South Asian Academy of Ophthalmology Journal

An Official Publication of the South Asian Academy of Ophthalmology

Volume 1 • Issue 1 • July-September 2026

https://journals.lww.com/saao

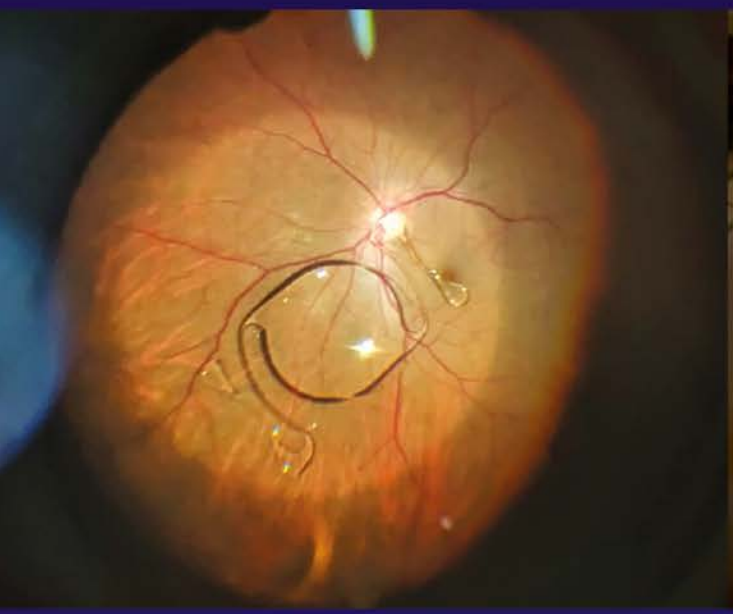

Wolters Kluwer

Medknow

South Asian Academy of Ophthalmology Journal

Editorial Board

South Asian Academy of Ophthalmology Journal

Volume 1 | Issue 1 | July-September 2026

Contents

Contents Contd...

Photo Essay

Letter to Editor

Editorial

See One, Simulate Many, Do One: A New Paradigm for Ophthalmic Surgical Education in South Asia

"Actual operative skill cannot be gained by observation, any more than skill in playing the violin can be had by hearing and seeing a virtuoso performing on that instrument." This profound observation by Allen O. Whipple perfectly encapsulates the current crisis in ophthalmic education. While observation is the first step in learning, it is a poor substitute for the tactile wisdom gained through performance. This distinction becomes a matter of urgent public health when we consider the staggering burden of blindness in our region. Recent data from the Global Burden of Disease Study highlights that South Asia continues to bear a disproportionately high share of the world's blindness. Despite decades of progress, the number of people blind or visually impaired due to cataract has risen over the past 30 years, driven by an aging population that is outpacing our surgical capacity.[1] We are facing a tsunami of cataract blindness that requires not just more ophthalmic surgeons but surgeons who are skilled, efficient, and safe from their very 1st day in independent practice.

The challenge we face is that our current training infrastructure is often unable to bridge the gap between theoretical knowledge and surgical competence. The transition from a supervised resident to an independent surgeon is fraught with anxiety and risk. A survey by the Academic and Research Committee of the All India Ophthalmological Society revealed a concerning reality where the median number of independent phacoemulsification surgeries performed by residents in many programs was negligible.[2] While residents may observe hundreds of procedures, their opportunities to actually maneuver instruments inside the eye are limited by the high-volume pressures of our hospitals and the understandable safety concerns for patients. This results in a generation of young ophthalmologists who are intellectually brilliant but surgically tentative. They understand the physics of fluidics but have not yet developed the muscle memory to manage a surging posterior capsule. This skill gap is the primary cause of complications such as posterior capsule rupture, which studies show occur significantly more frequently in surgeries performed by trainees compared to experienced staff.[3]

We must move beyond the antiquated apprenticeship model where a resident learns by operating on patients with no prior physical simulation. In the era of aviation, no pilot flies a passenger jet without hundreds of hours in a flight simulator. Similarly, we must embrace the era of ophthalmic simulation. The technology available today is transformative and must become a mandatory component of our curriculum. The *Eyesi Surgical* system by Haag Streit has established itself as a gold standard in virtual reality training. It offers an immersive environment where residents can practice complex maneuvers such as capsulorhexis and hydrodissection, repeatedly until they achieve a documented level of proficiency.[4] Studies have consistently shown that residents trained on the Eyesi demonstrate a significant reduction in complication rates when they eventually enter the operating room.[5]

However, we must also look at accessible solutions that fit the economically diverse landscape of South Asia. The *HelpMeSee* simulator is a remarkable innovation designed specifically to scale up training in manual small incision cataract surgery and phacoemulsification, offering high-fidelity simulation that mimics the feeling of real tissue.[6] Other systems, like the *MicroVisTouch,* provide haptic feedback, allowing the surgeon to feel the resistance of tissues, which is a critical sensory cue in surgery. For vitreoretinal training, the *RetinaVR* system offers a portable and affordable entry into the complex world of posterior segment surgery.[7] Beyond digital VR, we have synthetic eye models such as *SimulEYE* and the *Kitaro* dry lab and wet lab kits, which allow for repetitive practice of specific steps, like nuclear trenching or suturing, without the need for expensive electronic maintenance. These tools allow a resident to make their first hundred mistakes on plastic or digital avatars rather than on a human eye.

The integration of these simulators is not only about hand dexterity but also about building the mental resilience required for a high-pressure career. Surgical endurance is much like cycling up a steep mountain pass. It requires a rhythm, a calmness under pressure, and the ability to recover quickly from a stumble. As surgeons who also cycle, we often tell our students that the operating theater demands the same focus as a difficult climb. You must manage your energy, anticipate the terrain, and never panic. Simulation training builds this psychological fortitude by allowing

residents to face complications in a safe environment. When they encounter a vitreous loss in the simulator, they learn to manage it calmly. This mental conditioning is just as vital as manual skill.[8]

We must also foster a culture of mentorship that prioritizes patient safety through preparation. The old adage of "see one, do one, teach one" is dangerous in ocular microsurgery. A better approach is "see one, simulate many, do one." Institutions must invest in wet laboratories where residents can practice on animal eyes or synthetic tissues. Research confirms that structured wet laboratory training significantly improves performance scores and reduces operative time for beginning surgeons.[9] This investment pays for itself by reducing the cost of managing complications and improving patient trust.

The burden of blindness in South Asia is a call to action. We cannot meet this challenge with an army of hesitant ophthalmic surgeons. We need a workforce that is confident, competent, and compassionate. By adopting a proficiency-based progression model where simulation and wet laboratory mastery are prerequisites for live surgery, we can ensure that every patient, regardless of their economic status, receives surgery from a pair of safe and skilled hands. The technology exists. The data supports it. It is now up to us, the educators and leaders of South Asian ophthalmology, to make this the new reality for our residents. As we often say to our fellows, true confidence comes not from arrogance but from the quiet knowledge that you have prepared for every possibility.[10]

Suresh K. Pandey, Vidushi Sharma

SuVi Eye Institute and Lasik Laser Center, Kota, Rajasthan, India

Address for correspondence: Dr. Suresh K. Pandey, SuVi Eye Institute and Lasik Laser Center, C-13, Talwandi, Kota - 324 005, Rajasthan, India.
E-mail: suresh.pandey@gmail.com

Submitted: 25-01-2026 **Revised:** 26-01-2026
Accepted: 27-01-2026 **Published:** ***

REFERENCES

1. Vision Loss Expert Group of the Global Burden of Disease Study, GBD 2019 Blindness and Vision Impairment Collaborators. Global estimates on the number of people blind or visually impaired by cataract: A meta-analysis from 2000 to 2020. Eye (Lond) 2024;38:2156-72.
2. Gogate PM, Biswas P, Honavar SG, Sharma N, Sinha R, Sachdev MS, *et al*. Ophthalmology residency trainers' perspective on standardization of residency training in India. Indian J Ophthalmol. 2021;69:836-41. doi: 10.4103/ijo.IJO_2358_20.
3. Haripriya A, Chang DF, Reena M, Shekhar M. Complication rates of phacoemulsification and manual small-incision cataract surgery at Aravind Eye Hospital. J Cataract Refract Surg 2012;38:1360-9.
4. Al Ghamdi A, Al Mohaimeed M. Effectiveness of the eyesi surgical simulator for ophthalmology trainees: Systematic review and meta-analysis. Can J Ophthalmol 2024;59:172-80.
5. Thomsen AS, Bach-Holm D, Kjærbo H, Højgaard-Olsen K, Subhi Y, Saleh GM, *et al*. Operating Room Performance Improves after Proficiency-Based Virtual Reality Cataract Surgery Training. Ophthalmology. 2017;124:524-531. doi: 10.1016/j.ophtha.2016.11.015. Epub 2016 Dec 22.
6. Lansingh VC, Nair AG. More than simulation: The HelpMeSee approach to cataract surgical training. Indian J Ophthalmol 2024;72 Suppl 1:S12-5.
7. Antaki F, Doucet C, Milad D, Giguère CÉ, Ozell B, Hammamji K. Democratizing Vitreoretinal Surgery Training With a Portable and Affordable Virtual Reality Simulator in the Metaverse. Transl Vis Sci Technol. 2024;13:5. doi: 10.1167/tvst.13.4.5.
8. Pandey SK. The Infallible Doctor: Ending the Era of Medical Error with AI and Robotics. Noida, UP; Maple Press, In Press; 2026.
9. Alwadani S. Cataract surgery training using surgical simulators and wet-labs: Course description and literature review. Saudi J Ophthalmol. 2018;32:324-329. doi: 10.1016/j.sjopt.2018.01.003. Epub 2018 Feb 5.
10. Pokroy R, Du E, Alzaga A, Khodadadeh S, Steen D, Bachynski B, *et al*. Impact of simulator training on resident cataract surgery. Graefes Arch Clin Exp Ophthalmol 2013;251:777-81.

Access this article online

Website: https://journals.lww.com/saao

DOI: 10.4103/SAOJ.SAOJ_1_26

Quick Response Code

How to cite this article: Pandey SK, Sharma V. See one, simulate many, do one: A new paradigm for ophthalmic surgical education in South Asia. South Asian Acad Ophthalmol J 2026;XX:XX-XX.

Review Article

Evaluation of Trabecular Outflow in Minimally Invasive Glaucoma Surgery using Aqueous Angiography

ABSTRACT

Aqueous angiography (AA) allows for the real-time visualization of conventional aqueous humor outflow (AHO) pathways using intracameral injection of tracer dyes such as indocyanine green and fluorescein during a planned intraocular surgery. This review examines the current evidence on AA applications in evaluating trabecular minimally invasive glaucoma surgery (MIGS) procedures, including trabecular bypass stenting (iStent inject) and trabecular cutting procedures (bent ab interno needle goniectomy [BANG], Tanito microhook, and visco-BANG). Studies consistently demonstrate segmental AHO patterns with the highest flow in the nasal quadrant and lowest in the temporal quadrant. The use of dual dyes sequentially, AA has revealed distinct post-MIGS AHO patterns. AA has opened an avenue for targeted and individualized glaucoma surgery for glaucoma patients. AA also enables the assessment of intraoperative functionality of trabecular MIGS. This imaging technology can improve our understanding of AHO physiology and pathology to guide future therapeutic innovations.

Keywords: Aqueous angiography, glaucoma surgery, minimally invasive glaucoma surgery, trabecular outflow

INTRODUCTION

Glaucoma is an acquired progressive optic neuropathy that is currently the leading cause of irreversible blindness. The global burden of this disease is estimated to be 111.8 million by the year 2040.[1] Intraocular pressure (IOP) is a major risk factor for the progression of glaucoma. The inflow, outflow of aqueous humor along with episcleral venous pressure, determines IOP. The 70%–90% of aqueous humor outflow (AHO) occurs by the conventional (trabecular) outflow and the remaining 10%–30% by the unconventional (uveoscleral) outflow.

Aqueous humor being colorless with the lack of pigments makes it challenging to image the AHO pathways. Therefore, with the help of tracer dyes such as indocyanine green (ICG) dye and fluorescein dye, using the technique of aqueous angiography (AA), the trabecular AHO pathways are imaged.[2,3] AA allows for the real-time functional assessment of AHO *in vivo* in patients planned for an intraocular procedure. AA enables a surgeon to visualize 360° of perilimbal AHO channels and localize a region of high flow (area of increased angiographic signal intensity) and low flow (area of decreased angiographic signal intensity) [Figure 1].[2] Strohmaier *et al*. have documented that the region of high-flow corresponds to higher aqueous outflow and vice versa.[4]

Minimally invasive glaucoma surgery (MIGS) can be categorized based on the anatomical structures through which AHO is altered as (a) Enhancing AHO through Schlemm's canal surgery (trabecular MIGS) (example: bent ab interno needle goniectomy [BANG], iStent inject), (b) Enhancing AHO through uveoscleral routes (example: Miniject), (c) Enhancing AHO through subconjunctival space (for example: XEN),

Nitika Beri, Anuja Patil[1], Tanuj Dada[1]

Department of Ophthalmology, University College of Medical Sciences and GTB Hospital, Delhi, India, [1]Dr. Rajendra Prasad Centre for Ophthalmic Sciences, AIIMS, Delhi, India

Address for correspondence: Dr. Tanuj Dada,
Dr. Rajendra Prasad Centre for Ophthalmic Sciences,
AIIMS, Delhi, India.
E-mail: tanujdada@gmail.com

Submitted: 28-01-2026 **Revised:** 10-02-2026
Accepted: 12-02-2026 **Published:** ***

Access this article online

Website: https://journals.lww.com/saao

DOI: 10.4103/SAOJ.SAOJ_21_26

Quick Response Code

How to cite this article: Beri N, Patil A, Dada T. Evaluation of trabecular outflow in minimally invasive glaucoma surgery using aqueous angiography. South Asian Acad Ophthalmol J 2026;XX:XX-XX.

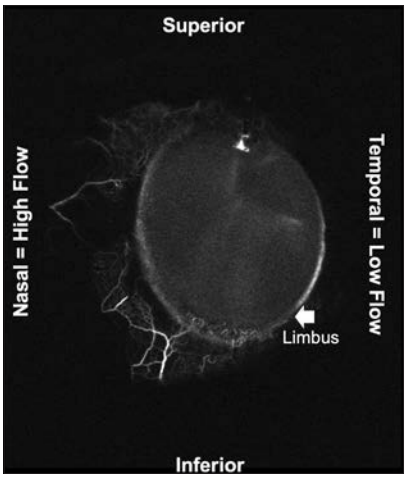

Figure 1: Aqueous angiography image with the nasal quadrant as increased angiographic signal intensity (high-flow region) and the temporal quadrant as decreased angiographic signal intensity (low-flow region). The arrow points toward the limbus

and (d) Reducing aqueous humor production through ciliary procedures (for example: Endocyclophotocoagulation). Within the trabecular MIGS category, there can be trabecular stenting procedures like iStent inject and trabecular cutting procedure like BANG. Using the technique of AA to visualize trabecular AHO, intraoperative status of AHO pre- and posttrabecular MIGS can be assessed in glaucoma patients. The focus of this review is to report trabecular outflow patterns using AA in glaucoma patients and the clinical application of AA.

METHOD OF LITERATURE REVIEW

The literature for this review was selected using PubMed and Google Scholar databases. A thorough systematic literature search was conducted utilizing keywords such as glaucoma, AA, MIGS, humans, and trabecular outflow. All pertinent review papers, original research articles, case series, and reports were examined and incorporated if they offered relevant information on the topic. The search was unrestricted by the publication year.

TECHNIQUE OF AQUEOUS ANGIOGRAPHY

Both ICG and fluorescein dye can be used either singly or as dual dyes (to query the effect of MIGS procedure). In the studies conducted in India, a concentration of 0.5%–0.1% of ICG dye and 2%-0.5% of fluorescein dye has been used.[5-9]

The machine, Spectralis HRA + OCT FLEX module (Heidelberg Engineering GmbH, Heidelberg, Germany) is used for performing AA. This machine allows us to image a supine patient in the operation theater (OT) with the help of multiple pivot joints and an integrated micromanipulator to control the alignment along the z-axis. The machine is wheeled into the OT prior and placed next to the OT table. The patient is cleaned and draped on the OT table as per the routine protocol. A 30G needle on a 1 ml syringe loaded with ICG/fluorescein dye is inserted by the surgeon at the superior 12'o clock position of the limbus. At this point, the microscope is removed and an assistant focuses the Spectralis HRA + OCT FLEX machine on the eye of the patient. The limbus and anterior chamber are brought to focus on infrared mode using a 30° lens (18–23 diopter focus). This is followed by the injection of 0.1 ml of dye by the surgeon with the simultaneous start of image recording in the tracer angiography mode of the machine by the assistant. The image is captured up to 60 s from the time of injection. These images are captured as a continuous video from the start of injection to up to 60 s. The 1 ml syringe with the needle is held in position throughout the image acquisition by the surgeon to prevent dye leak. Following this, the surgeon removes the needle and focuses the microscope to proceed with the surgical steps of the intraocular surgery planned.

To query the effect of MIGS on AHO, a different dye (from the one used previously) is used post-MIGS, with repetition of similar steps to capture the change in AHO post-MIGS procedure.

AQUEOUS HUMOR OUTFLOW PATTERNS STUDIED USING AQUEOUS ANGIOGRAPHY

AA evaluation of nonglaucomatous eyes has revealed segmental outflow with highest AHO in the nasal quadrant and the least in the temporal quadrant in both American and Asian populations.[5,10,11] AA evaluation in primary open angle glaucoma (POAG) also reported a segmental AHO with maximum AHO channels in the nasal quadrant and least in the temporal quadrant.[6]

Using dual dyes sequentially to query the effect of MIGS, or a single dye a pattern of early recruitment (earlier dye signal) was noted in cases of MIGS performed in the high-flow region by Huang *et al*. and Dada *et al*.[12,13] A pattern of new recruitment (re-opening of collapsed AHO channels) was noted in MIGS performed in the low-flow region by Huang *et al*. and Dada *et al*.[8,12]

Collapse of previously functional channels were noted by Beri *et al*. in a case of failed MIGS using AA.[14] BANG/trabecular cutting MIGS in the high-flow region led to scarring of the AHO channels and loss over a long-term follow-up. Therefore, trabecular cutting MIGS like BANG may be planned in a low-flow region (usually the temporal quadrant) to protect the high-flow region from scarring.

TRABECULAR MINIMALLY INVASIVE GLAUCOMA SURGERY PROCEDURES EVALUATED USING AQUEOUS ANGIOGRAPHY

Trabecular bypass stenting procedures

Trabecular bypass procedures like iStent inject were performed in AA targeted high-flow and low-flow regions in POAG patients, and patterns of AHO changes post iStent inject were reported by Huang *et al*. Istent inject in the high-flow region reported earlier recruitment of AHO channels, and in the low-flow region reported new recruitment of AHO channels.[12]

AA was used to assess the functionality/intraoperative patency of iStent inject and found that, despite anatomically well positioned iStent inject one of them was non-functional.[15] One of the reasons may be due to variations in AHO along the limbus (segmental AHO).[16]

Trabecular cutting procedures

AA evaluation in trabecular cutting procedure (BANG) in the nasal quadrant (high-flow region) has noted increased signal post BANG in pseudophakic glaucoma.[13] In a POAG patient, BANG in the low-flow region (temporal quadrant) led to re-opening of collapsed AHO channels.[8]

AA was used to assess the intraoperative patency/functionality of trabecular cutting MIGS, like Tanito microhook and visco-BANG in the temporal quadrant and found them to be functional.[17,18]

In a case of primary angle closure glaucoma (PACG), AA documented augmentation of AHO posttrabecular MIGS (Visco-BANG) with phacoemulsification and goniosynechialysis; indicating that MIGS in PACG may have a potential role, which is an area of active research at present.[7]

Aqueous angiography-guided minimally invasive glaucoma surgery

With AA allowing real time, intraoperative visualization of AHO channels of a patient, targeted and individualized glaucoma surgery can be planned with the hope to provide best results for the patients. A pilot randomized controlled trial by Dada *et al*. evaluated the postoperative success of performing MIGS (BANG) in the AA identified high-flow and low-flow regions.[9] They reported that better postoperative success was noted in patients who underwent BANG in the low-flow region over a follow-up of 6 months. It was the first study to suggest the concept of targeting the low-flow regions, such as the temporal quadrant, for MIGS procedures.[9] The modifications made to perform BANG in the temporal quadrant were that the position of the surgeon was shifted to the nasal side (opposite side of the temporal quadrant) along with the shift of eyepiece of the microscope, and the main port was made superonasal (example between 2 and 3'o clock hours in a right eye) to avoid obstruction by the nasal bridge.[9]

Huang *et al*., also performed targeted MIGS (iStent inject) in the high-flow and low-flow regions identified by AA.[12] However, they reported the change in AHO patterns post-MIGS and not clinical outcome for the patients.[12]

A summary of the studies of AHO and trabecular MIGS evaluated using AA are compiled in Table 1.

CLINICAL IMPLICATIONS FOR GLAUCOMA PRACTICE

With 70%–90% of AHO occurring by the conventional AHO pathway, visualizing this pathway in real-time intraoperatively can allow glaucoma surgeons to plan personalized and targeted glaucoma surgeries for their patients. Another advantage is that ICG dye stains the trabecular meshwork, thereby can help beginner surgeons in the identification of trabecular meshwork for MIGS procedures.[19] AA helps check the patency of MIGS procedures intraoperatively, which can allow re-adjustment if required in the same sitting. Ensuring the correct functional status of MIGS can help improve the clinical outcomes for the patients. Research on studying the changes in AHO post-MIGS can help us identify the cause of failure, thereby allowing us to take corrective measures and improve the efficacy of MIGS surgeries. A better understanding of AHO can give direction for innovation of newer MIGS in future with greater efficacy.

LIMITATIONS AND TECHNICAL CHALLENGES OF AQUEOUS ANGIOGRAPHY

The machine for AA imaging has limited availability as it is expensive. With further research and innovation, the cost may come down in future. AA is an invasive technique and requires a sterile operating theater for AHO pathways assessment. Repeated evaluation by AA is difficult to perform as there are limited indications to perform repeat invasive procedures in the eye. Vitreous staining and a focal nick of the anterior lens capsule have been noted with AA in various studies.[5,6,9,20] Vitreous staining was managed conservatively and the focal nick of the anterior lens capsule was included in the capsulorrhexis step of the phacoemulsification surgery.[5,6,9,20]

FUTURE DIRECTIONS IN OUTFLOW IMAGING

Further research on developing noninvasive modalities to image the AHO would be useful in patient management. The

Table 1: Studies of aqueous humor outflow and trabecular minimally invasive glaucoma surgery evaluated using aqueous angiography in adult humans

Authors	Year	Study type	Population/sample (*n*)	MIGS procedure	AA dye used	Key findings
Huang *et al*.[10]	2017	Clinical study	Nonglaucomatous patients (8)	None	ICG (0.4%)	Segmental outflow (Nasal quadrant=highest)
Huang *et al*.[11]	2018	Clinical study	Nonglaucomatous patients (8)	None	ICG (0.4%) and Fluor (2%)	Segmental outflow (Nasal=highest; Temporal=least) Dyes can be used sequentially
Huang *et al*.[12]	2019	Prospective comparative case series	POAG (14) and nonglaucomatous patients (1)	iStent inject (high and low-flow)	ICG (0.4%) and Fluor (2%)	Earlier signal intensity (high-flow); reopening of collapsed channels (low-flow)
Dada *et al*.[13]	2022	Case report	Pseudophakic Glaucoma (1)	BANG (nasal quadrant, high-flow)	ICG (0.5%)	Increased signal post-BANG
Dada *et al*.[8]	2023	Case report	POAG (1)	BANG (temporal quadrant/low-flow)	ICG (0.5%) and Fluor (2%)	Re-opening of collapsed channels
Dada *et al*.[15]	2024	Case report	POAG (1)	iStent inject	ICG (0.1%)	One stent nonfunctional despite correct position
Beri *et al*.[14]	2024	Case report	Failed MIGS patient (1)	BANG in high-flow (nasal quadrant)	ICG (0.1%)	Collapse of previously functional channels; fibrosis
Beri *et al*.[17]	2025	Case report	POAG (2)	Tanito microhook + Visco-BANG (temporal quadrant)	ICG (0.1%)	Patency of temporal trabecular cutting MIGS
Dada *et al*.[7]	2025	Case report	PACG patient (1)	Trabecular MIGS (visco-BANG) + phaco + GSL	ICG (0.1%) and Fluor (0.5%)	Augmentation of AHO post-MIGS in PACG
Dada *et al*.[9]	2025	Pilot RCT	POAG patients (30)	AA-guided BANG (high versus low-flow)	ICG (0.1%)	Better success in low-flow region (6 months)
Beri *et al*.[5]	2025	Cross sectional, observational	Nonglaucomatous (30)	None	ICG (0.1%)	Segmental AHO: Highest nasal, least temporal
Beri *et al*.[6]	2025	Cross sectional, observational	POAG patients (30)	None	ICG (0.1%)	Segmental AHO: Highest nasal, least temporal

AA: Aqueous angiography, ICG: Indocyanine green, Fluor: Fluorescein, POAG: Primary open angle glaucoma, PACG: Primary angle closure glaucoma, BANG: Bent ab interno needle goniectomy, GSL: Goniosynechialysis, Phaco: Phacoemulsification, AHO: Aqueous humor outflow, RCT: Randomized control trial, MIGS: Minimally invasive glaucoma surgery

image analysis of the captured AA image requires further refinement like the development of an in-built software for image analysis in the flex module of OCT machine or use of artificial intelligence for image assessment. Further studies are needed to study the efficacy of performing MIGS in the temporal (low-flow region) compared to the routine nasal quadrant.

CONCLUSION

AA has opened a new avenue for targeted and individualized MIGS procedures. It allows the evaluation of the functionality of trabecular MIGS and has demonstrated the changes in AHO patterns posttrabecular MIGS. The functional and real-time assessment of AHO in humans by AA will improve the understanding of both the physiology and pathology of AHO channels and help us to devise new treatment modalities for individualized targeted lowering of IOP in the near future. Further studies with larger sample size, varied ethnicities, along with randomized control trials are needed to validate the findings of these current studies and add further data to the literature.

Financial support and sponsorship

Nil.

Conflicts of interest

There are no conflicts of interest.

REFERENCES

1. Tham YC, Li X, Wong TY, Quigley HA, Aung T, Cheng CY. Global prevalence of glaucoma and projections of glaucoma burden through 2040: A systematic review and meta-analysis. Ophthalmology 2014;121:2081-90.
2. Beri N, Bukke AN, Gupta A, Huang AS, Angmo D, Sharma N, *et al.* Clinical applications of aqueous angiography in glaucoma. Indian J Ophthalmol 2024;72:S553-60.
3. Dada T, Verma S, Bukke AN, Strohmaier CA, Huang AS. Aqueous angiography-guided minimally invasive glaucoma surgery. J Curr Glaucoma Pract 2022;16:1-3.
4. Strohmaier CA, McDonnell FS, Zhang X, Wanderer D, Stamer WD, Weinreb RN, *et al.* Differences in outflow facility between angiographically identified high- versus low-flow regions of the conventional outflow pathways in porcine eyes. Invest Ophthalmol Vis Sci 2023;64:29.
5. Beri N, Patil A, Midha N, Angmo D, Bari A, Sharma N, *et al.* Quantitative assessment of functional aqueous humor outflow by aqueous angiography. J Glaucoma 2025;34:888-94.
6. Beri N, Patil A, Sharma A, Bari A, Sharma N, Dada T. Functional assessment of aqueous humor outflow by aqueous angiography in

primary open angle glaucoma. J Glaucoma 2025;34:669-78.
7. Dada T, Beri N, Patil A, Shaw E, Angmo D. Augmentation of aqueous outflow after trabecular MIGS in primary angle closure glaucoma demonstrated by aqueous angiography. J Glaucoma 2026;35:131-3.
8. Dada T, Bukke AN, Huang AS, Sharma N, Verma S. Recruitment of temporal aqueous outflow channels after bent needle ab-interno goniectomy demonstrated by aqueous angiography. J Glaucoma 2023;32:e15-8.
9. Dada T, Gupta A, Beri N, Huang AS, Sharma N, Angmo D, *et al*. Aqueous angiography-guided bent ab interno needle goniectomy in high versus low aqueous humor outflow regions in primary open angle glaucoma: A pilot randomized controlled trial. J Glaucoma 2025;34:317-24.
10. Huang AS, Camp A, Xu BY, Penteado RC, Weinreb RN. Aqueous angiography: Aqueous humor outflow imaging in live human subjects. Ophthalmology 2017;124:1249-51.
11. Huang AS, Penteado RC, Saha SK, Do JL, Ngai P, Hu Z, *et al*. Fluorescein aqueous angiography in live normal human eyes. J Glaucoma 2018;27:957-64.
12. Huang AS, Penteado RC, Papoyan V, Voskanyan L, Weinreb RN. Aqueous angiographic outflow improvement after trabecular microbypass in glaucoma patients. Ophthalmol Glaucoma 2019;2:11-21.
13. Dada T, Bukke AN. Aqueous angiography guided ab interno trabecular surgery for open-angle glaucoma. BMJ Case Rep 2022;15:e248261.
14. Beri N, Gupta A, Patil A, Dada T. Aqueous angiographic evaluation of failed trabecular MIGS reveals closure of previously functional aqueous outflow pathways. BMJ Case Rep 2024;17:e261032.
15. Dada T, Beri N, Mahalingam K, Sharma N. Functional assessment of trabecular bypass created by iStent inject using aqueous angiography. BMJ Case Rep 2024;17:e258741.
16. Dada T, Beri N. Analyzing the shortcomings of trabecular micro-bypass stents for surgical management of glaucoma. J Curr Glaucoma Pract 2024;18:1-3.
17. Beri N, Patil A, Angmo D, Dada T. Intraoperative functional assessment of temporal trabecular cutting MIGS using aqueous angiography. BMJ Case Rep 2025;18:e263543.
18. Dada T, Beri N, Sethi A, Sharma N. Viscodilation of Schlemm's canal combined with goniectomy using a 30 G needle (visco-bent ab interno needle goniectomy). J Curr Glaucoma Pract 2023;17:210-3.
19. Beri N, Bukke AN, Gupta A, Dada T. Dye-enhanced visualization of trabecular meshwork for canal-based minimally invasive glaucoma surgery. Digital Journal of Ophthalmology 2024; 30.
20. Beri N, Patil A, Verma S, Dada T. Staining of vitreous by indocyanine green dye post aqueous angiography. BMJ Case Rep 2024;17:e259610.

Review Article

Regional Differences of Retinopathy of Prematurity in South Asian Ophthalmology Region and Measures to Improve It

ABSTRACT

Retinopathy of prematurity (ROP) is an important cause of preventable childhood blindness worldwide and has emerged as a growing public health concern in developing countries. Improvements in neonatal care have increased the survival of premature and low birth weight infants, thereby increasing the number of infants at risk for ROP. Countries within the South Asian Ophthalmology (SAO) region share similar challenges related to screening, early detection, and timely management of this disease. This review summarizes the epidemiology, risk factors, and regional differences in the burden of ROP across countries in the SAO region including India, Nepal, Bangladesh, Pakistan, and Sri Lanka. The article also highlights gaps in screening infrastructure, variability in neonatal care practices, and delays in referral that contribute to visual morbidity. Innovative strategies such as telemedicine-based screening programs, including the Karnataka Internet Assisted Diagnosis of Retinopathy of Prematurity (KIDROP) model, and smartphone-based retinal imaging are discussed as potential solutions to improve accessibility and early diagnosis in resource-limited settings. Strengthening awareness among neonatologists, implementing standardized screening protocols, and expanding cost-effective tele-ophthalmology initiatives may significantly reduce the burden of ROP-related blindness in the region.

Keywords: Low birth weight, preterm, South East Asia, retinopathy of prematurity

INTRODUCTION

Retinopathy of prematurity (ROP) has been recognized as the fifth leading cause of childhood blindness in postindustrial and developed nations by the World Health Organization's (WHO's) Vision 2020 program.[1] Improved neonatal intensive care and survival of preterm children has boomed this condition in the underdeveloped nations also.[2] About 60% of childhood blindness in this part of the world is now a consequence of ROP.[2,3]

In ROP, there is an abnormal growth of blood vessels in the retina of the babies that have been born preterm and with low birth weight.[4] In 1942, Terry phrased the term "retrolental fibroplasia" to describe this condition where supplemental oxygen was regarded instrumental in the pathogenesis.[5] After all these years, it has been agreed that low gestational age, low birth weight, and prolonged exposure to auxiliary oxygen therapy have consistent and significant association with ROP.[6]

Access this article online	
Website: https://journals.lww.com/saao	Quick Response Code
DOI: 10.4103/SAOJ.SAOJ_2_25	

Eli Pradhan, Gunjan Prasai[1,2,3,4], Rajvardhan Azad[5,6]

Department of Ophthalmology, Tilganga Institute of Ophthalmology, Kathmandu, Nepal, [1]Department of Ophthalmology, University of Edinburgh, Edinburgh, Scotland, United Kingdom, [2]Netradham Eye Care Centre, Lalitpur, Nepal, [3]Department of Ophthalmology, Kathmandu Netralaya, Kathmandu, Nepal, [4]Department of Ophthalmology, Frontline Hospital, Kathmandu, Nepal, [5]Department of Ophthalmology, Akhanda Jyoti Eye Hospital, Patna, Bihar, India, [6]Raj Retina and Eye Centre, Patna, Bihar, India

Address for correspondence: Dr. Gunjan Prasai,
University of Edinburgh, Edinburgh, Scotland, United Kingdom.
Netradham Eye Care Centre, Lalitpur, Nepal.
Kathmandu Netralaya, Kathmandu, Nepal.
Frontline Hospital, Kathmandu, Nepal.
E-mail: prasaigunjan@gmail.com

Submitted: 06-06-2025 **Revised:** 29-01-2026
Accepted: 16-02-2026 **Published:** ***

How to cite this article: Pradhan E, Prasai G, Azad R. Regional differences of retinopathy of prematurity in South Asian Ophthalmology region and measures to improve it. South Asian Acad Ophthalmol J 2026;XX:XX-XX.

The world has so far seen three major epidemics of ROP. The first epidemic was during the 1940s and 1950s in the Western countries. It had occurred due to unregulated use of supplemental oxygen among preterm newborns without monitoring their blood gaseous levels. The birth weight of the neonates ranged from 800 g to 3400 g with an average of 1300 g.

The second epidemic occurred during the 1970s, again in Western countries, when rapid advances in neonatal care led to improved survival of very preterm infants. Even extremely low birth weight infants (<1000 g), those born at <30 weeks of gestation, and babies who were small for gestational age began to survive in greater numbers. These infants, often described at the time as suffering from the "oxygen radical disease of neonatology," frequently required supplemental oxygen therapy. However, inadequate monitoring and regulation of oxygen administration resulted in fluctuations between hypoxia and hyperoxia, contributing to the development of retinopathy of prematurity (ROP). A similar trend is now being observed in developing countries. With the expansion of neonatal care services, survival rates of extremely preterm and low birth weight infants have increased across many regions. However, this growth has often occurred without parallel improvements in training, monitoring, and infrastructure. Consequently, a larger number of infants are now at risk of developing ROP. Moreover, studies have also documented the occurrence of ROP in relatively more mature and heavier infants.[6]

METHODOLOGY

This review was conducted to synthesize current evidence on the regional differences in the epidemiology and management of ROP within the South Asian Ophthalmology (SAO) region and to identify effective strategies for improvement. A systematic approach was used to identify, select, and critically appraise relevant research.

Search strategy

A comprehensive literature search was performed using electronic databases including PubMed, Medline, Scopus, Google Scholar, and the Cochrane Library. The search was limited to articles published in English from January 2000 to December 2023. Key search terms and their combinations included "Retinopathy of prematurity," "ROP," "South Asia," "India," "Nepal," "Pakistan," "Bangladesh," "Sri Lanka," "Bhutan," "Afghanistan," "epidemiology," "incidence," "risk factors," "screening," and "telemedicine."

Inclusion and exclusion criteria

Studies were included if they reported original data on the incidence, risk factors, screening practices, or interventions for ROP within the SAO region. Review articles, meta-analyses, and relevant reports from major health organizations (e.g., WHO) were also considered for background and context. Editorials, letters without primary data, and studies focused exclusively on populations outside the SAO region were excluded.

Data extraction and synthesis

Titles and abstracts of the identified articles were screened for relevance by two independent reviewers. Full texts of potentially eligible studies were retrieved and assessed. Data on study design, population, sample size, key findings related to ROP burden, risk factors, and outcomes of screening and treatment strategies were extracted into a standardized form. Discrepancies were resolved through discussion with a third reviewer. The findings were synthesized narratively, with a focus on comparing epidemiological trends and highlighting innovative, context-appropriate solutions across different countries in the region.

Regional variations

Each year in Bangladesh, approximately 2500 babies are born that weigh ≤1500 g. Despite better facilities than the past, inadequate oxygen monitoring has led to even comparatively bigger babies, resulting in visual morbidity as a result of ROP.[7]

India with its large population is home to about 10% of the ROP population. In 2010, approximately 5000 children developed severe form of ROP and 2900 had sequelae, resulting in visual impairment.[8] In South India, from 2000 to 2017, a 20 times increment was seen in children diagnosed with ROP and 12 times rise in those that required medical intervention.[9] In North India, between 2013 and 2017, aggressive posterior ROP showed an increasing trend from 13% of cases in 2013 to 28% in 2017. Most notable was that about 15.6% of the children had retinal detachment (stages 4b/5) and were detected late due delay or no prior screening.[10] Another study in a well-equipped neonatal unit of a tertiary care center of India between 2017 and 2018 concluded significant risk factors as birth asphyxia, apnea, sepsis, anemia, neonatal seizure, blood transfusion, respiratory distress syndrome, phototherapy, antenatal steroid use, and multiple pregnancy.[11]

In Nepal, the incidence of ROP has been comprehended as 22%–30%. Among these, 3.2% had severe stages of ROP requiring intervention. Multiple studies in different centers concluded significant risk factors of developing ROP as oxygen supplementation, low birth weight, low gestational age, and sepsis.[12-14]

In Pakistan, the incidence of ROP was observed as 11.5%. In the same study, it was seen that ROP did not occur in infants more than 32 weeks of gestation and/or weighing more than 1500 g.[15] Multiple studies carried out in Pakistan established that low gestational age, oxygen administration, anemia, sepsis, multiple gestation, blood transfusion, intravenous antibiotics, and respiratory distress syndrome were significantly associated with development of ROP.[16-18]

In 2014 in Sri Lanka, for every 1000 live births, 248 were found to develop ROP. Analogous to other countries, the significant risk factors were supplemental oxygen or invasive ventilation for more than 7 days. Patent ductus arteriosus too was seen as a significant risk factor. In this study, babies <1500 g and <34 weeks of gestation were evaluated.[19]

However, the literature search could not find any articles on studies on ROP in Bhutan and Afghanistan, till now.

POSSIBLE SOLUTIONS

Telemedicine: Use of Karnataka Internet Assisted Diagnosis of Retinopathy of Prematurity model

A possible solution for ROP was evaluated in the Karnataka Internet Assisted Diagnosis of Retinopathy of Prematurity (KIDROP) model by means of in-person and telemedicine screening examinations between February 1, 2019, and June 30, 2021. Retinal images of babies after 30 weeks postmenstruation were used from an Indian telemedicine program, and an artificial intelligence (AI)-based vascular severity score was established. These variables were then used to predict treatment requiring ROP (TR-ROP) cases with the help of logistic models built by the AI using five-fold cross-validation. The study was carried out in three low-to-middle-income countries: India, Mongolia, and Nepal.

With the agency of this model, new TPR-ROP cases could be identified: 2.0 (0–11) weeks before in India, 0.5 (0–2.0) weeks before in Nepal, and 0 (0–5.0) weeks before in Mongolia. Moreover, if no repeat screening was done for low-risk infants, effective screening could be carried out with 45.0% (India, 664/1476), 38.4% (Nepal, 151/393), and 51.3% (Mongolia, 266/519) lesser examinations. Thus, this model has two major benefits. First, lesser number of low-risk babies can be examined without missing TR-ROP babies. Second, high-risk babies can be singled out earlier and monitored more closely before they develop TR-ROP.[20]

The KIDROP model demonstrated that telemedicine is a transformative and efficient strategy for ROP screening in low-resource settings, enabling earlier identification of high-risk infants when significantly reducing the screening burden by safely minimizing examinations for low-risk cases. This model has been adopted successfully throughout India and is an adoptable effective system for other countries too.

Use of smart phone

In today's era, where smartphones are present in almost every other hand, a study in Nepal has also acknowledged a possible potential of these devices to aid in screening ROP in low-resource countries. In this single-center study, a pediatric ophthalmologist examined 200 eyes of 100 at-risk babies whose retinal images were also concurrently taken by a well-trained photographer using an adapter, the Paxos Scope attached to a smartphone which were then evaluated separately by two retina specialists. For "grader one," the sensitivity was 87.5%, specificity was 82.1%, positive predictive value was 48.3%, and negative predictive value was 97.2%. For "grader two," sensitivity was 87.5%, specificity was 81.6%, positive predictive value was 47.5%, and negative predictive value was 97.2%. The measured κ coefficient for intergrader agreement was 0.94.[21] This study showed that smartphone-based retinal imaging, using an adapter like the Paxos Scope, is a promising, accessible, and reliable tool for screening ROP in low-resource settings, demonstrating good diagnostic accuracy and high agreement between specialists.

CONCLUSION

SAO countries have similar situations with the incidence as well as the risk factors for ROP although much of the evidence have not been explored in detail yet. Therefore, while we face the current ROP explosion, all of us in this region should tackle ROP more consciously, efficaciously, and scientifically. We can start by creating more awareness among neonatologists regarding more judicious use of oxygen supplementation as well as timely consultation and referral to ophthalmologists of at-risk babies. Similarly, we should also figure out ways to meet the screening demands such that no baby gets left out and those requiring treatment get them on time and adequately as well as cost-effectively so. We should start now, so that we do not have the next group of population filled with children barely starting their lives, who are severely visually debilitated owing to ROP.

Financial support and sponsorship

Nil.

Conflicts of interest

There are no conflicts of interest.

REFERENCES

1. World Health Organization. Vision 2020: The Right to Sight. Global

Initiative for the Elimination of Avoidable Blindness. Action Plan 2006–2011. Geneva, Switzerland: World Health Organization; 2006.
2. Gilbert C, Foster A. Childhood blindness in the context of VISION 2020 – The right to sight. Bull World Health Organ 2001;79:227-32.
3. Gilbert C, Fielder A, Gordillo L, Quinn G, Semiglia R, Visintin P, *et al*. Characteristics of infants with severe retinopathy of prematurity in countries with low, moderate, and high levels of development: Implications for screening programs. Pediatrics 2005;115:e518-25.
4. Gilbert C. Retinopathy of prematurity: A global perspective of the epidemics, population of babies at risk and implications for control. Early Hum Dev 2008;84:77-82.
5. Terry TL. Extreme prematurity and fibroblastic overgrowth of persistent vascular sheath behind each crystalline lens. Am J Ophthalmol 1942;25:203-4.
6. Sai Kiranmayee P, Kalluri V. India to gear up to the challenge of "third epidemic" of retinopathy of prematurity in the world. Indian J Ophthalmol 2019;67:726-31.
7. Nahar N, Badmus SA, Das SK, Malek MA, Rahman M, Khan MA. Retinopathy of prematurity in Bangladesh: An overview. Community Eye Health 2018;31:S25-6.
8. Blencowe H, Moxon S, Gilbert C. Update on blindness due to retinopathy of prematurity globally and in India. Indian Pediatr 2016;53 Suppl 2:S89-92.
9. Agarwal K, Balakrishnan D, Rani PK, Jalali S. Changing patterns of early childhood blinding conditions presenting to a tertiary eye center: The epidemic of retinopathy of prematurity in India. Indian J Ophthalmol 2019;67:816-8.
10. Tekchandani U, Katoch D, Dogra MR. Five-year demographic profile of retinopathy of prematurity at a tertiary care institute in North India. Indian J Ophthalmol 2021;69:2127-31.
11. Patel SS, *et al*. Risk factors for retinopathy of prematurity in a tertiary care neonatal unit. Int J Contemp Pediatr 2019;6:2235-41.
12. Adhikari S, Badhu BP, Bhatta NK, Rajbhandari RS, Kalakheti BK. Retinopathy of prematurity in a tertiary care hospital in Eastern Nepal. J Nepal Med Assoc 2008;47:24-7.
13. Chaudhry TA, Hashmi FK, Salat MS, Khan QA, Ahad A, Taqui AM, *et al*. Retinopathy of prematurity: an evaluation of existing screening criteria in Pakistan. Br J Ophthalmol. 2014;98:298-301.
14. Yadav R, Gupta S, Shrestha JB, Yadav R, Yadav TB. Perinatal risk factors for retinopathy of prematurity in preterm and low birth weight neonates. Nepal J Ophthalmol 2020;12:32-8.
15. Chaudhry TA, Hashmi FK, Salat MS, Khan QA, Ahad A, Taqui AM, *et al*. Retinopathy of prematurity: An evaluation of existing screening criteria in Pakistan. Br J Ophthalmol 2014;98:298-301.
16. Taqui AM, Syed R, Chaudhry TA, Ahmad K, Salat MS. Retinopathy of prematurity: Frequency and risk factors in a tertiary care hospital in Karachi, Pakistan. J Pak Med Assoc 2008;58:186-90.
17. Jamil AZ, Tahir MY, Ayub MH, Mirza KA. Features of retinopathy of prematurity in a tertiary care hospital in Lahore. J Pak Med Assoc 2015;65:156-8.
18. Hanif M, Ariff S, Ansar A, Ahmed K, Hussain AS. Characteristics of preterm with sight threatening retinopathy of prematurity. J Ayub Med Coll Abbottabad 2020;32:174-8.
19. Liyanage I, Perera K, Weerasekera M. A study on incidence and associated factors of retinopathy of prematurity in a tertiary care setting in Sri Lanka. Sri Lanka J Child Health 2017;46:322-7.
20. Coyner AS, Oh MA, Shah PK, Singh P, Ostmo S, Valikodath NG, *et al*. External validation of a retinopathy of prematurity screening model using artificial intelligence in 3 low- and middle-income populations. JAMA Ophthalmol 2022;140:791-8.
21. Adhikari S, Bajimaya S, Ranjitkar EP. Validation of smartphone-based screening for retinopathy of prematurity in a low-resource setting. J AAPOS 2021;25:274.e1-5.

Review Article

Artificial Intelligence in Ophthalmology – A Narrative Review

ABSTRACT

Artificial intelligence (AI) refers to the study and development of systems capable of simulating human thought processes and intelligent behavior. Over the past decade, AI has been integrated into diverse fields such as health care, education, business, and manufacturing. Within medicine, its adoption is still emerging; however, ophthalmology has become one of the specialties where AI has gained significant traction. This is largely due to the specialty's reliance on digital imaging, which provides a rich foundation for AI-driven diagnostic and decision-making tools. AI applications in ophthalmology now span disease screening, diagnosis, treatment planning, and surgical support, demonstrating strong potential to reduce preventable vision loss and improve patient outcomes. Despite these advances, challenges such as ethical concerns, data privacy, algorithmic bias, regulatory approval, and the "black-box" problem remain. Addressing these limitations through rigorous validation, transparent governance, and explainable models will be essential to ensure AI evolves into a safe, equitable, and transformative tool in global eye care. This review summarizes current applications of AI in ophthalmology, highlights diagnostic accuracy across subspecialties, and discusses challenges and future directions.

Keywords: Artificial intelligence, machine learning, ophthalmology

INTRODUCTION

Artificial intelligence (AI) broadly refers to the use of computer systems to perform tasks with limited human intervention. Its primary aim is to replicate aspects of human cognition, enabling machines to process information and support decision-making in ways that enhance efficiency in today's fast-paced environment.[1] Over recent years, AI has emerged as a transformative technology, representing one of the most significant developments in information technology.[2] Its rapid integration into health care, particularly ophthalmology, highlights its potential to revolutionize diagnostics, treatment, and patient care.

CATEGORIES OF ARTIFICIAL INTELLIGENCE BY CAPABILITY

1. Artificial narrow intelligence, which performs specific tasks like facial recognition or voice assistance but cannot operate beyond its scope[3]
2. Artificial general intelligence, a theoretical form of AI that could learn and adapt across diverse tasks at a human-like level, though it has not yet been achieved[4]
3. Artificial superintelligence, a hypothetical stage where machines surpass human intelligence entirely, raising significant ethical and societal concerns.[5]

TYPES OF ARTIFICIAL INTELLIGENCE BY FUNCTIONALITIES

AI can also be categorized according to the way systems function, process information, and interact with their environment. This framework highlights both current applications and potential future developments:

1. Reactive machines – The simplest form of AI, working only with current inputs and rule-based decisions. They

Kiu Mondal, Somen Misra, Riya Manna[1]

Department of Ophthalmology, AIIMS, Raipur, Chhattisgarh, India, [1]Department of Public Health, AIIMS, Raipur, Chhattisgarh, India

Address for correspondence: Dr. Kiu Mondal, Department of Ophthalmology, AIIMS, Raipur, Chhattisgarh, India.
E-mail: mondalkiu@gmail.com

Submitted: 30-01-2026 **Revised:** 15-02-2026
Accepted: 16-02-2026 **Published:** ***

Access this article online

Website: https://journals.lww.com/saao

DOI: 10.4103/SAOJ.SAOJ_27_26

Quick Response Code

How to cite this article: Mondal K, Misra S, Manna R. Artificial intelligence in ophthalmology – A narrative review. South Asian Acad Ophthalmol J 2026;XX:XX-XX.

cannot learn or adapt; examples include IBM's Deep Blue and Google's AlphaGo[6]
2. Limited memory AI – Uses recent data to improve decisions, seen in self-driving cars, fraud detection, and chatbots. These systems learn patterns but lack long-term memory[3]
3. Theory of mind AI – Still experimental, designed to understand human emotions, beliefs, and intentions. Prototypes such as MIT's Kismet and Sophia highlight its potential in health care and customer service[4]
4. Self-aware AI – A speculative concept where machines possess consciousness and autonomy. Currently confined to science fiction, it raises deep ethical and philosophical concerns.[5]

MACHINE LEARNING

Machine learning is an advanced branch of AI where models learn from datasets to identify patterns and make decisions without explicit programming. It is generally categorized into three types:[7]

1. Unsupervised learning – Works with unlabelled data to discover patterns or groupings
2. Supervised learning – Trains on labelled datasets with known outputs, improving reliability through expert annotations
3. Semi-supervised learning – Combines labeled and unlabeled data, enhancing accuracy and efficiency compared to using either alone.

Neural networks in machine learning

Neural networks are a specialized branch of machine learning designed to process data through interconnected layers of computational units, often referred to as "neurons." These systems typically begin with an input layer, where features – such as diagnostic variables – are defined in advance by programmers and subject experts. The information then passes through an intermediate layer, where complex transformations and computations occur, before reaching the output layer, which generates the final prediction or classification.[8]

Originally inspired by the functioning of biological neurons in the human brain, neural networks operate by transmitting the result of each node in one layer to multiple nodes in the next. This cascading process allows the network to capture intricate patterns in data. At the output stage, the system can produce either a continuous value (useful for regression tasks) or a probability score that corresponds to a specific category (for classification problems).

By mimicking the way neurons interact, neural networks provide a powerful framework for solving problems that involve large, complex datasets – ranging from medical diagnosis to image recognition and beyond.

Deep learning with convolutional neural networks

Deep learning refers to neural networks that contain many interconnected layers, often ranging from dozens to hundreds. These networks are called "deep" because of their complexity and the specialized training methods they require. Convolutional neural networks (CNNs) are a leading example, particularly effective in image analysis.[8]

CNNs learn by repeatedly examining labeled images, such as medical scans, and adjusting their internal parameters – known as weights – whenever their output differs from expert grading. Through this cycle of trial, error, and correction, the network gradually improves until its predictions closely match human assessments.[9] In practice, CNNs analyze pixel or voxel intensities, process them through multiple hidden layers, and generate either a diagnostic classification or a probability score at the output layer.

Once trained on large datasets, CNNs can evaluate new, unseen images with high accuracy. This ability to self-optimize through repetition and correction makes deep learning a powerful tool for tasks like medical diagnosis, pattern recognition, and computer vision.[10]

Several AI platforms based on CNNs are already commercially available for diabetic retinopathy screening. Notable examples include IDx–DR, which has received Food and Drug Administration (FDA) approval, and EyeArt, developed in California, which is classified as a European Union Class IIa medical device.[10] These systems demonstrate how deep learning models have progressed from research into real-world clinical practice, offering validated tools for largescale ophthalmic screening.

ARTIFICIAL INTELLIGENCE IN HEALTH CARE: APPLICATIONS AND MODALITIES

AI is playing an increasingly important role in healthcare, offering both virtual and physical solutions that enhance efficiency, accuracy, and patient care.[11] On the virtual side, AI supports clinical practice through digitized health records, automated scheduling, reminder systems, and drug dosage optimization, while also providing alerts for adverse interactions. It enables remote consultations, health monitoring through wearable devices, large-scale medical data management, disease diagnostics, and the creation of personalized treatment plans. In addition, AI assists in evaluating health plans for cost-effectiveness. Physical applications include robotic surgery for precision procedures,

adaptive prosthetics to improve mobility, robots designed for elderly care, surgical guidance systems, and automation of routine treatments. Together, these innovations are reshaping healthcare delivery by streamlining operations, improving diagnostic accuracy, and expanding access to quality care [Table 1].[10,12-17]

ROLE OF ARTIFICIAL INTELLIGENCE IN OPHTHALMOLOGY

AI is emerging as a powerful tool in ophthalmic care, offering new opportunities for early detection, accurate diagnosis, and tailored treatment planning.[18]

Ophthalmology is particularly well-suited for AI integration because of the abundance of digital imaging and measurable clinical data.[19] Techniques such as fundus photography, optical coherence tomography (OCT), and visual field analysis generate large datasets that can be used to train machine learning models for identifying and managing eye diseases.[20]

The incorporation of AI into ophthalmic practice is paving the way for more comprehensive and efficient clinical services.[21] With rising global life expectancy, age-related eye conditions are becoming increasingly common, placing additional pressure on healthcare systems.[22] AI can help address these challenges by detecting patients at risk of preventable vision loss earlier, supporting timely interventions, and ensuring medical resources are allocated more effectively through predictive analytics and personalized care strategies.[23] AI systems trained on these imaging modalities, combined with clinical data, are increasingly being developed to enhance diagnostic precision, support disease screening, and predict treatment outcomes. This integration of AI offers the potential to improve accuracy, efficiency, and patient care in ophthalmology.[7]

Dry eye disease

Dry eye disease (DED) is one of the most common ocular conditions, though prevalence estimates vary widely, ranging from 5% to 50% depending on the population studied.[24] Diagnosis typically involves tests such as tear breakup time, Schirmer's test, tear osmolarity, and tear meniscus height, along with advanced imaging techniques such as *in vivo* confocal microscopy, meibography, anterior segment OCT, interferometry, infrared thermography, and slit-lamp examination.[25] Harti *et al*. reported that AI, particularly deep learning applied to ocular imaging, shows strong potential for improving DED diagnosis.[26] Across modalities such as infrared meibography, OCT, and tear film interferometry, AI systems achieved high diagnostic accuracy, often comparable to or exceeding traditional tests. Infrared meibography was highlighted as the most clinically advanced approach due to its ability to directly visualize Meibomian gland morphology and its strong correlation with DED signs.

Table 1: Examples of artificial intelligence tools and their clinical implications in healthcare

AI tool	Implication in health care
Epic's Sepsis Model[12]	Predicts sepsis risk from electronic health record data
Tempus[13]	Integrates clinical and molecular data for cancer treatment decisions
IDxDR[10]	Diabetic retinopathy screening
Path AI[14]	Assist pathologists in cancer diagnosis
Brain IAC[15]	Capable of predicting brain cancer survival and dementia risk from MRI images
AliveCor Kardia Mobile[16]	AI-powered ECG analysis for arrhythmia detection
DeepMind Streams[17]	Predict acute kidney injury

AI: Artificial intelligence, MRI: Magnetic Resonance Imaging, ECG: Electrocardiography

Infectious keratitis

Infectious keratitis (IK) is an infection of the cornea that can lead to serious vision problems if not diagnosed and managed promptly. When left untreated, it may result in irreversible damage and permanent loss of sight. It is the leading cause of corneal scarring and is consistently ranked among the top five contributors to blindness worldwide, affecting populations in both developed and developing regions.[27]

Traditionally, IK is diagnosed and its underlying cause identified through slitlamp examination, corneal smears, and culture techniques. While these methods remain standard, recent research has increasingly explored the use of AI in anterior segment disease detection, including IK.[26,28]

Integrating AI into the diagnostic process offers a promising solution to the global shortage of ophthalmologists and has the potential to enhance both patient care and clinical outcomes. Machine learning models can be trained to detect subtle image features that are not visible to the human eye, enabling highly accurate identification of IK and its etiology.

Studies have shown that AI systems can analyze slit-lamp images with diagnostic performance comparable to that of experienced clinicians.[29] In addition, algorithms trained on confocal microscopy data have demonstrated strong capability in distinguishing fungal keratitis, further validating the role of AI as a supportive tool in ophthalmic diagnostics.[30] AI-based studies on IK show strong diagnostic performance, with accuracy ranging from about 70% to nearly 100% using slit lamp and confocal microscopy imaging [Table 2].[31-35]

Keratoconus

Keratoconus is a progressive corneal disorder that often begins in adolescence and remains challenging to detect in its early stages. While diagnosis typically relies on clinical

examination and corneal imaging, subtle cases without obvious clinical signs depend heavily on the interpretation of imaging techniques such as corneal topography and tomography by experienced specialists.

Before the advent of corneal cross-linking, transplantation was the only definitive treatment option for advanced keratoconus. Today, AI offers new possibilities by analyzing corneal images to identify keratoconus earlier, potentially preventing significant vision loss and reducing the need for transplantation. Despite the availability of cross-linking, keratoconus continues to be a leading indication for corneal transplantation.[36] Early and accurate diagnosis, therefore, remains critical to improving visual outcomes and minimizing the risk of invasive surgical intervention.

Current AI systems for detecting keratoconus are primarily supervised models, utilizing Pentacam indices alone or in combination with OCT parameters.[37] AI-based studies on keratoconus detection have shown excellent diagnostic accuracy, consistently above 98% across different devices and patient groups [Table 3].[38-42]

The Corvis ST uses a noncontact tonometer with a metered air pulse to induce corneal deformation, capturing high-speed Scheimpflug images during the process. Evidence suggests that biomechanical changes may precede tomographic or clinical signs of ectasia. By combining Pentacam tomography with Corvis ST biomechanical data, the Tomographic Biomechanical Index (TBI) – developed through machine learning – offers improved accuracy for early detection of keratoconus and ectasia. Lim and Lim confirm that TBI achieves greater sensitivity and specificity than tomography or biomechanics alone.[43]

Keratoplasty

The Eye Bank has reported a rising demand for corneal graft tissue, posing both financial and public health challenges. AI offers valuable support to corneal surgeons by enhancing decision-making for keratoplasty and related procedures. By combining clinical history, laboratory findings, and advanced imaging data, AI can improve surgical planning and predict outcomes more accurately. Machine learning models are capable of stratifying risk factors such as systemic and ocular allergies, eye-rubbing behaviour, and serum biomarkers, including IgE, Vitamin D, and Vitamin B12, along with detailed corneal indices from devices like the Pentacam HR in advanced keratoconus requiring keratoplasty.[44] Integrating these categorical and continuous variables enables AI to identify the most critical predictors of long-term success in procedures such as deep anterior lamellar keratoplasty. This approach allows for personalized treatment strategies, better patient selection, and early management of modifiable risk factors. Supporting this, Feizi *et al*. demonstrated that machine learning techniques are effective in forecasting graft rejection.[45]

Refractive surgery

The growing demand for achieving precise visual and refractive outcomes while minimizing postoperative complications has led to a surge in AI-based research within refractive surgery.[46] A key focus has been on preoperative screening to detect patients at risk of developing iatrogenic ectasia after corneal laser procedures. AI tools also assist in determining the most suitable type of refractive surgery and

Table 2: A brief summary of artificial intelligence-based infectious keratitis study

Author	Year	Type of keratitis	Sample size	Photography and Image Acquisition	Accuracy (%)	Sensitivity (%)	Specificity (%)
Kuo *et al*.[31]	2021	Bacterial	1512	Slit lamp/external - Resolution of 224 pixels ×224 pixels	70.30	74.10	64.30
Li *et al*.[32]	2021	Bacterial, Fungal, Viral	13557	Slit lamp/external - Resolution of 224 pixels ×224 pixels	98.00	97.70	98.20
Won *et al*.[33]	2023	Bacterial, Fungal	684	Slit lamp/external - Resolution of 500 pixels ×750 pixels	87.80	86.40	88.70
Hou *et al*.[34]	2021	Fungal	1870	Confocal microscopy	99.29	99.33	99.62
Liu *et al*.[35]	2019	Fungal	1213	Confocal microscopy	99.95	99.9	100

Table 3: Studies on the diagnostic accuracy of keratoconus using artificial intelligence

Author	Year	Sample size	Device	Keratoconus classes	Performance
Kamiya *et al*.[38]	2019	543	Tomey CASIA	Normal and 4 grades of keratoconus	Accuracy: 99%
Al-Timemy *et al*.[39]	2021	534	Pentacam	Normal and keratoconus	Accuracy: 98.3%
Ruiz Hidalgo *et al*.[40]	2016	860	Pentacam	Keratoconus, forme-fruste keratoconus, postrefractive surgery, astigmatism, and normal	Accuracy: 98.9%
Arbelaez *et al*.[41]	2012	3502	Sirius	Keratoconus, subclinical keratoconus, postcorneal surgery, and normal	Accuracy: 98.2%
Zhang *et al*.[42]	2024	1786	Corvis ST	Normal and keratoconus	Sensitivity: 92.49%, Specificity: 91.54%

in performing automated refraction. Presurgical screening remains critical for identifying high-risk candidates, and advanced technologies such as Pentacam, the Belin-Ambrosio enhanced ectasia display, and Orbscan are increasingly utilized to support these assessments.[47,48]

Cataract

Cataract surgery is among the most frequently performed procedures worldwide, with its prevalence continuing to rise in aging populations.[49] AI technologies, including machine learning, deep learning, and CNNs, are increasingly being applied across the preoperative, intraoperative, and postoperative phases of cataract management.[50] In the preoperative , AI assists in calculating intraocular lens (IOL) power and detecting cataracts using slit-lamp imaging.[51]

Recent innovations in IOL power prediction include several AI-driven models.[52] The Karmona formula is a purely machine learning ensemble model, while the Hoffer QST integrates AI into a classic vergence formula. The Nallasamy formula uses a two-layer ensemble trained on thousands of eyes, and the ZhuLu formula applies gradient boosting and support vector regression for highly myopic eyes. The Zeiss–AI formula combines paraxial ray tracing with AI optimization. Widely adopted AI-enhanced formulas also include the Kane formula (hybrid optics + AI), the HillRBF (radial basis function network), the Ladas Super Formula, and the Barrett Universal II.[53]

During surgery, AI contributes to risk assessment and monitoring of the surgical workflow.[54] Postoperatively, AI supports the prediction of complications such as posterior capsular opacification and IOL dislocation, while also helping to streamline patient follow-up care.[55]

Glaucoma

Glaucoma is a major cause of irreversible blindness, with persistent challenges in early diagnosis, monitoring disease progression, and predicting surgical outcomes.[56] AI has introduced new possibilities in glaucoma care by utilizing fundus photography, OCT, and multimodal data integration to detect subtle changes that may be overlooked by conventional methods.[57] Deep Learning models, including CNNs, Recurrent Neural Networks, Transformer models, and Generative Adversarial Networks, have demonstrated strong accuracy in identifying early glaucomatous features such as increased cup-to-disc ratio, rim thinning, and nerve fiber layer defects.[58] AI also improves the prediction of disease progression by combining structural and functional data from OCT and visual field assessments, enabling earlier intervention and individualized treatment strategies.[59,60] Furthermore, multimodal models that integrate imaging with electronic health records enhance forecasting of surgical success and complication risks, supporting personalized postoperative management and better patient outcomes.[61] AI-based glaucoma studies have demonstrated strong performance in diagnosis, progression prediction, and surgical outcome forecasting, with accuracy and sensitivity often exceeding 88% across diverse imaging and clinical datasets [Table 4].[62-67]

Diabetic retinopathy

Diabetic retinopathy is an escalating global health issue, and timely detection is essential for effective management. Since the FDA approved the first AI device for automated screening of diabetic retinopathy in 2018, the application of AI in this field has expanded rapidly, making it one of the most widely used AI-based procedures in the United States, second only to coronary artery disease.[68,69] A meta-analysis of 34 population-based studies assessed the effectiveness

Table 4: A brief summary of an artificial intelligence-based study of glaucoma

Study	Year	Data type	Data size	Task	Performance
Liu *et al*.[62]	2019	Color fundus photographs	274,413 images	Detects glaucomatous optic neuropathy	Sensitivity: 96.2%; Specificity: 97.7%
Hu *et al*.[63]	2023	Sequential fundus images	3671 images (from 405 eyes)	Glaucoma detection and progression forecast	Accuracy: 89.5%; Sensitivity: 87.6%; Specificity: 89.6%
Wu *et al*.[64]	2021	Spectralis spectral-domain OCT	470 eyes (224 healthy, 246 glaucoma)	Glaucoma diagnosis (discriminating normal from glaucomatous eyes and distinguishing between early, moderate, and severe glaucoma from normal conditions)	Accuracy: 88.18%, Sensitivity: 91.66%, Specificity: 85.07%
Hou *et al*.[65]	2023	Longitudinal OCT data	8785 follow-up sequences of 5 consecutive OCT tests from 3253 eyes	To predict visual field worsening from longitudinal OCT data	AUC: 0.97
Dixit *et al*.[66]	2021	Longitudinal VF data and clinical data	11,242 eyes	To detect when glaucoma progression is occurring based on longitudinal VF and clinical data	Accuracy: 91% to 93%; AUC: 0.89–0.93
Banna *et al*.[67]	2022	Preoperative systemic data, demographic data, and ocular data	230 trabeculectomy surgeries performed on 184 patients	To predict the complete success of trabeculectomy surgery at 1 year	Accuracy: 68%; AUC: 0.74

AUC: Area under curve, VF: Visual field, OCT: Optical coherence tomography

of various retinal imaging techniques, including tabletop, handheld, and smartphone fundus cameras, for screening in clinical practice.[70] The findings demonstrated strong diagnostic performance, with a pooled sensitivity of 94% and a specificity of 89% compared to human graders. Importantly, AI maintained high accuracy across both mydriatic and nonmydriatic images, with nonmydriatic imaging offering particular benefits in resource-limited environments.

Age-related macular degeneration

Age-related macular degeneration (AMD) is a complex condition and one of the leading causes of vision loss, projected to affect nearly 288 million individuals worldwide by 2040.[71] Deep Learning techniques have improved AMD diagnosis, particularly when multimodal imaging such as OCT angiography and OCT B-scans is used.[72] While drusen-based assessment alone can provide acceptable diagnostic outcomes at lower cost, multimodal approaches enhance accuracy.[73] In addition, machine learning models are increasingly applied to predict treatment needs, such as forecasting the likelihood of intravitreal injections, thereby supporting personalized patient management.[74]

Retinopathy of prematurity

Retinopathy of prematurity (ROP) is a vaso-proliferative retinal disease linked to prematurity and remains the leading cause of childhood blindness worldwide.[75] Its prevalence is rising due to improved survival of preterm infants in resource-limited settings where oxygen monitoring and screening are often inadequate.[76] Diagnosis of ROP is highly subjective, with significant variability between examiners, leading to inconsistent treatment decisions.[77] This underscores the need for more precise diagnostic approaches. AI offers a promising solution by enabling large-scale, standardized screening with objective image analysis. AI-based tools can improve diagnostic accuracy, reduce interobserver variability, enhance repeatability, and support timely triage and management, particularly in under-resourced healthcare systems.[78]

Ramanathan A *et al*. conducted a systematic review evaluating the application of AI in ROP.[79] The review included 27 studies, of which 19 utilized AI systems for diagnosing ROP, staging disease severity, detecting preplus or plus disease, and assessing retinal image quality. Reported diagnostic performance was strong, with sensitivity ranging from 71% to 100%, specificity between 74% and 99%, and area under the curve values of 91%–99%. AI techniques demonstrated accuracy and sensitivity comparable to those of ophthalmologists. In addition, eight studies assessed vascular severity scoring and showed that automated classification models could reliably differentiate disease severity. These findings underscore the potential of AI to provide consistent, objective, and scalable solutions for ROP screening and management.

INTEGRATION OF SMARTPHONE TECHNOLOGY AND ARTIFICIAL INTELLIGENCE FOR ADVANCED OPHTHALMIC CARE

Smartphones, with their advanced imaging capabilities, have evolved into valuable tools for medical diagnostics. In ophthalmology, their integration with AI has opened new possibilities for screening, monitoring, and managing eye diseases.[80] AI algorithms enhance the interpretation of ocular images captured through smartphone-based devices, enabling timely and cost-effective detection of conditions such as diabetic retinopathy, glaucoma, cataract, pediatric visual impairment, and ocular surface disorders [Table 5].[81-87] This convergence supports efficient

Table 5: Summary of representative studies using the integration of smartphone technology and artificial intelligence in ophthalmology

Author	Application	Data source	Performance
Natarajan *et al*.[81]	Diabetic retinopathy detection	Fundus photographs taken by the Remidio Non-Mydriatic Fundus on Phone	Sensitivity: 85.2%, specificity: 92.0%
Young *et al*.[82]	Retinopathy of prematurity detection and grading	Fundus photographs taken by smartphone (the Make-In-India Retcam/Keeler Monocular Indirect Ophthalmoscope devices)	Referral-warranted ROP (sensitivity: 80.0%, specificity: 59.3%) Treatment-requiring ROP (sensitivity: 100.0%, specificity: 58.6%)
Nakahara *et al*.[83]	Glaucoma detection	Fundus photographs taken by an iPhone 8 with the D-Eye lens (D-EYE S.r.l., Padova, Italy)	AUC: 0.842
Wu *et al*.[84]	IOP measurements	IOP measured by a smartphone tonometer prototype	The mean difference for Goldmann Applanation Tonometry: +0.24 mm Hg
Hu *et al*.[85]	Cataract grading	Ocular images taken by the smartphone-based slit-lamp	Accuracy was 93.5%
Murali *et al*.[86]	Amblyopia detection	Ocular images taken by a smartphone	Sensitivity: 88.2% Specificity: 75.6%
Tabuchi *et al*.[87]	Ptosis detection	Facial photographs taken by an iPad Mini 5	Sensitivity: 83.0% Specificity: 82.5%

IOP: Intraocular pressure, ROP: Retinopathy of prematurity, AUC: Area under curve

teleophthalmology, expands access to care, and improves diagnostic accuracy, particularly in resource-limited settings, making smartphone–AI platforms a transformative innovation in modern eye care.

Limitations and challenges

1. Ethical concern – AI in ophthalmology offers great potential for better diagnosis and treatment, but its use must be guided by careful ethical consideration to ensure it benefits everyone[88]
2. Data privacy – AI in health care depends on large datasets that include sensitive patient details such as medical histories, images, and treatment records. Protecting privacy requires strict ethical practices in how these data are collected, stored, and used[89]
3. Bias – Bias in AI poses a major ethical issue in ophthalmology. If algorithms are trained on unrepresentative datasets, they risk reinforcing inequalities and widening gaps in patient outcomes and access to eye care[90]
4. Data quality and representativeness – The effectiveness of AI in ophthalmology depends heavily on the quality and diversity of training datasets. Low-quality or nonrepresentative data can lead to poor model performance and limit generalizability across different patient populations[19]
5. Regulatory and legal challenges – Many AI systems in ophthalmology remain in the research stage without full clinical validation or regulatory approval. Unresolved issues around liability in cases of misdiagnosis and patient harm, along with evolving evaluation frameworks from regulatory authorities, present significant barriers to safe and widespread adoption[91]
6. The "black-box" problem – Many AI systems in ophthalmology function as opaque models, making it difficult to understand how inputs are transformed into outputs. This lack of transparency reduces trust among clinicians and patients.[92] While complex "black-box" algorithms often deliver higher accuracy in image analysis compared to simpler "white-box" models, they sacrifice interpretability.

Future directions

AI has the potential to transform medicine by enabling new discoveries through neural networks and hypothesis generation. To realize this promise, generative models must undergo rigorous testing on large, diverse datasets to ensure accuracy and reliability. Equally important is the establishment of strong governance and evaluation frameworks to safeguard against risks such as misleading or fake data analyses, ensuring AI contributes safely and effectively to healthcare.

CONCLUSION

AI is rapidly reshaping ophthalmology, offering innovative solutions for early detection, accurate diagnosis, and personalized treatment across a wide spectrum of eye diseases. From cataract and glaucoma to keratoconus, diabetic retinopathy, and ROP, AI demonstrates strong potential to improve clinical outcomes and reduce preventable vision loss. However, challenges such as ethical concerns, data privacy, bias, regulatory approval, and the "black-box" problem highlight the need for caution and accountability. Moving forward, rigorous validation, transparent governance, and explainable models will be essential to ensure AI evolves into a trusted, equitable, and transformative tool in global eye care.

Financial support and sponsorship

Nil.

Conflicts of interest

There are no conflicts of interest.

REFERENCES

1. Hamet P, Tremblay J. Artificial intelligence in medicine. Metabolism 2017;69S: S36-40.
2. Obermeyer Z, Emanuel EJ. Predicting the future – Big data, machine learning, and clinical medicine. N Engl J Med 2016;375:1216-9.
3. Simplilearn. Types of Artificial Intelligence Explained; 2025. Available from: https://www.simplilearn.com/tutorials/artificialintelligence tutorial/typesofartificialintelligence. [Last cited on 2026 Jan 24].
4. IBM Think. Understanding the Types of AI; 2024. Available from: https:// www.ibm.com/think/topics/artificial intelligencetypes. [Last cited on 2026 Jan 25].
5. Lumenalta. What are the Different Types of AI? Available from: https:// lumenalta.com/insights/whatarethe differenttypesofai. [Last cited on 2026 Jan 25].
6. IBM. Deep Blue: The Computer That Beat Kasparov. Armonk, NY: IBM Research; 1997.
7. Ting DS, Lee AY, Wong TY. An ophthalmologist's guide to deciphering studies in artificial intelligence. Ophthalmology 2019;126:1475-9.
8. Roach L. Artificial Intelligence. EyeNet Magazine; 2017. Available from: https://www.aao.org/eyenet/article/artificialintelligence. [Last cited on 2026 Jan 25].
9. Li Z, Wang L, Wu X, Jiang J, Qiang W, Xie H, *et al*. Artificial intelligence in ophthalmology: The path to the real-world clinic. Cell Rep Med 2023;4:101095.
10. Srivastava O, Tennant M, Grewal P, Rubin U, Seamone M. Artificial intelligence and machine learning in ophthalmology: A review. Indian J Ophthalmol 2023;71:11-7.
11. Amisha, Malik P, Pathania M, Rathaur VK. Overview of artificial intelligence in medicine. J Family Med Prim Care 2019;8:2328-31.
12. Cull J, Brevetta R, Gerac J, Kothari S, Blackhurst D. Epic sepsis model inpatient predictive analytic tool: A validation study. Crit Care Explor 2023;5:e0941.
13. Beaubier N, Bontrager M, Huether R, Igartua C, Lau D, Tell R, *et al*. Integrated genomic profiling expands clinical options for patients with cancer. Nat Biotechnol 2019;37:1351-60.

14. Tran KA, Kondrashova O, Bradley A, Williams ED, Pearson JV, Waddell N. Deep learning in cancer diagnosis, prognosis and treatment selection. Genome Med 2021;13:152.
15. Tak D, Garomsa BA, Chaunzwa TL, Zapaishchykova A, Climent Pardo JC, Ye Z, *et al*. A foundation model for generalized brain MRI analysis [Preprint]. medRxiv. 2024 Dec 2. doi:10.1101/2024.12.02.24317992.
16. Lim J, Lee HS, Han GI, Kang S, Jang JH, Jo YY, *et al*. Artificial intelligence-enhanced six-lead portable electrocardiogram device for detecting left ventricular systolic dysfunction: A prospective single-centre cohort study. Eur Heart J Digit Health 2025;6:476-85.
17. Tomašev N, Glorot X, Rae JW, Zielinski M, Askham H, Saraiva A, *et al*. A clinically applicable approach to continuous prediction of future acute kidney injury. Nature 2019;572:116-9.
18. Hashemian H, Peto T, Ambrósio R Jr., Lengyel I, Kafieh R, Muhammed Noori A, *et al*. Application of artificial intelligence in ophthalmology: An updated comprehensive review. J Ophthalmic Vis Res 2024;19:354-67.
19. Jin K, Ye J. Artificial intelligence and deep learning in ophthalmology: Current status and future perspectives. Adv Ophthalmol Pract Res 2022;2:100078.
20. Wang Z, Keane PA, Chiang M, Cheung CY, Wong TY, Ting DS. Artificial intelligence and deep learning in ophthalmology. Artif Intell Med 2022;13:1519-52.
21. Burton MJ, Ramke J, Marques AP, Bourne RR, Congdon N, Jones I, *et al*. The lancet global health commission on global eye health: Vision beyond 2020. Lancet Glob Health 2021;9:e489-551.
22. Holden BA, Wilson DA, Jong M, Sankaridurg P, Fricke TR, Smith EL III, *et al*. Myopia: A growing global problem with sight-threatening complications. Community Eye Health 2015;28:35.
23. Lin H, Long E, Ding X, Diao H, Chen Z, Liu R, *et al*. Prediction of myopia development among Chinese school-aged children using refraction data from electronic medical records: A retrospective, multicentre machine learning study. PLoS Med 2018;15:e1002674.
24. Chen H, McCann P, Lien T, Xiao M, Abraham AG, Gregory DG, *et al*. Prevalence of dry eye and Meibomian gland dysfunction in Central and South America: A systematic review and meta-analysis. BMC Ophthalmol 2024;24:50.
25. Vicnesh J, Oh SL, Wei JK, Ciaccio EJ, Chua KC, Tong L, *et al*. Thoughts concerning the application of thermogram images for automated diagnosis of dry eye-a review. Infrared Phys Technol 2020;106:1350-4495.
26. Harti ME, Andaloussi SJ, Ouchetto O. A comprehensive review comparing artificial intelligence and clinical diagnostic approaches for dry eye disease. Diagnostics (Basel) 2025;15:3071.
27. Shah S, Rana D, Purohit D, Malhotra S. Evaluation of therapeutic modalities and outcome in patients of infectious keratitis: A prospective observational study at a tertiary care eye hospital. Natl J Integr Res Med 2021;12:32-9.
28. Zhang Z, Wang Y, Zhang H, Samusak A, Rao H, Xiao C, et al. Artificial intelligence-assisted diagnosis of ocular surface diseases. Front Cell Dev Biol. 2023;11:1133680.
29. Vupparaboina KK, Vedula SN, Aithu S, Bashar SB, Challa K, Loomba A, *et al*. Artificial intelligence based detection of infectious keratitis using slit-lamp images. Investig Ophthalmol Vis Sci 2019;60:4236.
30. Lv J, Zhang K, Chen Q, Chen Q, Huang W, Cui L, *et al*. Deep learning-based automated diagnosis of fungal keratitis with *in vivo* confocal microscopy images. Ann Transl Med 2020;8:706.
31. Kuo MT, Hsu BW, Lin YS, Fang PC, Yu HJ, Chen A, *et al*. Comparisons of deep learning algorithms for diagnosing bacterial keratitis via external eye photographs. Sci Rep 2021;11:24227.
32. Li Z, Jiang J, Chen K, Chen Q, Zheng Q, Liu X, *et al*. Preventing corneal blindness caused by keratitis using artificial intelligence. Nat Commun 2021;12:3738.
33. Won YK, Lee H, Kim Y, Han G, Chung TY, Ro YM, *et al*. Deep learningbased classification system of bacterial keratitis and fungal keratitis using anterior segment images. Front Med (Lausanne) 2023;10:1162124.
34. Hou H, Cao Y, Cui X, Liu Z, Xu H, Wang C, *et al*. Medical image management and analysis system based on web for fungal keratitis images. Math Biosci Eng 2021;18:3667-79.
35. Liu Z, Cao Y, Li Y, Xiao X, Qiu Q, Yang M, *et al*. Automatic diagnosis of fungal keratitis using data augmentation and image fusion with deep convolutional neural network. Comput Methods Programs Biomed 2020;187:105019.
36. Kelly TL, Williams KA, Coster DJ, Australian Corneal Graft Registry. Corneal transplantation for keratoconus: A registry study. Arch Ophthalmol 2011;129:691-7.
37. Hwang ES, Perez-Straziota CE, Kim SW, Santhiago MR, Randleman JB. Distinguishing highly asymmetric keratoconus eyes using combined Scheimpflug and spectral-domain OCT analysis. Ophthalmology 2018;125:1862-71.
38. Kamiya K, Ayatsuka Y, Kato Y, Fujimura F, Takahashi M, Shoji N, *et al*. Keratoconus detection using deep learning of colour-coded maps with anterior segment optical coherence tomography: A diagnostic accuracy study. BMJ Open 2019;9:e031313.
39. Al-Timemy AH, Ghaeb NH, Mosa ZM, Escudero J. Deep transfer learning for improved detection of keratoconus using corneal topographic maps. Cognit Comput. 2022;14:1627-42. doi:10.1007/s12559-021-09880-3.
40. Ruiz Hidalgo I, Rodriguez P, Rozema JJ, Ní Dhubhghaill S, Zakaria N, Tassignon MJ, *et al*. Evaluation of a machine-learning classifier for keratoconus detection based on Scheimpflug tomography. Cornea 2016;35:827-32.
41. Arbelaez MC, Versaci F, Vestri G, Barboni P, Savini G. Use of a support vector machine for keratoconus and subclinical keratoconus detection by topographic and tomographic data. Ophthalmology 2012;119:2231-8.
42. Zhang P, Yang L, Mao Y, Zhang X, Cheng J, Miao Y, *et al*. CorNet: Autonomous feature learning in raw Corvis ST data for keratoconus diagnosis via residual CNN approach. Comput Biol Med 2024;172:108286.
43. Lim EW, Lim L. Review of preoperative tomographic and biomechanical corneal assessment for refractive surgery. Taiwan J Ophthalmol. 2025;15:1-12. doi:10.4103/tjo.TJO-D-24-00147.
44. Kundu G, Shetty R, D'Souza S, Khamar P, Nuijts RM, Sethu S, *et al*. A novel combination of corneal confocal microscopy, clinical features and artificial intelligence for evaluation of ocular surface pain. PLoS One 2022;17:e0277086.
45. Feizi S, Javadi MA, Bayat K, Arzaghi M, Rahdar A, Ahmadi MJ. Machine learning methods to identify risk factors for corneal graft rejection in keratoconus. Sci Rep 2024;14:29131.
46. Rampat R, Deshmukh R, Chen X, Ting DS, Said DG, Dua HS, *et al*. Artificial intelligence in cornea, refractive surgery, and cataract: Basic principles, clinical applications, and future directions. Asia Pac J Ophthalmol (Phila) 2021;10:268-81.
47. Lopes BT, Ramos IC, Salomão MQ, Guerra FP, Schallhorn SC, Schallhorn JM, *et al*. Enhanced tomographic assessment to detect corneal ectasia based on artificial intelligence. Am J Ophthalmol 2018;195:223-32.
48. Saad A, Gatinel D. Topographic and tomographic properties of forme fruste keratoconus corneas. Invest Ophthalmol Vis Sci 2010;51:5546-55.
49. Fang R, Yu YF, Li EJ, Lv NX, Liu ZC, Zhou HG, *et al*. Global, regional, national burden and gender disparity of cataract: Findings from the global burden of disease study 2019. BMC Public Health 2022;22:2068.
50. Nuliqiman M, Xu M, Sun Y, Cao J, Chen P, Gao Q, *et al*. Artificial intelligence in ophthalmic surgery: Current applications and expectations. Clin Ophthalmol 2023;17:3499-511.
51. Ladas J, Ladas D, Lin SR, Devgan U, Siddiqui AA, Jun AS. Improvement of multiple generations of intraocular lens calculation formulae with a novel approach using artificial intelligence. Transl Vis Sci Technol 2021;10:7.

52. Stopyra W, Grzybowski A. Innovations in intraocular lens power calculation-a review. J Clin Med 2025;14:6585.
53. Zhou Y, Dai M, Sun L, Tang X, Zhou L, Tang Z, *et al*. The accuracy of intraocular lens power calculation formulas based on artificial intelligence in highly myopic eyes: A systematic review and network metaanalysis. Front Public Health 2023;11:1279718.
54. Lindegger DJ, Wawrzynski J, Saleh GM. Evolution and applications of artificial intelligence to cataract surgery. Ophthalmol Sci 2022;2:100164.
55. Mohammadi SF, Hashemi H, Mazouri A, Rahman AN, Ashrafi E, Mehrjardi HZ, *et al*. Outcomes of cataract surgery at a referral center. J Ophthalmic Vis Res 2015;10:250-6.
56. Anderson RL, de Los Angeles Ramos Cadena M, Schuman JS. Glaucoma diagnosis: From the artisanal to the defined. Ophthalmol Glaucoma 2018;1:3-14.
57. Lan CH, Chiu TH, Yen WT, Lu DW. Artificial intelligence in glaucoma: Advances in diagnosis, progression forecasting, and surgical outcome prediction. Int J Mol Sci 2025;26:4473.
58. Phene S, Dunn RC, Hammel N, Liu Y, Krause J, Kitade N, *et al*. Deep learning and glaucoma specialists: The relative importance of optic disc features to predict glaucoma referral in fundus photographs. Ophthalmology 2019;126:1627-39.
59. Hood DC, La Bruna S, Tsamis E, Thakoor KA, Rai A, Leshno A, *et al*. Detecting glaucoma with only OCT: Implications for the clinic, research, screening, and AI development. Prog Retin Eye Res 2022;90:101052.
60. Mohammadzadeh V, Wu S, Besharati S, Yousefi S, Caprioli J. Prediction of visual field progression with baseline and longitudinal structural measurements using deep learning. Am J Ophthalmol 2024;262:141-52.
61. Salazar H, Misra V, Swaminathan SS. Artificial intelligence and complex statistical modeling in glaucoma diagnosis and management. Curr Opin Ophthalmol 2021;32:105-17.
62. Liu H, Li L, Wormstone IM, Qiao C, Zhang C, Liu P, *et al*. Development and validation of a deep learning system to detect glaucomatous optic neuropathy using fundus photographs. JAMA Ophthalmol 2019;137:1353-60.
63. Hu X, Zhang LX, Gao L, Dai W, Han X, Lai YK, *et al*. GLIM-Net: Chronic glaucoma forecast transformer for irregularly sampled sequential fundus images. IEEE Trans Med Imaging 2023;42:1875-84.
64. Wu CW, Shen HL, Lu CJ, Chen SH, Chen HY. Comparison of different machine learning classifiers for glaucoma diagnosis based on spectralis OCT. Diagnostics (Basel) 2021;11:1718.
65. Hou K, Bradley C, Herbert P, Wang SY, Lin K. Predicting visual field worsening with longitudinal OCT data using a gated transformer network. Ophthalmology 2023;130:854-62.
66. Dixit A, Yohannan J, Boland MV. Assessing glaucoma progression using machine learning trained on longitudinal visual field and clinical data. Ophthalmology 2021;128:1016-26.
67. Banna HU, Zanabli A, McMillan B, Shalaby A, El-Sayed AM. Evaluation of machine learning algorithms for trabeculectomy outcome prediction in patients with glaucoma. Sci Rep 2022;12:2473.
68. Abràmoff MD, Lavin PT, Birch M, Shah N, Folk JC. Pivotal trial of an autonomous AI-based diagnostic system for detection of diabetic retinopathy in primary care offices. NPJ Digit Med 2018;1:39.
69. Wu K, Wu E, Theodorou B, LiangW, Mack C, Glass L, *et al*. Characterizing the clinical adoption of medical AI devices through U.S. Insurance claims. NEJM AI 2023;1:11.
70. Joseph S, Selvaraj J, Mani I, Kumaragurupari T, Shang X, Mudgil P, *et al*. Diagnostic accuracy of artificial intelligence-based automated diabetic retinopathy screening in real-world settings: A systematic review and meta-analysis. Am J Ophthalmol 2024;263:214-30.
71. Wong WL, Su X, Li X, Cheung CM, Klein R, Cheng CY, *et al*. Global prevalence of age-related macular degeneration and disease burden projection for 2020 and 2040: A systematic review and meta-analysis. Lancet Glob Health 2014;2:e106-16.
72. Yoo TK, Choi JY, Seo JG, Ramasubramanian B, Selvaperumal S, Kim DW. The possibility of the combination of OCT and fundus images for improving the diagnostic accuracy of deep learning for age-related macular degeneration: A preliminary experiment. Med Biol Eng Comput 2019;57:677-87.
73. Chen Q, Leng T, Zheng L, Kutzscher L, Ma J, de Sisternes L, *et al*. Automated drusen segmentation and quantification in SD-OCT images. Med Image Anal 2013;17:1058-72.
74. Pfau M, Sahu S, Rupnow RA, Romond K, Millet D, Holz FG, *et al*. Probabilistic Forecasting of anti-VEGF treatment frequency in neovascular age-related macular degeneration. Transl Vis Sci Technol 2021;10:30.
75. Pertiwi A, Dian EY, Yeni DL. The use of artificial intelligence for diagnosing retinopathy of prematurity – A systematic review. Int J Retina. 2025;8:316. doi:10.35479/ijretina.2025.vol008.iss002.316.
76. Campbell JP, Singh P, Redd TK, Brown JM, Shah PK, Subramanian P, *et al*. Applications of artificial intelligence for retinopathy of prematurity screening. Pediatrics 2021;147:e2020016618.
77. Chiang MF, Jiang L, Gelman R, Du YE, Flynn JT. Interexpert agreement of plus disease diagnosis in retinopathy of prematurity. Arch Ophthalmol 2007;125:875-80.
78. Greenwald MF, Danford ID, Shahrawat M, Ostmo S, Brown J, Kalpathy-Cramer J, *et al*. Evaluation of artificial intelligence-based telemedicine screening for retinopathy of prematurity. J AAPOS 2020;24:160-2.
79. Ramanathan A, Athikarisamy SE, Lam GC. Artificial intelligence for the diagnosis of retinopathy of prematurity: A systematic review of current algorithms. Eye (Lond) 2023;37:2518-26.
80. Jin K, Li Y, Wu H, Tham YC, Koh V, Zhao Y, *et al*. Integration of smartphone technology and artificial intelligence for advanced ophthalmic care: A systematic review. Adv Ophthalmol Pract Res 2024;4:120-7.
81. Natarajan S, Jain A, Krishnan R, Rogye A, Sivaprasad S. Diagnostic accuracy of community-based diabetic retinopathy screening with an offline artificial intelligence system on a smartphone. JAMA Ophthalmol 2019;137:1182-8.
82. Young BK, Cole ED, Shah PK, Ostmo S, Subramaniam P, Venkatapathy N, *et al*. Efficacy of smartphone-based telescreening for retinopathy of prematurity with and without artificial intelligence in India. JAMA Ophthalmol 2023;141:582-8.
83. Nakahara K, Asaoka R, Tanito M, Shibata N, Mitsuhashi K, Fujino Y, *et al*. Deep learning-assisted (automatic) diagnosis of glaucoma using a smartphone. Br J Ophthalmol 2022;106:587-92.
84. Wu Y, Luttrell I, Feng S, Chen PP, Spaide T, Lee AY, *et al*. Development and validation of a machine learning, smartphone-based tonometer. Br J Ophthalmol 2020;104:1394-8.
85. Hu S, Wang X, Wu H, Luan X. Unified diagnosis framework for automated nuclear cataract grading based on smartphone slit-lamp images. IEEE Access 2020;8:174169-78.
86. Murali K, Krishna V, Krishna V, Kumari B. Application of deep learning and image processing analysis of photographs for amblyopia screening. Indian J Ophthalmol 2020;68:1407-10.
87. Tabuchi H, Nagasato D, Masumoto H, Tanabe M, Ishitobi N, Ochi H, *et al*. Developing an iOS application that uses machine learning for the automated diagnosis of blepharoptosis. Graefes Arch Clin Exp Ophthalmol 2022;260:1329-35.
88. UNESCO. Recommendation on the Ethics of Artificial Intelligence. Paris: UNESCO; 2023.
89. Chatterjee S, Sreenivasulu NS. Personal data sharing and legal issues of human rights in the era of artificial intelligence: Moderating effect of government regulation. Int J Electron Gov Res 2019;15:21-36.
90. Mittermaier M, Raza MM, Kvedar JC. Bias in AI-based models for medical applications: Challenges and mitigation strategies. NPJ Digit Med 2023;6:113.
91. Alowais SA, Alghamdi SS, Alsuhebany N, Alqahtani T, Alshaya AI, Almohareb SN, *et al*. Revolutionizing healthcare: The role of artificial intelligence in clinical practice. BMC Med Educ 2023;23:689.
92. Evans NG, Wenner DM, Cohen IG, Purves D, Chiang MF, Ting DS, *et al*. Emerging ethical considerations for the use of artificial intelligence in ophthalmology. Ophthalmol Sci 2022;2:100141.

Original Article

Evaluation of Structure–function Correlation Using Tablet Perimetry, Standard Perimetry, and Optical Coherence Tomography in Early Glaucoma

ABSTRACT

Purpose: The purpose of the study was to detect functional visual field changes using tablet perimetry with Melbourne Rapid Field (MRF) application and White-on-White perimetry using Humphrey Field analyzer and to correlate them with structural change on Spectral-domain Optical Coherence Tomography (SD-OCT) in patients with early glaucoma.

Methods: This cross-sectional observational study enrolled 44 participants with early glaucoma. All underwent HVF 24-2 SITA-FAST, MRF tablet perimetry (Version 3.0), and SD-OCT imaging at baseline and 6 months. The main outcome measures were association and correlation between MRF, HVF, and SD-OCT parameters. The previously published regression equation was subsequently used to model MRF MD values. Additional analysis included Bland–Altman agreement analysis for global indices, Lin's concordance coefficient, and intraclass correlation coefficients (ICC).

Results: Spearman coefficients showed a mild/moderate correlation between HVF and MRF global indices. Regression-adjusted MRF-MD values showed a high correlation with HVF MD. ICC for MRF and HVF MD ranged from 0.59 to 0.60. However, for regression-adjusted MRF MD values, the ICC was higher. For repeatability of outcomes, MRF-MD and HVF-MD were similar. For structure–function correlation at baseline and 6 months, MRF-MD showed mild correlation with retinal nerve fiber layer (RNFL) average thickness (0.34, 0.27) versus HVF-MD (0.29, 0.19). Regression-adjusted MRF correlated better with OCT values (0.43 and 0.33).

Conclusion: Regression-adjusted MRF-MD correlates well with HVF-MD. Direct output of MRF requires careful evaluation when used in conjunction with HVF testing. Both MRF and HVF also show a weak correlation with RNFL average thickness values. This indicates the need for both structural and functional tests while evaluating a glaucoma patient for a comprehensive evaluation.

Keywords: Melbourne rapid field, MRFg, SAP, white-on-white perimetry

INTRODUCTION

Glaucoma is an irreversible cause of blindness, which is characterized by structural damage to the retinal ganglion cells and their axons, and characteristic optic neuropathy with corresponding abnormalities of the visual field (VF).[1] As the "*silent thief of sight*," glaucoma already causes moderate-to-advanced VF loss in 41%–50% of all newly detected patients in Western nations at the time of the diagnosis.[2] Even with frequent follow-ups, 15.5% of glaucoma patients receiving treatment develop unilateral blindness, with 15.2% progressing in 2 years despite treatment.[3] More than 90% of cases of glaucoma remain undiagnosed in the community.[4] Only by

Access this article online	
Website: https://journals.lww.com/saao	Quick Response Code
DOI: 10.4103/SAOJ.SAOJ_8_26	

Itisha Goel, Parul Ichhpujani, Sahil Thakur[1], Uday Pratap Singh Parmar[2], Suresh Kumar Gupta

Department of Ophthalmology, Government Medical College and Hospital, Chandigarh, India, [1]Department of Ocular Epidemiology, Singapore Eye Research Institute, Singapore, [2]Department of Ophthalmology, Massachusetts Eye and Ear, Harvard Medical School, Boston, MA, USA

Address for correspondence: Dr. Parul Ichhpujani, Department of Ophthalmology, Government Medical College and Hospital, Sector-32, Chandigarh, India.
E-mail: parul77@rediffmail.com

Submitted: 26-01-2026 **Revised:** 27-01-2026
Accepted: 06-02-2026 **Published:** ***

How to cite this article: Goel I, Ichhpujani P, Thakur S, Parmar UP, Kumar S. Evaluation of structure–function correlation using tablet perimetry, standard perimetry, and optical coherence tomography in early glaucoma. South Asian Acad Ophthalmol J 2026;XX:XX-XX.

community and opportunistic screening can glaucoma suspects be identified early and treated timely. Following a diagnosis, it is necessary to undergo testing and follow-up visits for the rest of one's life to track the disease's development and customize treatment to lower the likelihood of permanent vision loss. As per the World Glaucoma Association (WGA) consensus guidelines, one structure and function assessment test is needed both for diagnosis and follow-up. The 8th WGA consensus meeting on "Progression of Glaucoma" says that glaucomatous optic neuropathy can progress structurally in the absence of functional progression and vice-versa.[5] Standard Automated Perimetry (SAP) using Humphrey Field analyzer (HFA) provides reliable, accurate, and reproducible VF in glaucoma patients, but it is expensive equipment with a large footprint, lacks portability, and therefore cannot be used for mass screening or in resource-deficient areas. With the evolution of virtual imaging, innovative yet handy technologies for glaucoma testing have bridged the gap between extensive clinical setups and communities in the periphery. Novel technologies have shifted attention from static testing methods to faster and portable methods that are likely to alter the paradigm of VF assessment.[6] Numerous imaging tools, such as scanning laser polarimetry, confocal scanning laser ophthalmoscopy, and spectral domain optical coherence tomography (SD-OCT), objectively give repeatable measurements and quantitative assessment of the optic disc and retinal nerve fiber layer (RNFL) change. The most used tool for structural assessment is SD-OCT, which produces a variety of cross-sectional pictures to measure the thickness of the RNFL. Literature is deficient as regards structure–function correlation between test results of SAP, tablet-based perimetry using Melbourne Rapid Field (MRF) application, and SD-OCT. If a concrete relationship is established, then tablet perimetry can be used as a reliable diagnostic modality, especially in the current and coming times when the use of bowl perimeter, such as the HFA, may be restricted due to increased risk of coronavirus disease 2019 or other respiratory viral infections. The current study is the first Indian study that attempts to ascertain the structure–function correlation in the North Indian population with early glaucoma using tablet perimetry with MRF application and SAP using HFA and SD-OCT.

METHODS

Study design

The current study was a hospital-based longitudinal, observational study conducted on the outpatients visiting the glaucoma services of a tertiary care center. Written informed consent was taken from all the participants before enrollment. The study adhered to the tenets of the Declaration of Helsinki and was approved by the Institutional Ethics Committee.

Sample size

The optimum sample size for the present cross-sectional study was calculated by taking minimum acceptable reliability and expected reliability between the two techniques, i.e., MRF application and HFA as 0.5 and 0.8, respectively, as per the study by Prea *et al*.,[7] with a significance level of 0.05 (two-tailed) and 90% power with several rates per subject as 2, and with 10% dropout rate, the minimum sample size required was 42.

The inclusion criteria for the study participants were patients with mild Primary open angle glaucoma (POAG) as per the Hodapp–Anderson–Parrish (HAP)[8] criteria, age 18 years or older, of either gender, best-corrected visual acuity (BCVA) >6/12 (20/40) or better, the spherical equivalent refractive error between −4 diopters (D) and +4D, and astigmatism ≤2.5D. A patient was labeled as having "glaucoma" in the presence of reproducible VF defects on the HFA 24-2 SITA-Fast program with corresponding structural defects in the optic disc on clinical examination in at least one eye. Each patient had undergone an average of 4 previous VFs to address the impact of the learning effect on VFs.

The exclusion criteria included patients with cataracts (nuclear sclerosis equal to or more than Grade 2 using LOCS III grading),[1] corneal opacity or degeneration, history of trauma or recent ophthalmic surgery, ocular inflammatory condition such as uveitis, history of diabetes, and concomitant retinal or macular disease. Any medical condition that precluded the patient from providing reliable and valid data (e.g., cognitive impairment, Parkinson's disease, Alzheimer's disease, and any other neurological or musculoskeletal disease). Any patient with an abnormal appearing disc, such as a tilted disc or congenital disc anomalies, was also excluded from the study.

Methodology

A careful, detailed history was taken in all cases. The patient's current symptoms, health problems, medications, and ocular comorbidities were also documented. The ocular examination consisted of documentation of the uncorrected visual acuity and BCVA using Snellen's visual acuity charts. Slit-lamp bio-microscopy of the anterior segment and fundus examination using a +90D lens and optic disc damage assessment. Measurement of intraocular pressure (IOP) was done using calibrated Goldmann Applanation tonometry (GAT). The VFs were considered satisfactory if false positive (FP) and false negative (FN) errors did not exceed 30% and fixation losses did not exceed 20%.

Procedure

All subjects underwent standard white-on-white perimetry on Humphrey's Field Analyzer HFA 750 II (Carl Zeiss-Humphrey

Systems, Dublin, California, USA), using the 24-2 SITA-Fast strategy using Stimulus Size 3. The test was carried out in a darkened room and took about 10 min per eye. The patient looked into the part of the instrument that consisted of a large semi-circular bowl covering their entire field of view. The instrument presented a series of stimuli (spots of light), one at a time, at a range of contrast levels at varying locations in the VF, whereas the patient fixated on a central point. The patient responded by clicking a button when a stimulus was detected. This process yielded a map of the parts of the patient's field of view; this map was subjected to statistical analysis comparing a patient's results to normative values for people with healthy vision.

The MRF application allowed assessment in two modes: A full threshold test of 4–5 min duration per eye and a screening test of approximately 90 s duration. The MRF perimeter software used a modified 24-2 grid, or a full test centered at fixation, which tests 30° ×20° of the VF, equivalent to the HFA 24-2 program. MRF used blind spot monitoring by presenting stimuli to the blind spot to estimate fixation accuracy during central fixation testing. In the radial pattern full test, 66 locations were used. The software controlled the difference in number and location as per the selected test. As the screen size was small, subtending around 15° ×12°, the patient had to fixate on the four corners of the screen at different times to gain eccentricities out to 30°. The spot size was increased with eccentricity to account for the tangent effect of the flat screen and to produce a fixed threshold across the central field (instead of a hill of vision). Targets were presented for 300 ms. It also provided audio commands that reminded participants to maintain fixation on the red fixation target. Fixation monitoring was done using a blind spot monitor with a 19 dB stimulus, which was nearly 40% larger in area than the Goldmann size II spot. Testing was performed by charting the blind spot at the beginning of each test, and a stimulus was presented in that location throughout the test using central fixation. FP and FN checks were presented throughout the test. FP checks were conducted by interspacing periods (1000–1400 ms) throughout the test, during which no stimulus was presented on the screen. An FP was recorded if the patient gave a response during that period.

The MRF software comes in several formats, and here we report findings for the MRF-glaucoma (MRF Glaucoma Lite, MRGg) version of this application. In short, MRFg is an application available for the Apple iPad (Apple, Cupertino, USA) that can be used by participants distant to the clinic in a self-monitoring mode.

Voice prompts for the test procedure were provided in multiple languages by the iPad software to guide the patient during the test. In the present study, we used an 11-inch iPad iOS 16.1 version, and voice prompts for all patients were provided in English. The response of the patient to the presentation of a stimulus was recorded by touching the screen or the spacebar on a Bluetooth keyboard connected to the iPad device. Touching the spacebar on the Bluetooth keyboard method was used in the current study to prevent smudging of the screen with fingerprints. The screen and keyboard were sanitized after each use [Figure 1].

One eye of each patient was randomly included in the study. Since all patients were new to MRF iPad-based perimeter software, two trial tests were given to the patients. Testing was performed in a dark room free from distractions, with undilated pupils, and the patient wore his/her habitual reading glasses (mono-focal, bifocal, or progressive) for normal near vision. When testing monocularly, the other eye was covered with an eye patch.

Before commencing the perimetry, the patients were given instructions in their vernacular language. The patient was seated comfortably, and the iPad tablet was placed in a customized plastic viewing chamber with a headrest maintaining a 33 cm viewing distance and the accompanying Bluetooth keyboard. The fellow eye was occluded. The iPad screen intensity was automatically set to 100% for each test by the software, and the iPad was turned on for at least 10 min before testing to ensure the stability of the luminous output.

Color-coded indicator in the MRF printout was classified as "Green" within normal limits (95% of normal), "Amber" borderline (<5% of normal), and "Red" outside normal limits (<1% of normal). FT on the printout stands for the foveal threshold [Figure 2].

In some MRF printouts, two values appear for mean Deviation, MD (dB), and an MRF MD (dB) (as an under-script). In such cases, MD (dB) refers to the value that has been adjusted using a correction factor (given by the developer), which approximates HFA MD (dB). MRF MD (dB), on the other hand, is the raw MD calculated from the MRF results before correction. For the sake of uniformity, we used the MD that was adjusted using the correction factor and was corrected for spot size and placement. MRF has spots in different locations (grid pattern), and MRF spots increase in size into the periphery. Therefore, MRF-MD will underestimate HFA MD, so a corrected MD is provided by the system.

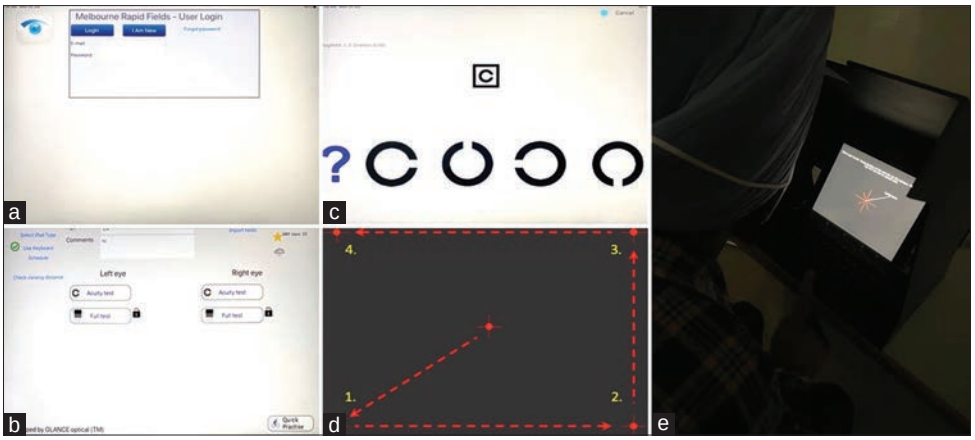

Figure 1: (a) Format of Melbourne Rapid Field (MRF) Login, (b) Overall MRF test display on iPad, (c) Visual acuity test, (d) Fixation changes during MRF testing, (e) Depiction of MRF test with patient's head over the headrest and index finger on the spacebar of the keyboard

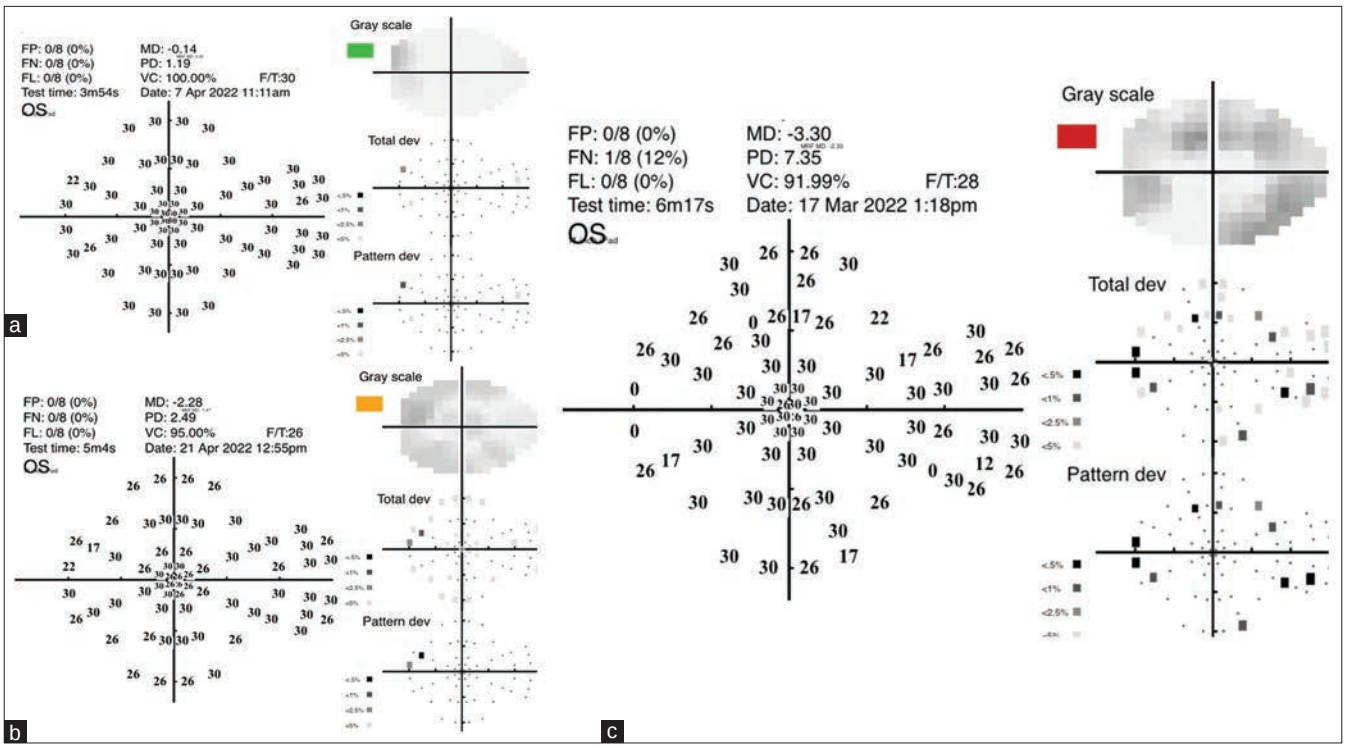

Figure 2: Color-coded indicator in the Melbourne rapid field (a) "Green" within normal limits (95% of normal) (b) "Amber" borderline (<5% of normal), (c) "Red" outside normal limits (<1% of normal)

MD: −0.31 (corrected value)
Melbourne rapid field MD: 0.20 (raw value)

Each patient underwent MRF iPad perimetry and HFA 24-2 SITA Fast perimetric testing on the same day, with a time interval of at least half an hour after the MRF iPad perimetry test. Study eyes did not undergo tonometry before field testing. These tests were repeated 6 months after enrolment.

RNFL thickness was measured using SD-OCT (Cirrus 5000, Carl Zeiss Meditec AG). Optic Disc Cube 200 × 200 protocol of Cirrus HD-OCT version 5.0.0.326 was used for scan acquisition. After each examination, image quality and the automatic segmentation of Bruch's membrane and ILM were manually reviewed. Data with a signal strength of < 6 were not considered. The RNFL parameter evaluated was the global RNFL average thickness (in micrometers).

Statistical analysis

Data were entered in a Microsoft Excel spreadsheet and analyzed using SYSTAT Software Inc. SYSTAT Software, Version 13.0. San Jose (CA) for Windows. Quantitative data were presented as mean and standard deviation (median and interquartile range for skewed/nonnormal data). Normality was checked using the Kolmogorov–Smirnov test.

Qualitative data were presented as ratios and proportions. For qualitative data, the Chi-square test was used to see the association between variables. Normally distributed quantitative data were analyzed using a *t*-test, and the Mann–Whitney *U*-test was used for nonnormal quantitative data. Spearman's correlation coefficient was used to see the correlation between quantitative variables. Lin's concordance coefficient was also calculated. Bland–Altman analysis was done to evaluate the limit of agreement between MRF-MD and HVF-MD. Intraclass correlation coefficient (ICC) was also calculated for our data. $P < 0.05$ was taken as a point of statistical significance.

RESULTS

Fifty treatment-naïve mild glaucoma patients were recruited, but due to the dropout of 2 participants for follow-up visits and unreliable data of 4 patients, despite repeated testing, data of only 44 participants were analyzed. All were started on a topical prostaglandin analog, Travoprost 0.004%, at bedtime after diagnosis. Additional drugs were added as per the IOP response. The mean age for the patients was 63.81 ± 11.31 years. Thirty-four (77.27%) were males, and ten (22.73%) were females. The baseline demographic characteristics are summarized in Table 1.

Tables 2 shows the comparison of VF test parameters for MRF, HVF 24-2 SITA-Fast program, and SD-OCT RNFL thickness. Table 3 shows the correlation between HVF, MRF, and average RNFL thickness at baseline and 6 months.

There was a poor correlation between HVF MD, PSD (dB), and raw, unadjusted MRF MD, PSD data (dB) at baseline and 6 months.

We modeled the MRF-MD values using the regression equation published previously.[7] This regression-adjusted MRF-MD was also compared while evaluating outcomes [Table 4].

There was a strong positive correlation between HVF-MD and regression-adjusted MRF-MD after using the regression equation. Therefore, we also suggest using this regression equation when considering the extrapolation of MRF data for analysis or comparison with VHF data. Structure and function correlation was also evaluated for our data using SD-OCT-average RNFL thickness. There was a weak, positive correlation between MRF-VC, HVF, and OCT Average RNFL. The correlation was slightly better with HVF-VFI than with MRF-VC.

Tables 5 and 6 show nil/poor concordance between HVF-MD and unadjusted MRF-MD, with wide limits of agreement and large bias. On adjustment using the regression equation, there is a "substantial" concordance between MRF-MD and HVF-MD. We also compared how the two tests performed successively at baseline and 6 months [Table 7]. MRF-MD had a lesser bias, higher concordance, and higher ICC than HVF-MD. Other indices from MRF also have better ICC than HVF indices. Figures 3 and 4 are visual field outcomes of two representative cases.

Table 1: Summary of baseline demographic and clinical data

Baseline data	Mean±SD (*n*=44), *n* (%)
Mean age	63.81±11.31 years
Mean age of males	61.86±12.82 years
Mean age of females	64.37±6.69 years
Gender	
Male (%), Female (%)	34 (77.27), 10 (22.73)
Pretreatment IOP, mean±SD (mmHg)	16.54±4.55
Anti-glaucoma medication	
Single drug	34 (52.27)
Two drugs	10 (22.72)
Previous cataract surgery	16 (36.36)
Systemic disease	
Hypertension	11 (25)
COPD (bronchial asthma)	4 (9.09)
Family history of glaucoma	7 (15.9)

COPD: Chronic obstructive pulmonary disorder, SD: Standard deviation, IOP: Intraocular pressure

Table 2: Comparison of visual field test parameters for Melbourne rapid field, Humphrey field analyzer 24-2 SITA-Fast program and spectral domain optical coherence tomography retinal nerve fiber layer thickness

Variable	Baseline, median (IQR)	6-months, median (IQR)	*P*
IOP (mmHg)	16 (6)	15 (2.5)	0.013
HVF MD (dB)	−2.54 (2.67)	−2.45 (3.1)	>0.05
HVF PSD (dB)	2.56 (2.66)	2.58 (2.07)	
HVF-VFI (%)	95 (5)	96 (4)	
MRF-VC (%)	98.25 (7.02)	97.5 (5.5)	
MRF MD (dB)	−1.15 (3.66)	−1.74 (3.57)	
MRF PSD (dB)	5.00 (3.89)	5.49 (2.13)	
SD-OCT RNFL thickness (micron)	71 (14.5)	70.5 (9.5)	

No statistically significant difference was there between baseline and 6 months. IOP: Intraocular pressure, HVF: Humphrey visual field, MD: Mean deviation, PSD: Pattern standard deviation, VFI: Visual field index, VC: Visual capacity, MRF: Melbourne rapid field, SD-OCT: Spectral domain optical coherence tomography, RNFL: Retinal nerve fiber layer, IQR: Interquartile range

DISCUSSION

In this study, we demonstrate that over a 6-month period, outputs from the MRF and HVF show concordance. However, MRF outputs require adjustment using a regression equation before meaningful comparison. We also demonstrate a weak correlation between functional VF outcomes and average RNFL thickness.

Table 3: Correlation between Humphrey visual field, Melbourne rapid field, and average retinal nerve fiber layer thickness at baseline and 6 months

	HVF MD (dB) Baseline	HVF PSD (dB) Baseline	MRF MD (dB) Baseline	MRF PSD (dB) Baseline	HVF MD (dB) 6 months	HVF PSD (dB) 6 months	MRF MD (dB) 6 months	MRF PSD (dB) 6 months
HVF MD (dB) Baseline	1.00							
HVF (dB) PSD Baseline	-0.61* <0.001	1.00						
Avg OCT Thickness(μm) Baseline	0.29 0.055	-0.37 0.011	1.00					
MRF MD (dB) Baseline	0.39* 0.007	-0.19 0.209	1.00					
MRF PSD (dB) Baseline	-0.29 0.050	0.14 0.332	-0.72* < 0.001	1.00				
HVF MD (dB) 6 months	0.67* <0.001	-0.41* 0.005	0.38* 0.009	-0.32* 0.031	1.00			
HVF PSD (dB) 6 months	-0.49* 0.0007	0.54* 0.0001	-0.48* 0.0008	0.43* 0.003	-0.74* <0.001	1.00		
Avg OCT Thickness(μm) 6months	0.32 0.032	-0.45 0.002	0.95 0.000	-0.01 0.929	0.35 0.016	-0.13 0.385	0.19 0.214	-0.35 0.017
MRF MD (dB) 6months	0.42* 0.004	-0.23 0.128	0.82* < 0.001	-0.53* 0.0002	0.38* 0.010	-0.48* 0.0008	1.00	
MRF PSD (dB) 6months	-0.24 0.111	0.23 0.120	-0.64* <0.001	0.63* <0.001	-0.31* 0.037	0.35* 0.017	-0.66* < 0.001	1.00

HVF: Humphrey visual field, MD: Mean deviation, PSD: Pattern standard deviation, MRF: Melbourne rapid field, OCT: Optical coherence tomography

Table 4: Intraclass correlation coefficient for baseline versus 6 months for Melbourne rapid field and Humphrey visual field outcomes

Global indices	ICC
HVF	
MD (dB)	0.62 (0.41–0.77)
PSD (dB)	0.37 (0.09–0.60)
VFI (%)	0.71 (0.52–0.82)
MRF	
MD (dB)	0.82 (0.69–0.90)
PSD (dB)	0.69 (0.50–0.82)
VC (%)	0.79 (0.65–0.88)

HVF: Humphrey visual field, MD: Mean deviation, PSD: Pattern standard deviation, VFI: Visual field index, VC: Visual capacity, MRF: Melbourne rapid field

The literature comparing perimetric results obtained using the MRF iPad-based application and the HFA is sparse. To our knowledge, this is the first Indian study to evaluate the correlation between functional tests, gold-standard HVF perimetry, tablet-based perimetry, and a structural test (OCT RNFL thickness) in patients with mild glaucoma receiving medical therapy.

A total of 50 patients were enrolled according to predefined inclusion and exclusion criteria. After excluding dropouts and unreliable test results, 44 participants were included in the final analysis, with a slightly skewed gender distribution (male:female ratio, 34:10). In our study, the mean test duration of MRF was 40 ± 5.2 s per eye, shorter than HVF 24-2 SITA-Fast ($P = 0.05$). Prea *et al*.[7] reported mean test durations of 276 ± 6 s for MRF, 258 ± 12.4 s for SITA-Fast, and 372 ± 6 s for SITA-Standard, indicating that MRF was significantly faster than SITA-Standard (by 96 s/eye) but marginally slower than SITA-Fast (by 18 s/eye). Kumar and Thulasidas[9] similarly reported that MRF testing was approximately 30 s per eye faster than HFA 24-2 SITA-Standard using a 9.7-inch iPad, comparable to our findings despite the use of an 11-inch iPad in our study. Similar results were also reported by Kong *et al*.[10]

The mean age of our study population (63.81 ± 11.31 years) was higher than that of the Indian cohort in the study by Prea *et al*.[7] (35.3 years) but lower than their UK cohort (70.1 years). Their overall mean age (57.9 years) was lower than that of our cohort. Another North Indian study by Kumar and Thulasidas[9] reported a lower mean age (52.28 ± 14.76 years). In our study, the mean age of male participants was 61.86 ± 12.82 years and that of females was 64.37 ± 6.69 years. Kong *et al*.[10] and Schulz *et al*.[11] reported higher mean ages of 69.5 ± 12.5 years and 64 ± 10.4 years, respectively, in their glaucoma cohorts, whereas the control group in the latter study was younger (53.8 ± 19.9 years).

A male predominance (77.3%) was observed in our study. This may reflect sociocultural factors in the Indian population, where male family members are more likely to seek medical care. Similar male predominance was noted by Kumar and

Table 5: Comparison of Humphrey visual field - mean deviation and Melbourne rapid field - mean deviation (unadjusted) at different time points

	LCC	ICC	Bias (dB)±SD	95% LOA (dB)
Baseline	0.32 (0.09–0.52)	0.33 (0.04–0.57)	0.28±3.08	−5.93–6.49
6 months	0.41 (0.19–0.58)	0.42 (0.14–0.63)	0.40±2.86	−5.37–6.17

LCC: Lin's concordance coefficient, ICC: Intraclass correlation coefficient, LOA: Limit of agreement, SD: Standard deviation

Table 6: Comparison of Humphrey visual field - mean deviation and regression-adjusted Melbourne rapid field - mean deviation at different time points

	LCC	ICC	Bias (dB)±SD	95% LOA (dB)
Baseline	0.82 (0.76−0.86)	0.82 (−0.05–0.97)	0.98±0.34	0.28–1.68
6 months	0.86 (0.80−0.90)	0.86 (−0.05–0.98)	1.01±0.43	0.14–1.87

LCC: Lin's concordance coefficient, ICC: Intraclass correlation coefficient, LOA: Limit of agreement, SD: Standard deviation

Table 7: Comparison of Humphrey visual field and Melbourne rapid field at baseline and 6 months

	LCC	ICC	Bias (dB)±SD	95% LOA (dB)
HVF-MD	0.62 (0.41–0.77)	0.63 (0.41–0.77)	−0.14±1.70	−3.57–3.30
MRF-MD	0.82 (0.69–0.90)	0.82 (0.69–0.89)	−0.01±1.95	−3.95–3.92

LCC: Lin's concordance coefficient, ICC: Intraclass correlation coefficient, LOA: Limit of agreement, SD: Standard deviation

Thulasidas[9] (60.7%) and Prea *et al*.[7] (62%). Gender distribution was not reported by Kong *et al*.[10] or Schulz *et al*.[11]

All patients in our study had been diagnosed with mild POAG as defined by HAP criteria. Kumar and Thulasidas[9] did not report glaucoma severity grading. In the multicentric study by Prea *et al*.,[7] stable ocular hypertensives, glaucoma suspects, and treated glaucoma patients with mild (42%), moderate (33%), and advanced (25%) VF loss were included. Kong *et al*.[10] assessed both normal and glaucoma patients with varying disease severity, while Schulz *et al*.[11] evaluated patients with manifest glaucoma, preperimetric glaucoma, and normal controls.

All participants in our study were on topical anti-glaucoma medications, with prostaglandin analogues (travoprost 0.004% once daily) as first-line therapy and timolol 0.5% twice daily as add-on therapy in selected cases. None underwent surgical intervention during the study period. Sixteen participants (36.36%) had undergone cataract surgery before enrollment, similar to the cohort reported by Prea *et al*.[7] In the study by Kong *et al*.,[10] all patients had well-controlled IOP on medical therapy. Schulz *et al*.[11] reported that seven patients had undergone cataract surgery and one had undergone trabeculectomy before enrollment.

These interstudy demographic and clinical differences highlight the heterogeneity of the published literature, which may partly explain variations in outcomes across functional and structural assessment modalities.

We observed a poor correlation between HVF 24-2 SITA-Fast MD/PSD and unadjusted (raw) MRF MD/PSD at both baseline and 6-month follow-up, with large bias and wide limits of agreement on Bland–Altman analysis. However, after applying regression adjustment, MRF-MD showed substantial concordance with HVF-MD, with reduced bias, improved agreement, and higher ICCs. Prea *et al*.[7] similarly demonstrated near-perfect concordance between baseline and 6-month MRF outcomes following regression adjustment (coefficient of accuracy = 0.95; ICC = 0.98), exceeding that observed with either SITA strategy.

Kong *et al*.[10] and Schulz *et al*.[11] used linear regression analysis to demonstrate strong correlations between MRF and HFA global indices (MD, PSD, and VFI). Prea *et al*.[7] reported a stronger association between MRF and SITA-Standard (0.83) than between MRF and SITA-Fast (0.77). Collectively, prior studies have reported excellent agreement between MRF and HFA for MD, PSD, and VFI/VC. However, an important limitation of earlier work is that outcomes were reported only after regression adjustment, underscoring that raw MRF MD values are not directly interchangeable with HVF MD. This distinction is critical when both modalities are used longitudinally in the same patient.

Prea *et al*.[7] also cited unpublished data indicating that larger iPad screen sizes reduce test duration, with the 12.9-inch iPad Pro shortening test time by 72 ± 48 s compared with a 9.7-inch device, likely due to reduced fixation shifts. Faster testing is particularly advantageous in high-volume clinics, community screening programs, and home monitoring for elderly patients.

We found a strong correlation between MRF-VC and HVF-VFI at baseline and at 6 months (R^2 = 39.1% and 46.2%, respectively), with the strongest association observed at 6 months.

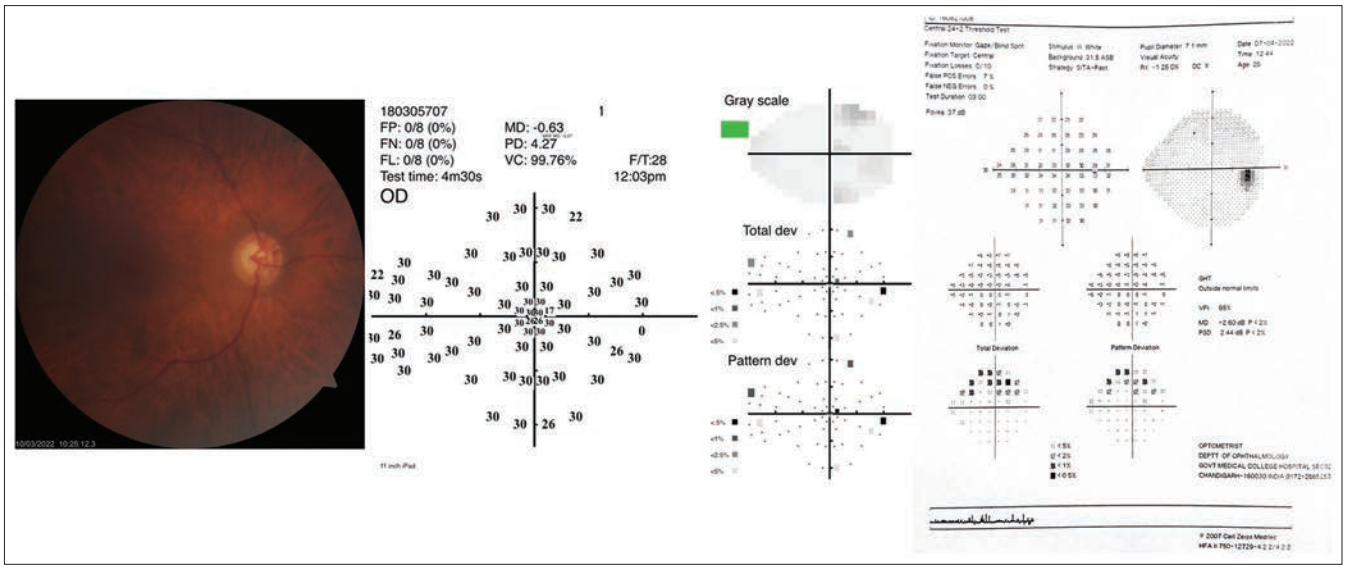

Figure 3: Representative visual field (VF) outcome in a patient having VF defect. Fundus photo (Extreme Left Panel), Melbourne Rapid Field (MRF) outcome (Central Panel), and Humphrey Field analyzer SITA-FAST Threshold plot (Extreme Right Panel) are shown. Note, all normal locations for the MRF return 30 dB

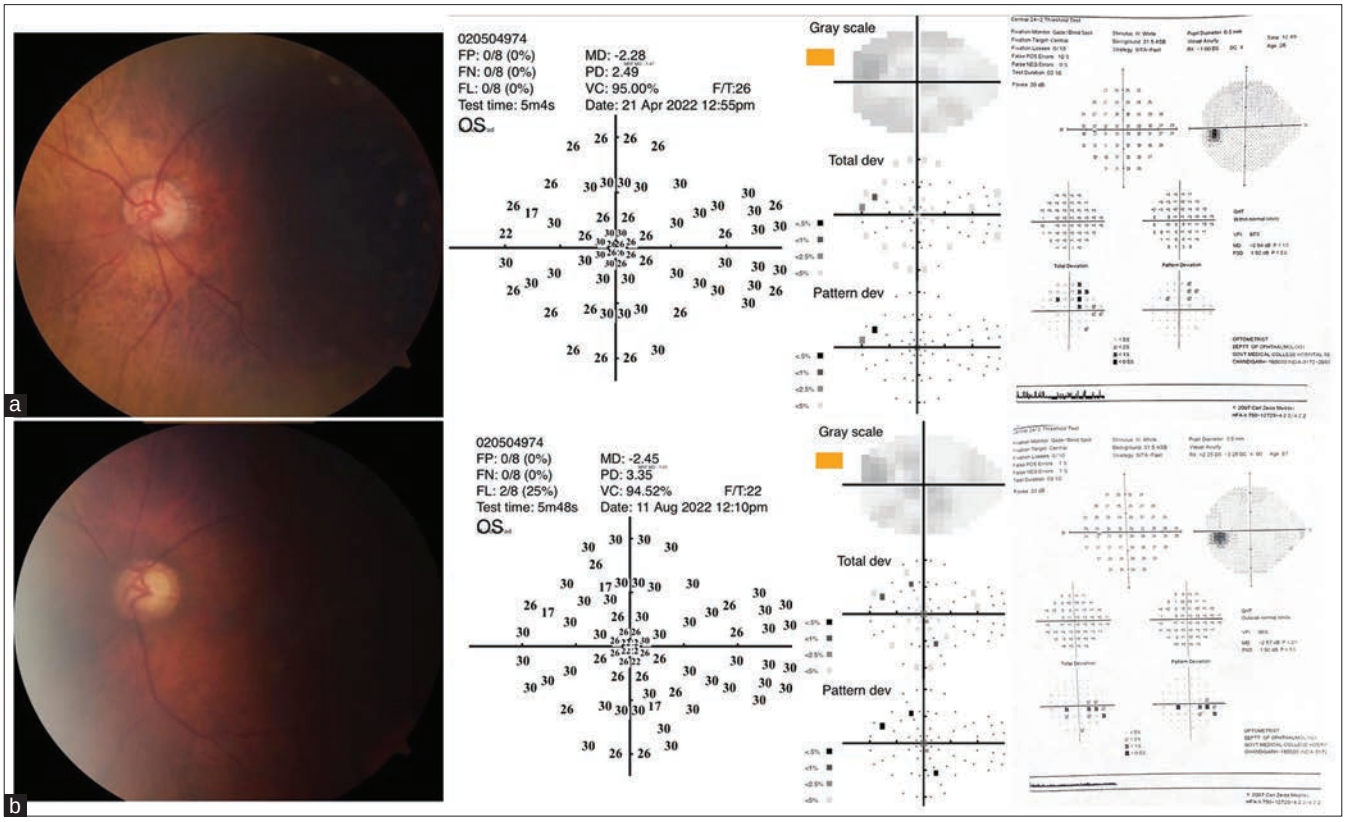

Figure 4: Fundus photo (Extreme Left Panel), Melbourne Rapid Field outcome (Central Panel), and Humphrey Field analyzer SITA-FAST Threshold plot (Extreme Right Panel) are shown for two patients at baseline (a) and at 6 months (b)

Several limitations of the MRF application warrant consideration. To enhance dynamic range, MRF employs lower background luminance than HFA, and nonuniform background illumination may pose challenges in community settings. Although contrast ratios appear consistent across similar devices, fixation monitoring remains limited. Incorporation of real-time eye or head tracking using the iPad camera or external gaze-tracking systems could improve reliability, though at increased cost. Current reliance on voice prompts to maintain fixation may be suboptimal during community deployment; expansion to additional regional languages or user-recorded prompts could enhance usability.

Offline ("internet-free") functionality would further facilitate deployment in resource-limited settings. Ergonomic modifications, such as the addition of a chin rest, may assist elderly patients with postural instability. Importantly, all published studies to date, including ours, have been conducted in controlled clinical environments; real-world robustness of MRF requires validation in community settings.

The presence of dual MD values (MD and MRF-MD) in some printouts introduces uncertainty regarding longitudinal comparisons. Moreover, MRF results cannot be directly substituted for HVF values without regression correction, representing a significant limitation of the application.

Consistent with previous studies, we observed a weak structure–function correlation between VF indices and average RNFL thickness.[12-14] This likely reflects the inclusion of patients with early glaucoma and the use of only global RNFL metrics. Future studies should incorporate quadrant-wise RNFL, Ganglion cell–inner plexiform layer (GCIPL) analysis, and additional OCT parameters to better elucidate structure–function relationships.

The main limitation of our study is the relatively small sample size; however, power calculations suggest adequacy for the primary outcome. Pointwise comparisons between MRF and HVF were not performed, and OCT analysis was limited to average RNFL thickness due to a lack of quadrant-wise and GCIPL data.

CONCLUSION

MRF offers utility as a complementary means of functional vision assessment along with SAP but cannot replace it. Following the initial screening using these cutting-edge "wireless" perimetry applications, conventional HVF testing – which is still the gold standard – can be employed with more effectiveness and cost-efficiency. There is still a considerable need to develop tools that can better demonstrate the structure–function correlation in glaucoma. Till such tools are developed and validated, patients will continue to require multiple structural and functional investigations to help clinicians make diagnostic and therapeutic decisions.

Financial support and sponsorship

Nil.

Conflicts of interest

There are no conflicts of interest.

REFERENCES

1. Che Hamzah J, Daka Q, Azuara-Blanco A. Home monitoring for glaucoma. Eye (Lond) 2020;34:155-60.
2. Gagrani M, Ndulue J, Anderson D, Kedar S, Gulati V, Shepherd J, *et al*. What do patients with glaucoma see: A novel iPad app to improve glaucoma patient awareness of visual field loss. Br J Ophthalmol 2022;106:218-22.
3. Prea SM, Kong GY, Guymer RH, Vingrys AJ. Uptake, persistence, and performance of weekly home monitoring of visual field in a large cohort of patients with glaucoma. Am J Ophthalmol 2021;223:286-95.
4. Kang JM, Tanna AP. Glaucoma. Med Clin North Am 2021;105:493-510.
5. Lerner SF, Lin S, Mansouri K. The world glaucoma association during the COVID-19 pandemic. J Glaucoma 2020;29:505-6.
6. The Evolution of Portable Visual Field Testing. Available from: https://www.reviewofophthalmology.com/article/the-evolution-of-portable-visual-field-testing. [Last accessed on 2024 Jan 14].
7. Prea SM, Kong YX, Mehta A, He M, Crowston JG, Gupta V, *et al*. Six-month longitudinal comparison of a portable tablet perimeter with the Humphrey field analyzer. Am J Ophthalmol 2018;190:9-16.
8. Hodapp E, Parrish RK II, Anderson DR. Clinical Decisions in Glaucoma. St Louis: Mosby-Year Book; 1993.
9. Kumar H, Thulasidas M. Comparison of perimetric outcomes from Melbourne Rapid Fields tablet perimeter software and Humphrey Field Analyzer in glaucoma patients. J Ophthalmol 2020;2020:8384509.
10. Kong YX, He M, Crowston JG, Vingrys AJ. A comparison of perimetric results from a tablet perimeter and Humphrey field analyzer in glaucoma patients. Transl Vis Sci Technol 2016;5:2.
11. Schulz AM, Graham EC, You Y, Klistorner A, Graham SL. Performance of iPad-based threshold perimetry in glaucoma and controls. Clin Exp Ophthalmol 2018;46:346-55.
12. Garway-Heath DF, Poinoosawmy D, Fitzke FW, Hitchings RA. Mapping the visual field to the optic disc in normal tension glaucoma eyes 11 the authors have no proprietary interest in the development or marketing of any product or instrument mentioned in this article. Ophthalmology 2000;107:1809-15.
13. Ajtony C, Balla Z, Somoskeoy S, Kovacs B. Relationship between visual field sensitivity and retinal nerve fiber layer thickness as measured by optical coherence tomography. Invest Ophthalmol Vis Sci 2007;48:258-63.
14. Nouri-Mahdavi K, Hoffman D, Tannenbaum DP, Law SK, Caprioli J. Identifying early glaucoma with optical coherence tomography. Am J Ophthalmol 2004;137:228-35.

Original Article

A Clinical Study of Bilateral Acute Depigmentation of the Iris Following Photorefractive Keratectomy

ABSTRACT

Objective: To describe a clinical study of bilateral acute depigmentation of the iris (BADI) occurring after photorefractive keratectomy (PRK).

Methods: This retrospective study included 14 patients (28 eyes) who presented with acute ocular pain and photophobia after uneventful PRK surgery performed at a tertiary eye care center by two refractive surgeons over 2 years (January 2022 and December 2023). All patients developed iris stromal depigmentation with pigment dispersion in the anterior chamber during the follow-up.

Results: The mean age of the patients was 26.5 ± 4.93 years; 11 were female and 3 were male. The mean preoperative refractive spherical equivalent was 3.58 ± 1.65 Diopters. Simple myopia was present in 11.76% of eyes, while 88.23% had compound myopic astigmatism. Four patients (seven eyes) developed transient elevation of intraocular pressure. The mean time to symptom onset was 19.57 ± 9.40 days after surgery. Systemic and immunological investigations were within the normal limits in all patients.

Conclusion: This study represents the largest reported cohort of BADI following PRK. The findings suggest a possible association with postoperative topical moxifloxacin exposure.

Keywords: Corneal epithelium, intraocular pressure, moxifloxacin, pigment dispersion syndrome, surface ablation, trabecular meshwork, visual acuity

INTRODUCTION

Bilateral acute depigmentation of the iris (BADI) was identified as a novel clinical entity in the early 21st century.[1] The condition presents with acute pigment dispersion in the anterior chamber and trabecular meshwork, followed by diffuse stromal depigmentation of the iris.[2] The involvement of both eyes is typical and may show asymmetry in severity. Clinical examination shows pigment release without inflammatory cells in the anterior chamber. Iris transillumination defects are absent, pupillary architecture is preserved, and elevations in intraocular pressure are usually mild and transient.[3] These features separate BADI from bilateral acute iris transillumination (BAIT), which shows epithelial pigment loss, pupillary abnormalities, and sustained elevation of intraocular pressure.[3]

Patients with BADI commonly present with acute photophobia, ocular pain, redness, and circumcorneal congestion. The clinical picture often resembles acute iridocyclitis at initial assessment, which can lead to diagnostic difficulty. Slit-lamp examination shows dense pigment dispersion within the anterior chamber without inflammatory cells or keratic precipitates. Iris stromal depigmentation becomes evident over time during the follow-up examinations, which contributes to delayed clinical recognition.[1,4] The etiopathogenesis of BADI and BAIT has not been clearly

Nimrata Bajaj Dhami, Abhinav Dhami, Gobinder Singh Dhami

Department of Ophthalmology, Dhami Eye Care Hospital, Ludhiana, Punjab, India

Address for correspondence: Dr. Nimrata Bajaj Dhami, Dhami Eye Care Hospital, 82-b Kitchlu Nagar, Ludhiana - 141 001, Punjab, India.
E-mail: nimratabajaj@gmail.com

Submitted: 30-01-2026 **Revised:** 02-02-2026
Accepted: 20-02-2026 **Published:** ***

Access this article online

Website: https://journals.lww.com/saao

DOI: 10.4103/SAOJ.SAOJ_26_26

Quick Response Code

How to cite this article: Dhami NB, Dhami A, Dhami GS. A clinical study of bilateral acute depigmentation of the iris following photorefractive keratectomy. South Asian Acad Ophthalmol J 2026;XX:XX-XX.

defined. Studies have reported a temporal relationship between symptom onset and prior exposure to systemic antibiotics, particularly oral moxifloxacin.[5,6] Similar pigment dispersion syndromes have also been described following systemic fluoroquinolone therapy and after intracameral moxifloxacin administration during intraocular surgery. These observations indicate an association between both systemic and local moxifloxacin exposure and the development of iris pigment dispersion disorders.[6,7] Iris depigmentation syndromes following corneal refractive procedures have been reported rarely. Available literature consists mainly of isolated case reports, and data on clinical features, triggers, and outcomes are sparse. The temporal association between refractive surgery, postoperative medication exposure, and the onset of symptoms requires evaluation in larger patient groups. The aim of this study was to describe the clinical presentation, course, and outcomes of patients who developed BADI after photorefractive keratectomy (PRK).

METHODS

Study design and patient selection

The medical records of patients who underwent elective PRK for correction of ametropia at a tertiary eye care center were retrospectively reviewed. The procedures were performed by two refractive surgeons over 2 years (January 2022 and December 2023). Patients who developed postoperative redness, watering, and photophobia, with or without elevation of intraocular pressure, or who showed worsening of these symptoms during routine postoperative treatment were included for the analysis. The study followed the Declaration of Helsinki and received approval from the institutional ethics committee. Written informed consent for PRK was obtained from all patients before surgery.

Patients aged 18 years or older with stable refraction for at least 6 months, no contact lens use for 4 weeks, normal preoperative corneal topography, and a postoperative residual stromal bed thickness >300 μm were included. Patients with prior ocular surgery, ocular trauma, ectatic corneal disorders, uveitis, preexisting ocular disease, diabetes mellitus, pregnancy, lactation, or collagen vascular disease were excluded. Baseline evaluation included manifest and cycloplegic visual acuity assessment, slit-lamp biomicroscopy, intraocular pressure measurement using Goldmann applanation tonometry, corneal topography with Pentacam HR (Oculus Optikgeräte GmbH), corneal pachymetry and epithelial mapping using anterior segment optical coherence tomography (Cirrus 500 HD-OCT, Zeiss), and dilated fundus examination. Peripheral retinal lesions predisposing to retinal detachment were treated by a retinal specialist at least 2 weeks before surgery.

Surgical technique

The eye received topical proparacaine hydrochloride 0.5% before surgery. Preparation followed aseptic protocol and an eyelid speculum was placed. Corneal epithelial removal used alcohol-assisted debridement. A Merocel sponge soaked in 20% diluted ethanol was applied within a well for 30 s, followed by epithelial removal with a spatula and irrigation. The planned central epithelial removal depth measured 45–60 μm based on the epithelial profile. The optical zone measured 6.0–6.5 mm and was selected according to refractive error, astigmatic correction, corneal thickness, and visual requirements. Laser ablation was performed in PRK mode using the EX500 Alcon WaveLight excimer laser system with a peak fluence of 400 mJ/cm^2 and a repetition rate of 500 Hz. Mitomycin-C 0.02% was applied with a Wekcel sponge for 10–60 s according to the refractive correction. The cornea was irrigated with cold balanced salt solution. A high oxygen permeability soft bandage contact lens was placed at end of surgery and removed between the postoperative day 3 and day 5 after epithelial healing.

Postoperative management and follow-up

Postoperative treatment included topical moxifloxacin 0.5% four times daily for 2 weeks, preservative free artificial tears six times daily for 1 month, and oral analgesics as required. After bandage contact lens removal, topical fluorometholone acetate 0.1% was started four times daily and tapered weekly over 4 weeks. Follow-up visits were scheduled on the postoperative day 1, day 3, day 10, and at 1, 3, and 6 months, with annual review thereafter. Each visit included slit-lamp examination. Visual acuity, intraocular pressure measurement, and direct ophthalmoscopy were performed from the postoperative day 3 onward.

RESULTS

Patient demographics and refractive profile

The medical records of 14 patients (28 eyes) who developed acute postoperative symptoms after uneventful PRK were retrospectively reviewed. All procedures were performed by two surgeons (NBD, GSD) between January 2022 and December 2023. Demographic data of symptomatic patients are presented in Table 1. The mean patients' age was 26.5 ± 4.93 years (range 18–36 years), with 3 males and 11 females. The mean preoperative methicillin-resistant

Table 1: Demographic characteristics of symptomatic patients

Parameter	Mean±SD	Range
Age (years)	26.5±4.93	18 to 36
MRSE (diopter)	−3.58±1.65	−1.25 to −6.75
Optical zone (mm)	6.33±0.13	6.0 to 6.5

SD: Standard deviation, MRSE: Mean refractive spherical equivalent

Staphylococcus epidermidis was −3.58 ± 1.65 D (range −1.25 to −6.75 D). Simple myopia was present in 11.76% of eyes, while 88.23% had compound myopic astigmatism. The mean optical zone used for PRK ablation was 6.33 ± 0.13 mm (range 6.0–6.5 mm). No eye required enhancement following PRK.

Clinical presentation and ocular findings

The mean time to symptom onset after PRK was 19.57 ± 9.40 days (range 11–45 days). All patients presented with acute pain, redness, and photophobia. Slit-lamp examination showed circumcorneal congestion and dense pigment dispersion in the anterior chamber without inflammatory cells or keratic precipitates [Figure 1]. Posterior segment examination was normal in all patients. Gonioscopy showed hyperpigmentation of the trabecular meshwork. Anterior segment optical coherence tomography demonstrated normal iris configuration in all eyes.

Systemic evaluation

All patients underwent systemic evaluation by a physician to exclude associated systemic conditions. Investigations included complete blood count, blood glucose levels, erythrocyte sedimentation rate, C-reactive protein, Mantoux test, venereal disease research laboratory test, viral serology for human immunodeficiency virus, hepatitis B, hepatitis C, TORCH Toxoplasma gondii, Rubella virus, Cytomagelovirus, Herpes simplex virus complex, serum angiotensin-converting enzyme levels, antinuclear antibody testing, human leukocyte antigen B27 typing, rheumatoid factor, and routine urine analysis. All systemic investigations were within the normal limits.

Management and intraocular pressure changes

All symptomatic patients received topical homatropine 2% three times daily, prednisolone acetate 1% four times daily with weekly tapering, and carboxymethyl cellulose 0.5% four times daily. Systemic therapy was not administered to any patient. Four patients (seven eyes), accounting for 25% of affected eyes, developed a transient rise in intraocular pressure during the acute phase. In these cases, intraocular pressure was controlled with a short course of brimonidine–timolol combination eye drops and tablet acetazolamide 250 mg once daily was administered temporarily to manage the acute pressure elevation. IOP was controlled over a median duration of 1 week, with no further resurgence reported during disease course.

Clinical course and follow-up outcomes

Clinical improvement was noted in all patients, with resolution of symptoms after a median treatment duration of 1 month. During the follow-up, the iris showed patchy areas of stromal depigmentation [Figure 2]. Final examination demonstrated normal pupillary size and light reaction in most eyes. Mild pupillary distortion persisted in 13 eyes (46.42%) [Figure 3]. Table 2 details the clinical characteristics of the symptomatic patients. All patients maintained visual acuity 6/6 in each eye throughout the study period. The mean photopic pupil diameter was 2.9 ± 1.8 mm, with a range of 2.5–5.3 mm. The mean scotopic pupil diameter was 5.2 ± 2.2 mm, ranging from 4.8 to 6.7 mm. The mean duration of follow-up was 6.57 ± 2.84 months, with a range of 3–11 months. No recurrent episodes were observed during the follow-up period.

DISCUSSION

BADI and BAIT belong to the same spectrum of acute pigment dispersion disorders but differ in clinical phenotype and disease course.[8] The first comprehensive report of 26 cases from Turkey in 2006 described an anterior segment

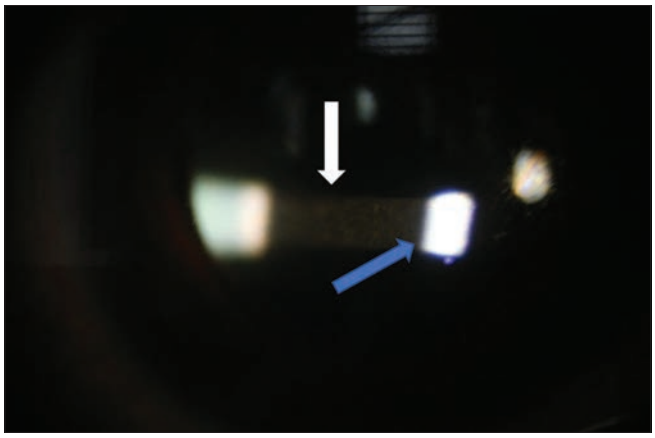

Figure 1: Shows 1 mm × 1 mm oblique slit-beam illumination photograph taken at high magnification depicting florid pigment dispersion in the anterior chamber (white arrows) in the acute phase of disease and note the absence of any keratic precipitates on endothelium (blue arrow)

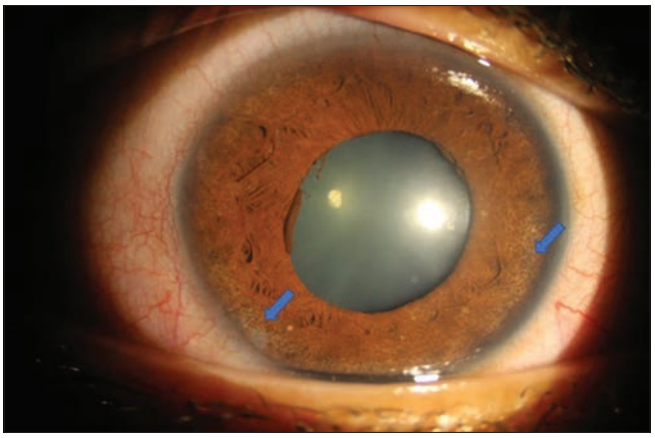

Figure 2: Diffuse beam slit-lamp photograph with diffuse depigmented patches on iris (blue arrows). This photograph was taken on day 10 during the acute phase of bilateral acute depigmentation of the iris and under pharmacological dilatation of 2% homatropine eye drops

Table 2: Clinical characteristics and follow-up details of symptomatic patients

Age/gender	Eye	Preoperative MRSE (diopter)	Time to symptom onset post-PRK (days)	IOP spike during acute phase	Pupillary distortion after resolution	Follow-up (months)
21/male	OD	−5.25	14	+	−	11
	OS	−5.50	14	+	−	11
25/female	OD	−4.75	14	−	+	11
	OS	−4.375	14	−	+	11
27/female	OD	−3.25	18	+	+	9
	OS	−2.50	18	+	+	9
28/female	OD	−1.25	14	−	+	9
	OS	−1.50	14	−	−	9
33/female	OD	−3.75	13	−	+	8
	OS	−4.00	13	−	−	8
32/female	OD	−2.50	11	−	−	9
	OS	−2.50	11	−	−	9
26/female	OD	−4.125	11	−	+	5
	OS	−4.25	11	−	−	5
18/female	OD	−1.625	27	−	+	3
	OS	−1.50	27	−	−	3
23/female	OD	−6.25	27	−	−	3
	OS	−6.625	27	−	−	3
24/male	OD	−2.50	12	−	+	5
	OS	−2.875	12	+	+	5
36/male	OD	−3.00	24	−	−	4
	OS	−2.875	24	−	−	4
22/female	OD	−6.75	19	+	+	6
	OS	−6.75	19	+	+	6
29/female	OD	−1.50	45	−	−	4
	OS	−1.75	45	−	+	4
27/female	OD	−3.875	25	−	−	5
	OS	−3.125	25	−	−	5

+ = present; - = absent, MRSE: Mean refractive spherical equivalent, PRK: Photorefractive keratectomy, IOP: Intraocular pressure, OD: Right eye, OS: Left eye

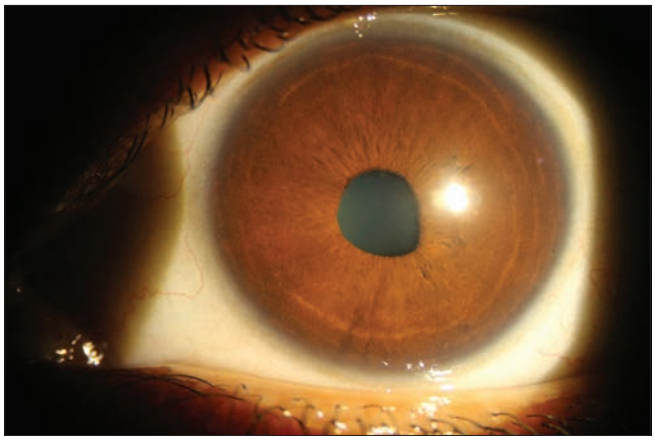

Figure 3: Diffuse beam slit-lamp photograph with white arrow depicting mild pupillary distortion. This photograph was taken at a 3-month follow-up after the resolution of bilateral acute depigmentation of the iris-symptoms, without any pharmacological dilatation

presentation with pigment dispersion in the anterior chamber, trabecular meshwork, anterior lens capsule, and a Krukenberg spindle on the corneal endothelium, without evidence of intraocular inflammation.[9] Patients present with acute photophobia, ocular pain, and ciliary congestion, with bilateral involvement that may be symmetrical or asymmetrical and can resemble acute iridocyclitis, which complicates the diagnosis.[10-12]

BAIT is the more severe form and is characterized by pigment release from the iris pigment epithelium, iris transillumination defects, pupillary changes, and sustained increase in the intraocular pressure. Pupils often appear fixed and dilated due to sphincter dysfunction. Persistent ocular hypertension may occur and can require surgical management. Studies have shown cases with uncontrolled intraocular pressure that needs tube shunt implantation. The increase in the intraocular pressure in BAIT is typically greater in magnitude and duration than that observed in BADI, which requires close monitoring of the pressure to reduce the risk of optic nerve damage. BADI represents a milder and nonprogressive variant. Pigment originates from the iris stroma and results in diffuse patchy depigmentation that begins near the iris root and generally spares the peri-pupillary region. Pupillary configuration is usually preserved, intraocular pressure elevation is transient, and final visual acuity remains unaffected.[12]

BADI requires differentiation from the conditions with overlapping anterior segment findings, particularly viral iridocyclitis and pigment dispersion syndrome. Viral iridocyclitis may show sectoral iris atrophy with elevation of intraocular pressure but usually affects one eye and is associated with inflammatory keratic precipitates and anterior chamber cells, findings not observed in BADI. Pigment dispersion syndrome represents a chronic disorder characterized by sustained elevation of intraocular pressure, midperipheral iris transillumination defects, and posterior iris bowing, features that are absent in BADI.[8] BADI and BAIT show an acute disease course with pigment dispersion resolving over weeks to months, which differentiates them from chronic pigmentary disorders.[9,12] The etiopathogenesis of BADI has not been clearly defined. Previous case reports have reported preponderance with female sex and prior exposure to systemic moxifloxacin or other oral antibiotics used for respiratory infections.[13] In the present series, no patient reported prior systemic illness or oral antibiotic use. Female patients constituted 78% of the study population, while males accounted for 22%. A similar female predominance has been reported in previously published series, including the original cohort described by Tuğal-Tutkun and later reports from Brazil and India.[9,12]

Case reports have described BADI and BAIT following local or intraocular exposure to moxifloxacin in the absence of systemic use. Reported settings include intracameral moxifloxacin administration during glaucoma surgery,[14] use for endophthalmitis prophylaxis in cataract surgery,[7] and exposure after phakic intraocular lens implantation.[15] These observations indicate an association between local moxifloxacin exposure and acute iris pigment dispersion. Intracameral administration results in higher anterior chamber drug concentrations than topical or systemic routes, which may account for the severity of pigmentary changes observed in some cases.[7,14]

Reports have described iris pigmentary changes following corneal refractive procedures combined with postoperative moxifloxacin exposure. Cases have been documented after femtosecond-assisted Laser-Assisted In Situ Keratomileusis (LASIK) and PRK.[16-18] Olcay *et al*. reported bilateral iris atrophy with transillumination defects after LASIK, and noted a possible association with intraoperative pressure changes, although postoperative medication use was not specified.[16] Studies have reported the occurrence of BADI and BAIT after PRK in patients who received postoperative topical moxifloxacin thus indicating an association between surface ablation procedures and subsequent acute iris pigment dispersion.[17,18] Surface ablation procedures include the removal of the epithelium, which may alter the function of the corneal barrier and permit an increased intraocular exposure to topical medications. This mechanism explains the occurrence of acute iris pigment dispersion after refractive surgery in the presence of topical antibiotic use.[17,18]

The first reported case of BADI from China described the recurrent episodes following systemic moxifloxacin and levofloxacin use for tympanitis, with serological evidence of elevated cytomegalovirus and rubella immunoglobulin G levels.[19] Atilgan *et al*. described a 23-year-old woman with BADI who showed spontaneous iris re-pigmentation over 3 years after systemic moxifloxacin therapy for pneumonia.[20] Dhami *et al*. reported a young male patient who developed BAIT after PRK while using postoperative topical moxifloxacin-soaked bandage contact lenses thus highlighting increased drug exposure in eyes with epithelial disruption.[21] Kawali *et al*. conducted a retrospective analysis of 22 patients from India and reported topical fluoroquinolone use in 17 patients, while three patients had no documented antibiotic exposure, indicating variability in exposure patterns.[22] Perone *et al*. reviewed 79 cases of BAIT and noted frequent association with moxifloxacin use, along with regional clustering and inconsistent antibiotic histories.[23] Bringas Calvo and Iglesias Cortiñas described bilateral uveitis with pigment dispersion after systemic moxifloxacin treatment for pneumonia, and similar findings have been described after the use of fluoroquinolone using different routes.[24]

This study provides the detailed clinical documentation of BADI following PRK. The findings describe the occurrence of this condition after surface refractive surgery and document its clinical course and outcomes. The exposure to topical moxifloxacin on a de-epithelialized corneal surface was observed in all cases, which may permit increased intraocular drug penetration. Laboratory investigations such as aqueous humor polymerase chain reaction for viral pathogens were not performed, which restricts the evaluation of infectious causes. The absence of a comparison group limits the assessment of drug-related causation. BADI and BAIT should be considered in the differential diagnosis of acute pigment dispersion occurring after refractive surgery or fluoroquinolone exposure, particularly in cases with poor response to corticosteroid therapy.

CONCLUSION

This study documents the largest series to date of BADI occurring after PRK. The findings expand the current knowledge of postoperative pigment dispersion

disorders following surface refractive surgery. Increased use of refractive procedures requires the awareness of uncommon postoperative anterior segment conditions. The etiopathogenesis of BADI remains uncertain, with the factors such as topical fluoroquinolone exposure, surgical intervention, and host susceptibility under consideration. Further clarification requires studies using anterior chamber sampling with PCR testing for viral pathogens and prospective multicenter designs with uniform diagnostic criteria and extended follow-up. Accurate recognition and reporting remain necessary to distinguish BADI and BAIT from uveitis and to guide the appropriate clinical management.

Financial support and sponsorship

Nil.

Conflicts of interest

There are no conflicts of interest.

REFERENCES

1. Tugal-Tutkun I, Araz B, Taskapili M, Akova YA, Yalniz-Akkaya Z, Berker N, *et al*. Bilateral acute depigmentation of the iris: Report of 26 new cases and four-year follow-up of two patients. Ophthalmology 2009;116:1552-7, 1557.e1.
2. Barraquer F, Mejía LF. Bilateral acute depigmentation of the iris: First report on the American continent and 5 years follow up of two patients. J Emmetropia. 2012;3:119–23.
3. Amin R, Nabih A, Khater N. Bilateral acute depigmentation of the iris in two siblings simultaneously. Am J Ophthalmol Case Rep 2018;10:257-60.
4. Willermain F, Deflorenne C, Bouffioux C, Janssens X, Koch P, Caspers L. Uveitis-like syndrome and iris transillumination after the use of oral moxifloxacin. Eye (Lond) 2010;24:1419.
5. Tranos P, Lokovitis E, Masselos S, Kozeis N, Triantafylla M, Markomichelakis N. Bilateral acute iris transillumination following systemic administration of antibiotics. Eye (Lond) 2018;32:1190-6.
6. Morshedi RG, Bettis DI, Moshirfar M, Vitale AT. Bilateral acute iris transillumination following systemic moxifloxacin for respiratory illness: Report of two cases and review of the literature. Ocul Immunol Inflamm 2012;20:266-72.
7. Light JG, Falkenberry SM. Unilateral bilateral acute iris transillumination-like syndrome after intracameral moxifloxacin injection for intraoperative endophthalmitis prophylaxis. JCRS Online Case Rep 2019;7:3-5.
8. Tuğal-Tutkun İ, Altan Ç. Bilateral acute depigmentation of iris (BADI) and bilateral acute iris transillumination (BAIT)-an update. Turk J Ophthalmol 2022;52:342-7.
9. Tugal-Tutkun I, Urgancioglu M. Bilateral acute depigmentation of the iris. Graefes Arch Clin Exp Ophthalmol 2006;244:742-6.
10. Gonul S, Bozkurt B. Bilateral acute iris transillumination (BAIT) initially misdiagnosed as acute iridocyclitis. Arq Bras Oftalmol 2015;78:115-7.
11. Langevin S, Gershkovich A, Marr BP. A case of bilateral acute depigmentation of the iris in one of two identical twins. BMC Ophthalmol 2020;20:13.
12. Costa FV, Silva AG, Pedroso LA, Biancardi AL, Curi AL. Bilateral acute depigmentation of the iris (BADI) and bilateral acute iris transillumination (BAIT): A case series from a center in Brazil. Arq Bras Oftalmol 2024;87:e2023.
13. Wefers Bettink-Remeijer M, Brouwers K, van Langenhove L, De Waard PW, Missotten TO, Martinez Ciriano JP, *et al*. Uveitis-like syndrome and iris transillumination after the use of oral moxifloxacin. Eye (Lond) 2009;23:2260-2.
14. Sánchez-Sánchez C, Puerto B, López-Caballero C, Contreras I. Unilateral acute iris depigmentation and transillumination after glaucoma surgery with mitomycin application and intracameral moxifloxacin. Am J Ophthalmol Case Rep 2020;18:100639.
15. Jones M, Reynhout J, Schirber S, Khachikian S. Moxifloxacin-associated acute pigment dispersion and iris transillumination after phakic lens surgery. JCRS Online Case Rep 2024;12:e00124.
16. Olcay K, Cakir A, Sagdic SK, Duzgun E, Yildirim Y. Bilateral iris atrophy after the femtosecond assisted laser *in situ* keratomileusis surgery. Case Rep Ophthalmol Med 2015;2015:127806.
17. Menon MG, Prasad SN. Bilateral acute depigmentation of the iris following refractive surgery – An untold story. Acta Sci Ophthalmol 2024;7:24-6.
18. Veas R, Caraccioli E, Anguita R. Bilateral acute iris transillumination after refractive surgery. JFO Open Ophthalmol 2023;4:100055.
19. Wang T, Wu WM, Zhang FY, Jia X. Clinical analysis of bilateral acute depigmentation of the iris: First reported case in China. Int J Ophthalmol 2022;15:1560-2.
20. Atilgan CU, Kosekahya P, Caglayan M, Berker N. Bilateral acute depigmentation of iris: 3-year follow-up of a case. Ther Adv Ophthalmol 2018;10:2515841418787988.
21. Dhami NB, Dhami A, Dhami GS, Malhi R, Gupta V. Bilateral acute iris transillumination after photorefractive keratectomy: A case report. Indian J Ophthalmol Case Rep 2023;3:26-9.
22. Kawali A, Mahendradas P, Shetty R. Acute depigmentation of the iris: A retrospective analysis of 22 cases. Can J Ophthalmol 2019;54:33-9.
23. Perone JM, Chaussard D, Hayek G. Bilateral acute iris transillumination (BAIT) syndrome: Literature review. Clin Ophthalmol 2019;13:935-43.
24. Bringas Calvo R, Iglesias Cortiñas D. Acute and bilateral uveitis secondary to moxifloxacin. Arch Soc Esp Oftalmol 2004;79:357-9.

Case Report

Aurolab Aqueous Drainage Implant with a Ripcord Stent for Childhood Glaucoma in Axenfeld–Rieger Syndrome

ABSTRACT

Axenfeld–Rieger syndrome (ARS) represents a spectrum of congenital anterior segment dysgenesis, in which angle malformations predispose affected children to early-onset glaucoma. We report the case of a 6-year-old girl who presented with bilateral scleral bluish discoloration, microcornea, decreased vision, and characteristic ocular features of ARS, along with systemic manifestations including dental anomalies and redundant umbilical skin. Her intraocular pressure remained uncontrolled in the left eye (OS) despite full adherence to maximally tolerated topical therapy, and surgical intervention was planned owing to advanced glaucomatous optic disc cupping in OS. A superotemporal Aurolab aqueous drainage implant (350 mm^2; Aurolab, Madurai, India) with an intraluminal (4-0 Prolene) ripcord stent was placed in OS. This case highlights the challenges of managing glaucoma associated with anterior segment dysgenesis and suggests the potential value of incorporating a ripcord stent in high-risk pediatric eyes to reduce the risk of early postoperative hypotony.

Keywords: Aurolab aqueous drainage implant, Axenfeld–Rieger syndrome, glaucoma, glaucoma drainage device, ripcord stent

INTRODUCTION

Axenfeld-Rieger syndrome (ARS) is a rare genetic disorder characterized by a spectrum of anterior segment dysgenesis abnormalities. It is most commonly inherited in an autosomal dominant condition and is associated with mutations in PITX2 and FOXC1 genes. It is also associated with systemic abnormalities like dental anomalies, craniofacial dysmorphism and cardiac defects. Glaucoma in ARS can be present at birth or can develop in later life.[1-4] It is bilateral but asymmetrical. It is treated with antiglaucoma medications initially. But majority of them are refractory to medical therapy eventually needing surgical management. Surgical management is more efficacious than medical management and includes procedures such as trabeculotomy, trabeculectomy, and glaucoma drainage devices (GDDs).[4-7]

CASE REPORT

A 6-year-old girl was brought by her parents with concerns of bluish discoloration of both sclerae and progressive visual difficulties, which they had observed for several months. They reported that the child increasingly held reading material close to her face and had difficulty viewing distant objects at school. There were no complaints of watering, redness, or photophobia. Her developmental history was normal, and the parents reported no prior medical, ophthalmic, or laboratory evaluations. The family history was unremarkable.

Nishwath Bala Krishnan, Vijayalakshmi A. Senthilkumar

Department of Glaucoma, Aravind Eye Hospital and Postgraduate Institute of Ophthalmology, Madurai, Tamil Nadu, India

Address for correspondence: Dr. Vijayalakshmi A. Senthilkumar, Department of Glaucoma, Aravind Eye Hospital and Postgraduate Institute of Ophthalmology, Madurai, Tamil Nadu, India.
E-mail: vijimmc@gmail.com

Submitted: 01-02-2026 **Revised:** 26-02-2026
Accepted: 28-02-2026 **Published:** ***

Access this article online

Website: https://journals.lww.com/saao

DOI: 10.4103/SAOJ.SAOJ_41_26

Quick Response Code

How to cite this article: Krishnan NB, Senthilkumar VA. Aurolab aqueous drainage implant with a ripcord stent for childhood glaucoma in Axenfeld–Rieger syndrome. South Asian Acad Ophthalmol J 2026;XX:XX-XX.

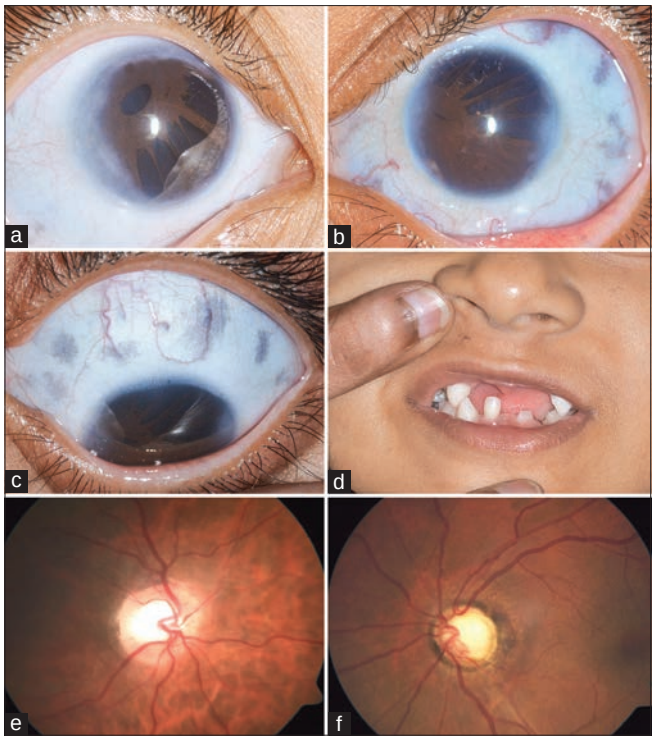

Figure 1: (a and b) Slit-lamp photograph showing microcornea, marked iris hypoplasia, polycoria, posterior embryotoxon in right eye (OD) and left eye (OS) respectively, (c) Bluish scleral discoloration in OS, (d) Dental anomalies such as widely spaced and conical teeth, (e and f) Fundus photo demonstrating a cup–disc ratio of 0.6 in OD and 0.85 with bipolar thinning in OS

Ophthalmic evaluation showed uncorrected visual acuities of 20/200 in both eyes (OU), improving to 20/60 in the right eye (OD) and 20/200 in left eye (OS) with best correction. Slit-lamp examination revealed classical features of Axenfeld–Rieger syndrome (ARS), including bluish scleral discoloration, decreased corneal diameter (horizontal 8.0 mm and vertical 8.5 mm), marked iris hypoplasia, polycoria, posterior embryotoxon, and broad peripheral anterior synechiae [Figure 1a-c]. Anterior chamber depth measurements were limited due to the distorted anterior segment anatomy; however, clinically, the chambers were shallow (Van Herrick Grade 1). Intraocular pressure (IOP) by Goldmann tonometry measured 16 mmHg in OD and 26 mmHg in OS. Central corneal thickness in OU was markedly increased (OD-649 µm and OS-643 µm), and the axial length was noted to be 21.25 mm in OD and 22.67 mm in OS. Gonioscopic examination in OU revealed iridocorneal adhesions and dysgenetic angle structures. Dilated fundus examination showed a cup–disc ratio (CDR) of 0.6 with a pink neuroretinal rim and CDR of 0.85 with bipolar thinning in OS [Figure 1e and f]. Considering the markedly increased central corneal thickness, the true IOP was interpreted with caution; however, the advanced optic disc cupping and documented pressure elevation despite therapy supported the diagnosis of uncontrolled glaucoma in OS.

General examination revealed dental anomalies such as widely spaced and mildly conical teeth [Figure 1d] along with redundant umbilical skin, both of which are recognized systemic features of ARS disorders. No overt craniofacial or cardiac abnormalities were noted clinically. Initial management included a fixed drug combination of topical 2% dorzolamide hydrochloride and 0.5% timolol maleate eye drops twice daily in OU. One month later, IOP remained elevated in OS (28 mmHg), prompting the addition of 0.005% latanoprost eye drops at night. Although glaucoma drainage device (GDD) implantation in OS was advised, the parents were initially reluctant to consent to invasive surgery. Drug compliance was excellent, but despite 3 months of maximally tolerated therapy, pressures increased to 34 mmHg in OS, with progressive cupping. In view of inadequate medical response, the child was taken up for surgical intervention.

In the present case, a nonvalved implant was preferred over a valved device because the child had markedly dysgenetic angle structures and shallow anterior chamber, increasing the risk of early hypotony-related complications. Nonvalved implants with staged flow control allow gradual IOP reduction and may reduce the risk of excessive early filtration.[1,2] Valved devices, although providing immediate IOP reduction, are associated with a hypertensive phase that may affect long-term success.[3] Angle surgery such as goniotomy or trabeculotomy was considered less favorable due to the presence of extensive peripheral anterior synechiae and abnormal angle anatomy.[4] Trabeculectomy was also avoided, given the high risk of bleb failure and complications in pediatric eyes with anterior segment dysgenesis.[5,6]

A nonvalved Aurolab aqueous drainage implant (AADI 350) with a ripcord stent was implanted under general anesthesia. A 3-clock-hour fornix-based conjunctival peritomy was created in the superotemporal quadrant followed by appropriate posterior blunt dissection of Tenon's capsule. Priming of the tube was done with a 27-gauge cannula to rule out manufacturing defects, and a 4-0 Prolene intraluminal ripcord stent was introduced into the tube lumen using the *ab externo* ripcord technique [Figure 2a]. The tube was externally ligated with two 6-0 Vicryl sutures to prevent early hypotony. The AADI plate was positioned approximately 8–10 mm posterior to the limbus and secured with 9-0 Nylon sutures. A 23-gauge needle track, approximately 4 mm in length, was created after marking 4 mm from the limbus and 2 mm medial to the tube entry site [Figure 2b and c]. The tube was then inserted through this track into the anterior chamber [Figure 2d] and secured to the sclera with a 10-0 Nylon suture. The Prolene stent was placed in the sub-Tenon's space temporally, and the conjunctiva was closed in a watertight manner using 8-0 Vicryl sutures.

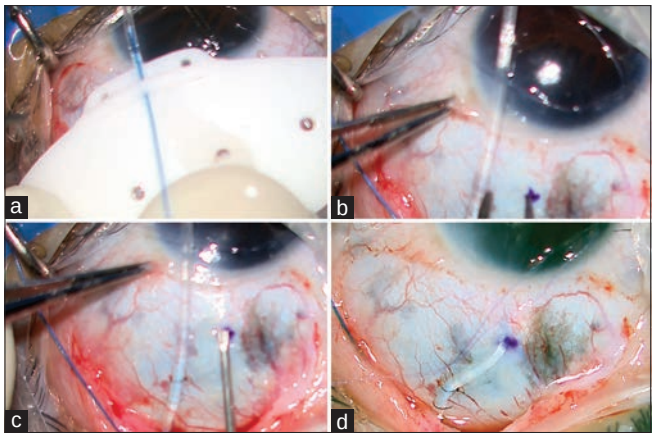

Figure 2: (a) Intraoperative photo showing a 4-0 Prolene *ab externo* ripcord technique, (b-d) the patch-free Aurolab aqueous drainage implant surgery technique using a 4 mm long scleral track. A 23-gauge needle track, approximately 4 mm in length, was created after marking 4 mm from the limbus and 2 mm medial to the tube entry site

Postoperatively, the child was maintained on topical antibiotic-steroid combination and aqueous suppressants, which were gradually tapered over subsequent visits as IOP stabilized. On postoperative day 1, the tube was well positioned without corneal touch or iris incarceration. Over the subsequent weeks, as the Vicryl ligature dissolved, the tube opened and pressures steadily decreased. The OS ultimately stabilized in the midteens without further surgical intervention, and no complications such as tube exposure, corneal decompensation, or motility disturbances were observed until the last follow-up at 18 months. The Prolene ripcord stent did not require removal during the entire follow-up period. The OD remained medically controlled.

DISCUSSION

ARS represents a spectrum of congenital anterior segment dysgenesis in which angle malformations predispose affected children to early-onset glaucoma.[7,8] Glaucoma develops in nearly 50%–60% of patients with ARS and is often refractory to medical management, necessitating surgical intervention.[7-10] GDDs offer similar efficacy to trabeculectomy, but the incidence of endophthalmitis is significantly lower with GDDs.[9] Valved GDDs, such as the Ahmed valve, provide an immediate IOP lowering effect and pose a lower risk of hypotony in the early postoperative period. However, bleb encapsulation and a hypertensive phase occurring 4–8 weeks after surgery can reduce the long-term success and survival of the Ahmed GDD.[1-3] Nonvalved GDDs, such as the Baerveldt implant, require the use of a dissolvable ligature to delay aqueous outflow, allowing for controlled IOP reduction. This delayed IOP-lowering effect helps prevent plate encapsulation and improves the long-term survival of the device.[1,2] To our knowledge, reports specifically describing the combined use of an *ab externo* ripcord stent and patch-free AADI implantation in ARS are scarce.[11,12] This case, therefore, contributes practical surgical insight into flow modulation strategies in complex pediatric anterior segment dysgenesis.

The AADI, which is inspired by the Baerveldt 350-mm^2 implant, has been shown in published studies to provide comparable long-term IOP control in pediatric glaucoma at a fraction of the cost, making it a valuable option in resource-limited settings.[11,12] This case illustrates the complexity of managing glaucoma in ARS, where anatomical distortion, early-onset disease, and limited response to medical therapy often necessitate surgical intervention. Importantly, it emphasizes the crucial role of a ripcord stent in high-risk pediatric eyes to minimize the risk of postoperative hypotony and its related complications. In addition, a patch-free technique was employed, obviating the need for a donor patch graft. While this approach reduces surgical time and cost, careful scleral tunnel construction and meticulous conjunctival closure are essential to minimize the long-term risk of tube erosion. Long-term follow-up remains important to monitor for late exposure.[12]

Comparative studies have shown that AADI demonstrates IOP reduction comparable to the Baerveldt implant and similar long-term success rates to the Ahmed glaucoma valve in pediatric refractory glaucoma.[1-3,11,12] However, the sustained pressure control achieved with nonvalved devices may offer theoretical advantages in complex pediatric eyes when adequate flow restriction is employed. Beyond ocular control, multidisciplinary systemic evaluation is essential, as ARS is associated with significant dental, cardiac, periumbilical, and craniofacial abnormalities. Careful intraoperative planning and an individualized surgical technique were key to achieving a favorable outcome.

Declaration of patient consent

The authors certify that they have obtained all appropriate patient consent forms. In the form, the legal guardian has given his consent for images and other clinical information to be reported in the journal. The guardian understands that names and initials will not be published and due efforts will be made to conceal patient identity, but anonymity cannot be guaranteed.

Financial support and sponsorship

Nil.

Conflicts of interest

There are no conflicts of interest.

REFERENCES

1. Budenz DL, Barton K, Feuer WJ, Schiffman J, Costa VP, Godfrey DG, *et al.* Treatment outcomes in the Ahmed Baerveldt comparison study after 1 year of follow-up. Ophthalmology 2011;118:443-52.
2. Christakis PG, Tsai JC, Kalenak JW, Zurakowski D, Cantor LB, Kammer JA, *et al.* The Ahmed versus Baerveldt study: Three-year treatment outcomes. Ophthalmology 2013;120:2232-40.
3. Nouri-Mahdavi K, Caprioli J. Evaluation of the hypertensive phase after insertion of the Ahmed glaucoma valve. Am J Ophthalmol 2003;136:1001-8.
4. Mandal AK, Pehere N. Early-onset glaucoma in axenfeld-rieger anomaly: Long-term surgical results and visual outcome. Eye (Lond) 2016;30:936-42.
5. Sidoti PA, Belmonte SJ, Liebmann JM, Ritch R. Trabeculectomy with mitomycin-C in the treatment of pediatric glaucomas. Ophthalmology 2000;107:422-9.
6. Zepeda EM, Branham K, Moroi SE, Bohnsack BL. Surgical outcomes of glaucoma associated with axenfeld-rieger syndrome. BMC Ophthalmol 2020;20:172.
7. Chang TC, Summers CG, Schimmenti LA, Grajewski AL. Axenfeld-rieger syndrome: New perspectives. Br J Ophthalmol 2012;96:318-22.
8. Reis LM, Maheshwari M, Capasso J, Atilla H, Dudakova L, Thompson S, *et al*. Axenfeld-rieger syndrome: More than meets the eye. J Med Genet 2023;60:368-79.
9. Gedde SJ, Herndon LW, Brandt JD, Budenz DL, Feuer WJ, Schiffman JC, *et al*. Postoperative complications in the tube versus trabeculectomy (TVT) study during five years of follow-up. Am J Ophthalmol 2012;153:804-14.e1.
10. Khan AM, Ahmad K, Alarfaj M, Alotaibi H, AlJaloud A, Malik R. Surgical outcomes of the Aurolab aqueous drainage implant (AADI) versus the Ahmed glaucoma valve for refractory paediatric glaucoma in middle Eastern children. BMJ Open Ophthalmol 2021;6:e000831.
11. Puthuran GV, Palmberg PF, Wijesinghe HK, Pallamparthy S, Krishnadas SR, Robin AL. Intermediate-term outcomes of Aurolab aqueous drainage implant in refractory paediatric glaucoma. Br J Ophthalmol 2020;104:962-6.
12. Puthuran GV, Palmberg P, Wijesinghe HK, Srivastav KS, Krishnadas SR, Lee Robin A. Aurolab aqueous drainage implant with and without scleral patch graft in refractory adult and pediatric glaucomas: A comparative study. Am J Ophthalmol 2020;216:226-36.

Case Report

Posterior Dislocation of Kelman Multiflex Anterior Chamber Intraocular Lens – An Uncommon Presentation

ABSTRACT

Ocular trauma, though not uncommon, has a reported prevalence of approximately 3.75% in the Indian population. Traumatic dislocation of an intraocular lens (IOL) is a relatively rare but potentially serious complication following cataract surgery. We report an uncommon case of traumatic dislocation of a Kelman Multiflex anterior chamber intraocular lens (ACIOL), highlighting key vitreoretinal surgical considerations for safe explantation . In this case, active aspiration using the vitrectomy probe alone was utilized to levitate the ACIOL into the pupillary plane. This approach simplified the procedure by eliminating additional manipulative steps, thereby reducing overall surgical time while ensuring controlled and safe IOL retrieval. Subsequently, scleral-fixated intraocular lens implantation was performed using a three-piece IOL, with haptics externalized and secured by flange formation through cauterization of the exposed haptic ends. This approach represents a safe, effective, and minimally invasive strategy, ensuring optimal lens stability and favourable postoperative outcomes while minimizing intraocular manipulation.

Keywords: Anterior chamber intraocular lens, dislocation, Kelman Multiflex, vitrector-assisted aspiration

INTRODUCTION

Ocular trauma, though not an uncommon scenario, has a prevalence of 3.75% among the Indian population.[1] Ocular trauma resulting in dislocation of intraocular lens (IOL) is relatively rare but a serious complication following cataract surgery, with an incidence ranging between 0.2% and 3%.[1] The specific occurrence of an anterior chamber IOL (ACIOL) dislocating into the posterior segment is, however, a rarer phenomenon. Posterior chamber IOL (PCIOL) dislocation may arise from progressive zonular weakness or capsular instability, whereas ACIOL dislocation results from improper placement, due to inadequate support by the iris, or because of ocular trauma. A posterior dislocation of ACIOL may result in sight-threatening complications, including retinal detachment, macular edema, and monocular diplopia.[2] Managing a traumatic IOL dislocation, though challenging, requires prompt surgical management for adequate stabilization and better visual rehabilitation. A deeper understanding of such occurrences is important as it helps unveil new aspects of visual recovery. This case illustrates an uncommon instance of traumatic vitreous dislocation of a Kelman Multiflex ACIOL and brings attention to key surgical considerations involved in safe explantation, vitreoretinal handling, and appropriate secondary IOL fixation.

Arun Bhatti, Nithya Raghunandan, Pradnya Shrikant Rao, J. Vidya

Department of Ophthalmology, M. S. Ramaiah Medical College, Bengaluru, Karnataka, India

Address for correspondence: Dr. Arun Bhatti, Department of Ophthalmology, M. S. Ramaiah Medical College, MSR Nagar, New Bel Road, MSRIT Post, Bengaluru - 560 054, Karnataka, India.
E-mail: arun.bhatti@yahoo.com

Submitted: 27-01-2026
Accepted: 29-01-2026 **Published:** ***

Access this article online

Website: https://journals.lww.com/saao

DOI: 10.4103/SAOJ.SAOJ_10_26

Quick Response Code

How to cite this article: Bhatti A, Raghunandan N, Rao PS, Vidya J. Posterior dislocation of Kelman Multiflex anterior chamber intraocular lens – An uncommon presentation. South Asian Acad Ophthalmol J 2026;XX:XX-XX.

CASE REPORT

A 72-year-old male patient presented with sudden diminution of vision in the left eye (LE) following blunt trauma sustained 1 month prior. The patient had undergone cataract surgery in the LE 10 years ago. On examination, the visual acuity in the right eye (RE) was 6/6, and LE was counting finger 1 m. On examination of LE, the anterior segment revealed a round, mid-dilated pupil. Pupillary zone was aphakic; there was no sphincter tear, angle recession, or iridodialysis. On dilated fundus examination, a Kelman Multiflex type ACIOL was noted in the mid-vitreous cavity. B scan confirmed the presence of IOL, and there was no retinal detachment. The patient underwent pars plana vitrectomy with dislocated ACIOL retrieval. Perfluoro carbon liquid (PFCL) was utilized intraoperatively to safeguard the macula, providing a protective tamponade during the manipulation and retrieval of the dislocated lens. Secondary Scleral Fixated IOL (SFIOL) implantation was considered. Postoperative period was uneventful. Following the surgery, the patient's vision was 6/12 in the LE on 1-month follow-up.

DISCUSSION

Dislocation of the ACIOL, while rare, can lead to significant visual impairment and other serious complications.[3] ACIOL dislocation can occur due to several mechanisms, broadly grouped into intraoperative, early postoperative, and late postoperative causes. The most plausible mechanism in our case was improper primary placement of the ACIOL, compounded by subsequent blunt ocular trauma, causing sudden anterior chamber deformation and resultant haptic dislodgment. Notably, there was no evidence of iris defects, iridodialysis, or sphincter tears. Although not unprecedented, instances, in which ACIOL dislocation with iris architecture and pupil appearing largely normal are rare and typically occur following ocular trauma after cataract surgery.[4] A detailed preoperative assessment, including a thorough history and retinal examination with scleral depression and B scan, is crucial for planning appropriate surgical intervention. The management strategy for dislocated ACIOL typically involves PPV to remove the displaced lens, followed by secondary IOL implantation.[4] The dislocated IOL was visualised on the posterior pole [Figure 1]. Traditional methods of IOL retrieval often involve grasping the IOL within the posterior segment by intraocular forceps.[5] This technique, while commonly practiced, can present difficulties, especially with plate-haptic IOL, which are challenging to secure with forceps.[5] Moreover, the manipulation of instruments near the retina increases the risk of retinal damage, IOL re-dislocation, or even retinal detachment.[5] Another well-established technique is using a silicon tip flute needle to induce active aspiration to retrieve the dislocated IOL.[6] However, in our case, active aspiration using the vitrectomy probe alone was employed to levitate the ACIOL to the pupillary plane.[5] PFCL was utilized intraoperatively to safeguard the macula, providing a protective tamponade during the manipulation and retrieval of the dislocated lens. Maintaining the optic aligned parallel to the iris plane is crucial while inducing active vacuum, as improper orientation can exert focal traction or contact on the peripheral retina, predisposing to iatrogenic retinal breaks.[6] This technique streamlines the procedure by avoiding time-consuming steps, thereby shortening total surgical duration while maintaining precise control and ensuring safer IOL retrieval. This technique also eliminates the need for specialized forceps. Once the IOL was levitated to the pupillary plane, it was retrieved from the anterior chamber through the preformed sclerocorneal tunnel using appropriate forceps held in the nondominant hand [Figure 2]. In this case, SFIOL implantation was performed using a three-piece IOL, with the haptics externalized and flanged into the sclera by cauterization of the exposed haptic ends. This technique is easy and can be well adopted by novice surgeons; long-term outcomes are generally favorable with precise surgical management.[7]

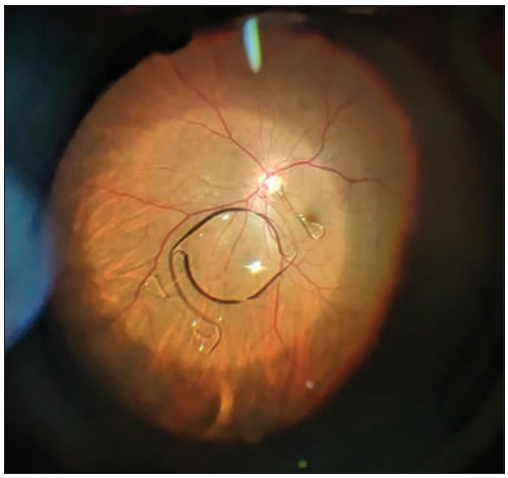

Figure 1: Kelman Multiflex anterior chamber intraocular lens seen on the macular surface

CONCLUSION

Ocular trauma resulting in ACIOL dislocation, although rare, requires prompt recognition and timely intervention. In our case, active aspiration using the vitrectomy probe alone was employed to safely levitate the ACIOL to the pupillary plane, followed by SFIOL implantation using a flanged three-piece IOL. This approach represents a safe, effective, and minimally invasive strategy,

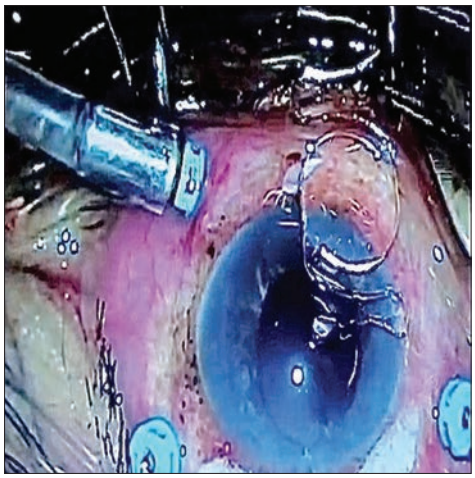

Figure 2: Kelman Multiflex anterior chamber intraocular lens retrieved from the vitreous cavity

ensuring optimal lens stability and favorable postoperative outcomes while minimizing intraocular manipulation.

Declaration of patient consent

The authors certify that they have obtained all appropriate patient consent forms. In the form, the patient(s) has/have given his/her/their consent for his/her/their images and other clinical information to be reported in the journal. The patients understand that their names and initials will not be published and due efforts will be made to conceal their identity, but anonymity cannot be guaranteed.

Financial support and sponsorship

Nil.

Conflicts of interest

There are no conflicts of interest.

REFERENCES

1. Shah M, Shah S. Prevalence of eye injury in India: A meta-analysis. J Clin Ophthalmol Res 2024;12:3-7.
2. Bryn Mawr Communications. A dropped anterior chamber IOL - Retina Today [Internet]. Retina Today. Available from: https://retinatoday.com/articles/2021-oct/a-dropped-anterior-chamber-iol.
3. Sitompul R. Intraocular lens dislocation after cataract surgery in Tambolaka, Southwest Sumba, Indonesia: A case report. Case Rep Ophthalmol 2018;9:179-84.
4. Esquenazi S. Management of a displaced angle-supported anterior chamber intraocular lens. Ophthalmic Surg Lasers Imaging 2006;37:65-7.
5. Icoz M, Usta SA. Modified double-flanged technique in the management of dislocated posterior intraocular lenses. Graefes Arch Clin Exp Ophthalmol 2025;263:1925-32.
6. Olson JL, Velez-Montoya R, Erlanger M, Mackenzie D. Management of a dislocated intraocular lens with a suction-based grasping tool. J Cataract Refract Surg 2013;39:154-7.
7. Rao GN, Kumar S, Sinha N, Rath B, Pal A. Outcomes of three-piece rigid scleral fixated intraocular lens implantation in subjects with deficient posterior capsule following complications in manual small incision cataract surgery. Heliyon 2023;9:e20345.

Case Report

Unusual Tiny Dermoid of Caruncle

ABSTRACT

Dermoids and lipodermoids of epibulbar origin are choristomas with tissues derived from the epithelium. These may be associated with oculoauriculovertebral dysplasia, characterized by ocular lipodermoid or dermoid, preauricular skin appendages, vertebral malformations, and fistulas. We report a rare, tiny dermoid cyst of a caruncle in a 22-year-old young male who presented to our department with a cyst in the left eye near the caruncle for the last 3 months. The cyst was gradually increasing in size and was painless. There was no history of any congenital illness. On examination, a cyst was present on the caruncle, measuring appro 5 mm 3 mm and bilobular in shape, and yellowish in colour. Extraocular movements were full and free in both eyes, and the rest of the anterior and posterior segments were normal in both eyes. There was no preauricular tag, postural/spinal abnormalities, or cleft palate. We made a provisional diagnosis of a dermoid cyst of the caruncle. The cyst was excised under local anesthesia and sent for histopathological examination. On histopathology, epithelial-lined dermal appendages were present, which confirmed the diagnosis of a dermoid.

Keywords: Caruncle, dermoid, Goldenhar

INTRODUCTION

Dermoids and lipodermoids of epibulbar origin are choristomas with tissues derived from the epithelium. These are the most frequent epibulbar tumors in children.[1] The cornea, limbus, bulbar conjunctiva, and other areas of the orbit can have these choristomas, which are congenital lesions that are normal tissue in an abnormal location.[2] These may be associated with oculoauriculovertebral dysplasia, characterized by ocular lipodermoid or dermoid, preauricular skin appendages, vertebral malformations, and fistulas.[1] We report a rare, tiny dermoid cyst of a caruncle in a 22-year-old young male.

CASE REPORT

A 22-year-old male presented to our department with a cyst in the left eye near the caruncle for the last 3 months. The cyst was gradually increasing in size and was painless. It was not associated with redness or discharge. There was no history of any congenital illness. On examination, a cyst was present on the caruncle, measuring approximately 5 mm × 3 mm. The lesion was bilobular in shape, yellowish in color, adherent and was not translucent [Figure 1a]. His visual acuity was 6/6 in both eyes, and his intraocular pressure was normal. Extraocular movements were full and free in both eyes, and the rest of the anterior and posterior segments were normal in both eyes. There was no preauricular tag, postural/spinal abnormalities, or cleft palate. We made a provisional diagnosis of a dermoid cyst of the caruncle. The cyst was excised under local anesthesia and sent for histopathological examination. Intraoperatively, adhesions on the caruncle were found, which were released. On histopathology, epithelial-lined dermal appendages were present, which confirmed the diagnosis of a dermoid [Figure 1b].

Nazia Anjum, Nitin Kumar, Poonam Sharma[1]

Department of Ophthalmology, All India Institute of Medical Sciences, Vijaypur, Jammu and Kashmir, India, [1]Department of Pathology, All India Institute of Medical Sciences, Vijaypur, Jammu and Kashmir, India

Address for correspondence: Dr. Nazia Anjum, Faculty Block, Ground Floor, All India Institute of Medical Sciences, Vijaypur - 181 134, Jammu and Kashmir, India.
E-mail: naziaanjummarch@gmail.com

Submitted: 02-02-2026 **Revised:** 13-02-2026
Accepted: 15-02-2026 **Published:** ***

Access this article online

Website: https://journals.lww.com/saao

DOI: 10.4103/SAOJ.SAOJ_47_26

Quick Response Code

How to cite this article: Anjum N, Kumar N, Sharma P. Unusual tiny dermoid of caruncle. South Asian Acad Ophthalmol J 2026;XX:XX-XX.

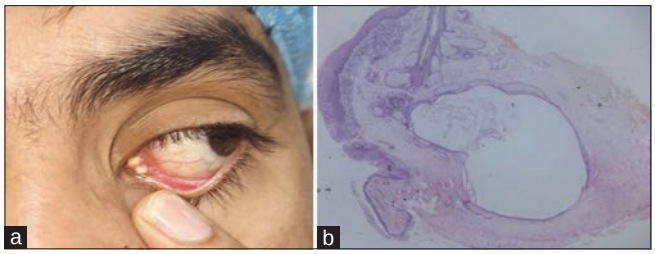

Figure 1: (a) Photograph of the left eye showing a dermoid of caruncle, (b) Histology of the lesion showing epithelial-lined dermal appendages

DISCUSSION

Lesions of the caruncle are not common. A study conducted in Wilmer Institute reported that nevi, papillomas, and sebaceous gland hyperplasia were the most commonly encountered lesions, accounting for 65% of the total caruncular lesions.[3] Dermoids are one of the most frequent cysts of the orbit. These are benign, congenital tumors of the orbit that are typically located superonasally or superotemporally, closer to the frontozygomatic suture.[4,5] They are made up of keratinized stratified squamous epithelium and a few dermal derivatives, such as sebaceous glands and hair follicles.[4] The majority of superficial cysts are seen in early childhood and are frequently reported to have an anatomic mean diameter that ranges from approximately 0.5 to 3 cm.[5-7]

We report a case of a dermoid presenting at an atypical location. Goldenhar syndrome is known to be more frequently associated with dermoids. Goldenhar is a rare congenital syndrome characterized by ocular anomalies, vertebral anomalies, auricular appendages, and aural fistula.[8] In our case, there was no systemic association, and there was no other ocular abnormality. Dermoids are usually located on the limbus or in the superonasal or superotemporal orbit, but in our case, it was located on the caruncle, which was unique. After histopathological confirmation, the patient was reassured.

CONCLUSIONS

Dermoid and lipodermoids can be located at atypical locations such as the caruncle. Dermoids are usually associated with other systemic conditions, but can present alone.

Declaration of patient consent

The authors certify that they have obtained all appropriate patient consent forms. In the form, the patient has given his consent for his images and other clinical information to be reported in the journal. The patient understands that his name and initials will not be published and due efforts will be made to conceal his identity, but anonymity cannot be guaranteed.

Financial support and sponsorship

Nil.

Conflicts of interest

There are no conflicts of interest.

REFERENCES

1. Balogh M. Lipodermoid: A case report. Clin Eye Vis Care 1995;7:79-82.
2. Elsas FJ, Green WR. Epibulbar tumors in childhood. Amyloid 1975;1:0.5.
3. Luthra CL, Doxanas MT, Green WR. Lesions of the caruncle: A clinicohistopathologic study. Surv Ophthalmol 1978;23:183-95.
4. Shields JA, Shields CL. Orbital cysts of childhood – Classification, clinical features, and management. Surv Ophthalmol 2004;49:281-99.
5. Cavazza S, Laffi GL, Lodi L, Gasparrini E, Tassinari G. Orbital dermoid cyst of childhood: Clinical pathologic findings, classification and management. Int Ophthalmol 2011;31:93-7.
6. Kumar R, Vyas K, Jaiswal G, Bhargava A, Kundu J. Deep orbital dermoid cyst bulging into the superior orbital fissure: Clinical presentation and management. J Ophthalmic Vis Res 2017;12:110-2.
7. Bansal R, Honavar SG, Talloju SS, Mulay K. Orbital dermoid cyst. Indian J Ophthalmol 2022;70:709.
8. Vinay C, Reddy RS, Uloopi KS, Madhuri V, Sekhar RC. Craniofacial features in Goldenhar syndrome. J Indian Soc Pedod Prev Dent 2009;27:121-4.7

Case Report

Occult Nucleus Drop Masquerading as Endophthalmitis

ABSTRACT

Postoperative endophthalmitis is a serious complication following intraocular surgeries. Patients may present with endophthalmitis in the setting of retained lens fragments. We report a case of occult nucleus dislocation, where the nuclear fragment was lodged between the Wieger's ligament and the zonules. The patient presented with signs and symptoms mimicking endophthalmitis. He was managed with pars plana vitrectomy (PPV), removal of retained lens fragment and instillation of intravitreal antibiotics. A high index of suspicion, thorough clinical examination and meticulous scleral indentation during PPV has enabled us to manage the case efficiently. This case report also emphasizes the importance of proper record keeping for all surgeries.

Keywords: Endophthalmitis masquerade, occult nucleus drop, Wieger's ligament, zonules

INTRODUCTION

Postoperative endophthalmitis is a serious complication following intraocular surgeries, mostly from microbial contamination from the adnexa and environment during surgery.[1] While there are high chances of infectious causes, noninfectious ones should be considered as a differential. Noninfectious endophthalmitis has diverse etiologies, and includes systemic autoimmune diseases, local ocular inflammations, endophthalmitis related to lens material, and endophthalmitis attributable to intraocular foreign bodies.[2] Patients may present with endophthalmitis in the setting of retained lens fragments after phacoemulsification. In such cases, the preferred initial management may be pars plana vitrectomy (PPV), removal of retained lens fragments, and injection of intravitreal antibiotics. In eyes with endophthalmitis and opaque media, ultrasonography (USG) is a useful screening modality.[3]

CASE REPORT

A 72-year-old male was referred to us with dimness of vision, pain, watering, and redness in the right eye (RE) for 2 months. His vision in RE was finger counting – 1 m and 0.80 logMAR in the left eye (LE). He gave a history of cataract surgery in RE done 4 months ago. On examination, there was mild conjunctival congestion, minimal hypopyon in the anterior chamber, fixed mid-dilated pupil, and posterior chamber intraocular lens (PCIOL) in RE [Figure 1]. In LE, the patient had a Grade IV nuclear cataract. Fundus evaluation of RE revealed plenty of vitreous floaters and vitreous hemorrhage.

Video available on: https://drive.google.com/file/d/1aoPWvutH7nFGSBkXGkSb1UjVYeTNzC1x/view?usp=sharing

Access this article online	
Website: https://journals.lww.com/saao	Quick Response Code
DOI: 10.4103/SAOJ.SAOJ_57_26	

Haimanti Choudhury, Himadri Choudhury[1], Shubham Pisal[2], Hirendra Kumar Choudhury[3]

Department of Cataract and Oculoplasty, Choudhury Eye Hospital and Research Centre, Silchar, Assam, India, [1]Department of Vitreoretina and Uvea, Choudhury Eye Hospital and Research Centre, Silchar, Assam, India, [2]Department of Ophthalmology, Choudhury Eye Hospital and Research Centre, Silchar, Assam, India, [3]Department of Cataract and Glaucoma, Choudhury Eye Hospital and Research Centre, Silchar, Assam, India

Address for correspondence: Dr. Haimanti Choudhury, Department of Cataract and Oculoplasty, Choudhury Eye Hospital and Research Centre, Shyamaprasad Road, Shillongpatty, Silchar - 788 001, Assam, India.
E-mail: drhaimanti@gmail.com

Submitted: 13-02-2026 **Revised:** 15-02-2026
Accepted: 16-02-2026 **Published:** ***

How to cite this article: Choudhury H, Choudhury H, Pisal S, Choudhury HK. Occult nucleus drop masquerading as endophthalmitis. South Asian Acad Ophthalmol J 2026;XX:XX-XX.

Intraocular pressure (IOP) in RE was 9 mmHg and in LE was 12 mmHg, done by rebound tonometer. On B scan of RE, there were dense echoes in mid vitreous. The case was suspected as delayed endophthalmitis and was planned for PPV with vitreous biopsy and intravitreal antibiotics under local anesthesia [Figure 2a].

While performing PPV, meticulous scleral indentation was done, which revealed a nuclear material (about one-third of the nucleus) lodged in ciliary zonules [Figure 2b]. It was maneuvered through the pars plana and dropped in the posterior segment [Figure 2c]. Then, the dropped nucleus was removed with phaco fragmatome [Figure 2d and Video 1]. Intravitreal antibiotics (vancomycin 1 mg/0.1 mL and ceftazidine 2.25 mg/0.1 mL) were instilled. On postoperative day 1, the vision was hand movement. Anterior segment evaluation showed congestion, reduced hypopyon, and fixed semi-dilated pupil. IOP in RE was 12 mmHg, and in LE was 20 mmHg. On fundus examination, the retina was on. Vitreous biopsy was reported sterile after 72 h.

After 2 weeks, the vision in RE improved to 0.60 logMAR. IOP in RE was 18 mmHg. Anterior segment was quiet, there was no hypopyon, and PCIOL was *in situ* [Figure 3]. After 3 months, Best corrected visual acuity (BCVA) improved to 0.20 logMAR with +1.00 Dioptre spherical and – 2.50 Dioptre cylinder at 90°.

DISCUSSION

Retained lens material is a known and rare cause of postoperative endophthalmitis after phacoemulsification.[3] Irvine *et al*. reported four cases who developed endophthamitis secondary to prolonged exposure of nucleus material; the duration after which the patients presented ranged from 1 month to 1 year of cataract extraction.[4] In the present case, the patient was operated in the camp setting where residents usually perform surgery under consultant supervision. There was no mention of any intraocular complications, and PCIOL was placed in the sulcus. Patient was not aware of any intraoperative complication, nor did his discharge summary had any mention of anterior vitrectomy. In the immediate postoperative period (postcataract), the patient reported having suboptimal vision and mild pain. He was put on prolonged topical Moxifloxacin Dexamethasone combination eye drop. He used the eye drop up to 2 months from surgery. After cessation of eye drop, he complained of further diminution of vision and a constant nagging pain in the RE. He reported to his place of surgery after another 2 months, following which he was referred to us. Preoperative evaluation (prior to PPV) also did not reveal any vitreous in

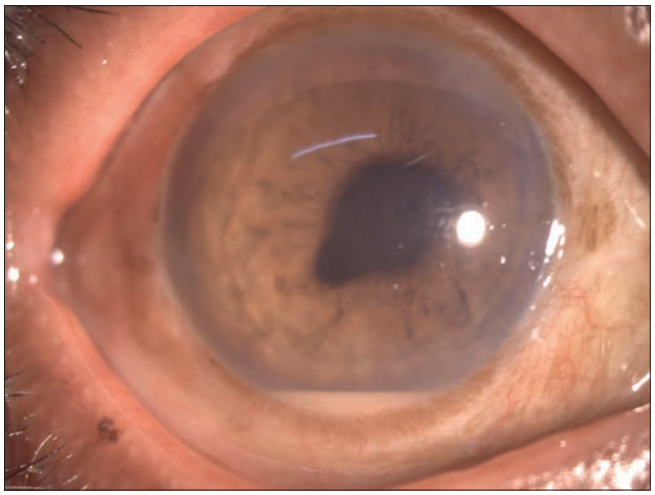

Figure 1: Anterior segment at presentation, showing mild conjunctival congestion, hypopyon in the anterior chamber, and posterior chamber intraocular lens

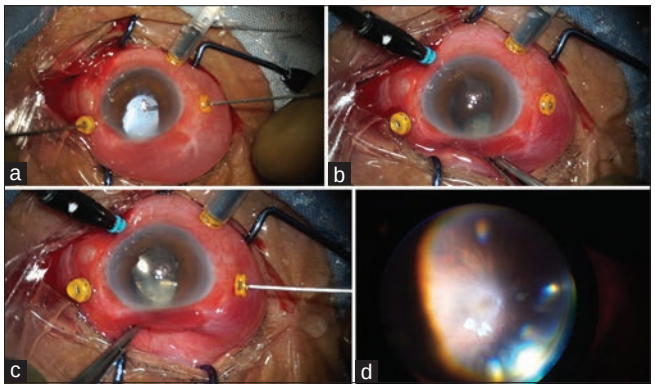

Figure 2: (a) Pars plana vitrectomy (PPV) started. (b) Scleral indentation being done during PPV, which reveals nuclear material. (c) Scleral indentation maintained, vitrector is maneuvered through the pars plana and drops the nuclear fragment into the posterior segment. (d) Dropped nuclear fragment over retina, which was removed with a phaco fragmatome

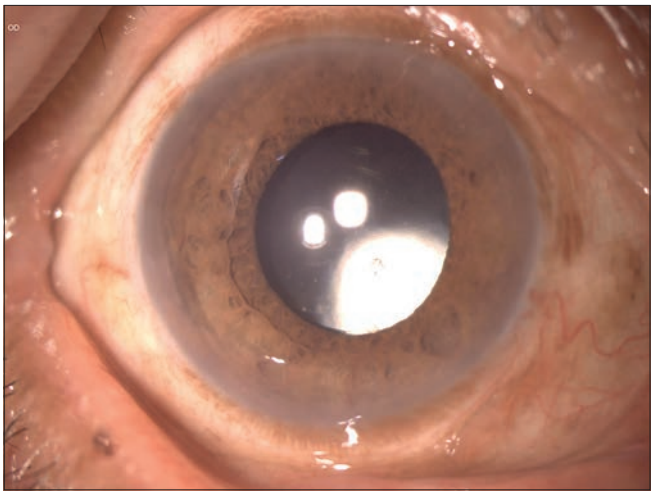

Figure 3: Postoperative day 14 shows a quiet anterior segment, no hypopyon, and posterior chamber intraocular lens *in situ*

the anterior chamber. Usually USG B scan can detect the dropped nucleus, but in our case, since the dislocated nuclear material was lodged anteriorly in the ciliary zonules, it was not perceived on B scan.

In such cases where etiology is rare, history is of utmost importance in diagnosing and preventing further delay in management. Dropped nucleus is an intraoperative complication which occurs due to posterior capsular rupture (PCR). In phacoemulsification, the pressure gradient from the infusion causes the nucleus material to propel posteriorly through PCR.[5] The incidence of this complication is more in residents as compared to consultants.[6] Though such cases have been reported earlier, what makes this case unique is the way the nuclear dislocation was missed by the operating surgeon. The nuclear material was not exactly dropped in the vitreous, rather it was lodged between the Wieger's ligament and the zonules. The absence of vitreous in the anterior chamber suggests that the anterior vitreous phase was not disturbed, and there was no vitreous loss in the first surgery. The retained nuclear material has acted as a nidus for chronic inflammation, thus resulting in features mimicking endophthalmitis. A high index of suspicion, thorough clinical examination, and scleral indentation during PPV have enabled us to manage the case efficiently. This case report also emphasizes the importance of proper record-keeping for all surgeries.

Declaration of patient consent

The authors certify that they have obtained all appropriate patient consent forms. In the form, the patient has given his consent for his images and other clinical information to be reported in the journal. The patient understands that name and initials will not be published, and due efforts will be made to conceal identity, but anonymity cannot be guaranteed.

Financial support and sponsorship

Nil.

Conflicts of interest

There are no conflicts of interest.

REFERENCES

1. Althiabi S, Aljbreen AJ, Alshutily A, Althwiny FA. Postoperative endophthalmitis after cataract surgery: An update. Cureus 2022;14:e22003.
2. Safneck JR. Endophthalmitis: A review of recent trends. Saudi J Ophthalmol 2012;26:181-9.
3. Kim JE, Flynn HW Jr., Rubsamen PE, Murray TG, Davis JL, Smiddy WE. Endophthalmitis in patients with retained lens fragments after phacoemulsification. Ophthalmology 1996;103:575-8.
4. Irvine WD, Flynn HW Jr., Murray TG, Rubsamen PE. Retained lens fragments after phacoemulsification manifesting as marked intraocular inflammation with hypopyon. Am J Ophthalmol 1992;114:610-4.
5. Hu JY, Ti SE, Chee SP. Risk factors affecting visual outcomes following dropped nucleus after cataract surgery. Eye (Lond) 2024;38:253-8.
6. Halim J, Micheletti E, Dari ML, Mandal N, Khan SR. Incidence and outcomes of dropped nucleus after phacoemulsification cataract surgery between 2020 and 2024. J Clin Transl Ophthalmol 2025;3:26.

Case Report

Donor-related Multidrug-resistant *Klebsiella pneumoniae* Causing Severe Interface Keratitis Following Deep Anterior Lamellar Keratoplasty

ABSTRACT

Postoperative interface infectious keratitis (IIK) is a rare but sight-threatening complication following deep anterior lamellar keratoplasty (DALK). Early identification of the causative organism and prompt initiation of targeted therapy are critical for preserving vision. We report the case of a 17-year-old male who developed rapidly progressive interface infiltrates involving the graft-host junction on postoperative day 1 after an uneventful DALK. Microbiological analysis of the donor corneoscleral rim and graft tissue revealed multidrug-resistant *Klebsiella pneumoniae*, sensitive only to colistin. The infection was successfully managed with urgent therapeutic penetrating keratoplasty (TPK) and intensive topical colistin therapy. At 3 months, the patient achieved a best-corrected visual acuity of 20/30. This case highlights that urgent surgical intervention, early microbiological diagnosis, and timely initiation of organism-specific therapy are key to the successful management of post-DALK IIK.

Keywords: Colistin, donor-to-host transmission, interface infectious keratitis, *Klebsiella pneumoniae*, multidrug-resistant

INTRODUCTION

Deep anterior lamellar keratoplasty (DALK) is a widely accepted technique for treating corneal ectasia and stromal pathologies, offering better outcomes with fewer complications by preserving the endothelium. However, one of the emerging concerns is postoperative microbial keratitis, known as interface infectious keratitis (IIK). It can be a devastating and potentially sight-threatening complication if not managed timely, especially in donor-related contamination with multidrug-resistant (MDR) organisms.

Although many microbes can cause IIK, Candida species are the most common. Only four cases due to *Klebsiella pneumoniae* (KP) have been reported.[1-4] Thus, more data are needed on its presentation and management to enable early recognition and prevent severe outcomes. This case highlights the earliest signs at presentation, its differentiating clinical features from fungal etiology, and key points for successful management.

Access this article online	
Website: https://journals.lww.com/saao	Quick Response Code
DOI: 10.4103/SAOJ.SAOJ_9_26	

CASE REPORT

A 17-year-old male with advanced keratoconus underwent DALK in the left eye. Preoperatively, UCVA was 6/24 in the right eye, improving to 6/9 with correction, and 3/60 in the left eye with no improvement due to apical scarring. After

Rakhi Kusumesh, Ashmita Adhikari, Nisha Jha, Abhishek Kumar, Surbhi Sinha

Cornea and Refractive Services, Regional Institute of Ophthalmology, Indira Gandhi Institute of Medical Sciences, Patna, Bihar, India

Address for correspondence: Dr. Rakhi Kusumesh, Cornea and Refractive Services, Regional Institute of Ophthalmology, Indira Gandhi Institute of Medical Sciences, Patna, Bihar, India.
E-mail: drkrakhi@yahoo.com

Submitted: 27-01-2026 **Revised:** 16-02-2026
Accepted: 16-02-2026 **Published:** ***

How to cite this article: Kusumesh R, Adhikari A, Jha N, Kumar A, Sinha S. Donor-related multidrug-resistant *Klebsiella pneumoniae* causing severe interface keratitis following deep anterior lamellar keratoplasty. South Asian Acad Ophthalmol J 2026;XX:XX-XX.

informed consent, DALK was performed under peribulbar anesthesia using a manual layer-by-layer dissection. After baring the DM, an 8.5 mm donor cornea was secured with 10-0 nylon sutures. The procedure was uneventful. The donor was a 65-year-old patient from the intensive care unit (ICU). Cornea with 3 mm scleral rim was excised within 3 h of death, and the tissue was preserved in Cornisol. Transplantation was performed on day 5. Preoperative evaluation showed mild stromal edema, central and paracentral Descemet's membrane folds with an endothelial cell (EC) density of 2010 cells/mm^2.

On postoperative day 1, the patient developed pain, mucopurulent discharge, ciliary congestion, and visual axis interface infiltrates [Figure 1a and b]. Anterior segment optical coherence tomography confirmed deposits at the graft-host junction [Figure 1c]. Suspecting bacterial or fungal infection, we initiated fortified antibiotics, topical natamycin, and cycloplegics; donor rim and storage media were sent for microbiology. In view of the rapid progression of the infiltrates, the lamellar graft along with host DM was excised on the same day, followed by the first therapeutic penetrating keratoplasty (TPK) performed with a 10 mm donor cornea (EC: 1732 cells/mm^2). Host trephination was oversized by 1.5 mm to include the involved graft host junction. The anterior chamber was irrigated with vancomycin (1 mg/0.1 mL) and voriconazole (50 µg/0.1 mL). The excised graft, host DM, and corneal scrapings underwent microbiological analysis. However, the full-thickness stromal infiltrates reappeared in the graft with hypopyon despite intensive fortified antibiotic drops [Figure 1d].

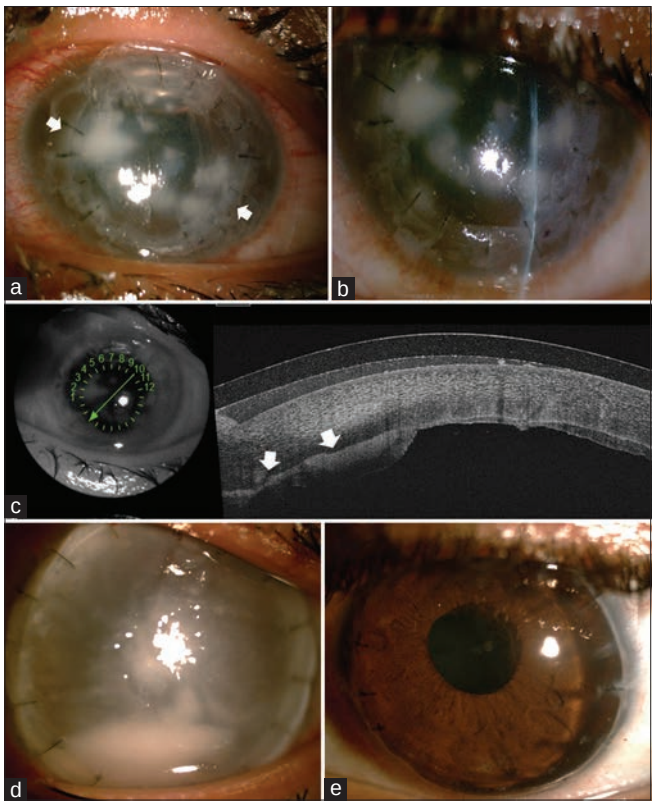

Figure 1: (a) Presence of multiple white-colored infiltrates at the graft-host interface involving the visual axis and graft-host junction (white arrow) following an uneventful deep anterior lamellar keratoplasty, (b) worsening of keratitis with coalescence of infiltrates, (c) infiltrates involving interface and graft-host junction on anterior segment optical coherence tomography (white arrow), (d) recurrence of infiltrate and hypopyon after first therapeutic penetrating keratoplasty (TPK), (e) patient 20/30 vision following second TPK with optical grade donor cornea and intense medical therapy with topical colistin

Cultures from donor rim, storage media, explanted graft, and corneal scraping revealed KP, confirming donor-transmitted infection. Table 1 summarizes culture results across surgical stages. The strain was resistant to multiple antibiotics and sensitive only to colistin, thus labeled MDR-KP. Hourly topical colistin (0.19%) with broad-spectrum antibiotics, corticosteroids, and cycloplegics was initiated, but no improvement was seen within 24 h.

As the infiltrate recurred and involved the graft as well as the graft–host junction, a second TPK was performed using an 11-mm optical-grade donor cornea (EC: 3022 cells/mm^2). However, microbiological culture of this sample showed no growth. The anterior chamber was irrigated with colistin (1 mg/mL). Postoperatively, topical colistin was maintained two-hourly, alongside corticosteroids and cycloplegics. The infection resolved completely by postoperative day 1 [Figure 1e] with no recurrence. Colistin (4×/day) and tapering corticosteroids continued for 6 weeks. At 3 months, the graft remained clear with BCVA of 6/9. The mate cornea from the same donor used for penetrating keratoplasty in another patient (preservation-to-transplant interval: 1 day) yielded an uneventful outcome.

Table 1: Microbiological culture results from different surgical stages and sample sources in the management of postdeep anterior lamellar keratoplasty interface infectious keratitis

Surgery performed	Sample (culture report)
DALK	Recipient cornea (not performed) Donor rim (MDR-KP) Storage media (MDR-KP)
First TPK	Previous lamellar graft (MDR-KP) Donor rim (no growth) Storage media (no growth)
Second TPK	First TPK graft (no growth) Donor rim (no growth) Storage media (no growth)

DALK: Deep anterior lamellar keratoplasty, TPK: Therapeutic penetrating keratoplasty, MDR-KP: Multidrug-resistant *Klebsiella pneumoniae*

DISCUSSION

Postkeratoplasty microbial keratitis remains one of the most devastating complications. In DALK, IIK was first reported by in 1999. Since then, to the best of our knowledge, 19 cases have been reported.[5] In contrast to PK, DALK offers a close environment for developing infectious keratitis due to the corneal interface between the donor graft and the host cornea. Among causative microbes, Gram-negative KP is a nosocomial pathogen, difficult to control and often MDR with limited therapeutic options. Thus, early identification and targeted therapy are essential.

In literature, clinical characteristics, course, and outcome of IIK in DALK have mainly been described in fungal etiology. IIK caused by KP shares a similar clinical picture like the presence of scattered white or cream-colored interface deposits. However, early graft-host junction involvement, presence of hypopyon, and rapid progression with coalescing infiltrates and overlying inflammation differentiate it from fungal IIK. Time of onset is another key differentiator. All reported cases documented their very acute onset either on postoperative day 1 or 2, likely due to donor-host transmission and high virulence of the organism.[1-4] In contrast, fungal infections may manifest as late as 2.5 months postoperatively.[6] Table 2 summarizes the clinical features and outcomes of post-DALK IIK caused by KP.

Our case and two previous reports showed positive donor tissue rim culture for KP, confirming the donor-to-host transmission.[1,4] In both, the donors were ICU patients; one had renal failure with diabetes mellitus. It is known that prolonged hospitalization and extended death-enucleation time increase microorganism prevalence in donor corneas.[7] A higher incidence of gram-negative bacilli from cadaveric eyes has been reported among organisms. Although it is unclear whether positive corneal rim cultures correlate with postoperative infection, the risk of developing postoperative infection seems more significant.[7] Thus, a positive rim culture must prompt close patient monitoring.

Management of post-DALK IIK remains challenging due to the deeper location of infiltrates, limited scraping access, poor topical drug penetration, and the need of urgent surgical intervention. In addition, no treatment algorithm has been defined yet. Literature shows that almost all reported cases required repeat DALK or PK, irrespective of etiology.

Our case was particularly challenging due to (1) the rapid progression of keratitis, (2) early graft-host junction involvement, (3) the donor-host transmission, (4) the

Table 2: Clinical features, donor profile, and outcomes of postdeep anterior lamellar keratoplasty interface infectious keratitis caused by *Klebsiella pneumoniae*

Author and year	Indication	Onset of symptoms	Clinical features	Re DALK or TPK	Culture of excised lamellar graft	Donor detail	Status of mate donor cornea	Drug sensitivity profile	Final outcome at 3 months
Zarei-Ghanavati S, *et al.*, 2010	Keratoconus	POD 2	Multiple infiltrates in the donor-recipient interface	TPK on POD 3	KP	KP Preservation=Optisol GS Culture of donor rim-KP	NA	Ceftazidime	20/20 at the end of 3 months
Egrilmez S, *et al.*, 2013	Keratoconus	POD 1	Multiple white infiltrates in the donor-recipient interface and at graft-host junction	TPK on POD 2	KP	Donor was in ICU Culture-no yield	NA	Meropenem and imipenem	20/24 at the end of 1 year
Bajracharya L, *et al.*, 2015	Granular dystrophy	POD 1	Whitish infiltrate at graft-host junction with severe AC reaction	Re DALK on POD 1 TPK on POD 5	KP	Donor age-36 years Preservation-MK media for 4 days Culture of rim-no detail	NA	Imipenem, tigecyclin, gatifloxacin	20/60 at 6 weeks
Basak S, *et al.*, 2019	Post-HSVK scar	POD 2	Infiltrates at interface along graft host the junction and hypopyon	TPK on POD 2	KP, *E. coli*	Donor-diabetic, renal failure KP	NA	Colistin	20/40 at 3 months
Current Study	Keratoconus	POD 1	Multiple white infiltrates in the donor-recipient interface and at graft-host junction	TPK on POD 1 Then repeat TPK on POD 4	KP	Donor was in ICU, preservation to tranplantation time-6 days Culture-KP Preservation=Cornisol	No postoperative infection	Colistin	20/30 at the end of 3 months

TPK: Therapeutic penetrating keratoplasty, POD: Postoperative day, MK: McCarey Kaufman, HSVK: Herpes simplex virus keratitis, *E. coli*: *Escherichia coli*, KP: *Klebsiella pneumonia*, NA: Not available, DALK: Deep anterior lamellar keratoplasty, GS: Gentamicin-streptomycin, AC: Anterior chamber, ICU: Intensive care unit

need for urgent surgery, and the most challenging part, (5) the presence of MDR-KP. To manage MDR Gram-negative bacteria, Colistin has reemerged as a treatment for MDR Gram-negative infections. Jain *et al*. first reported the use of topical colistin for corneal graft infections with MDR Pseudomonas aeruginosa in 2014.[8] In our case, topical colistin (0.19%) combined with repeat keratoplasty achieved complete resolution without recurrence.

In summary, urgent keratoplasty, early identification of the causative organism, and timely initiation of targeted therapy were key to the successful management of post-DALK IIK in our patient.

Declaration of patient consent

The authors certify that they have obtained all appropriate patient consent forms. In the form, the patient has given his consent for his images and other clinical information to be reported in the journal. The patient understands that name and initials will not be published and due efforts will be made to conceal identity, but anonymity cannot be guaranteed.

Acknowledgments

We thank Dr. Lalan Kumar Arya (Ocular microbiologist) and Miss Anita Kumari, who performed microbiological examinations of all samples.

Financial support and sponsorship

Nil.

Conflicts of interest

There are no conflicts of interest.

REFERENCES

1. Zarei-Ghanavati S, Sedaghat MR, Ghavami-Shahri A. Acute *Klebsiella pneumoniae* interface keratitis after deep anterior lamellar keratoplasty. Jpn J Ophthalmol 2011;55:74-6.
2. Egrilmez S, Palamar M, Sipahi OR, Yagci A. Extended spectrum beta-lactamase producing *Klebsiella pneumoniae*-related keratitis. J Chemother 2013;25:123-5.
3. Bajracharya L, Sharma B, Gurung R. A case of acute postoperative keratitis after deep anterior lamellar keratoplasty by multidrug resistant *Klebsiella*. Indian J Ophthalmol 2015;63:344-6.
4. Basak S, Basak SK, Saha S. Acute interface infectious keratitis with multidrug resistant *Klebsiella* and *Escherichia coli* following deep anterior lamellar keratoplasty. Indian J Ophthalmol 2020;68:1678-80.
5. Gao Y, Li C, Bu P, Zhang L, Bouchard CS. Infectious interface keratitis (IIK) following lamellar keratoplasty: A literature review. Ocul Surf 2019;17:635-43.
6. Kodavoor SK, Dandapani R, Kaushik AR. Interface infectious keratitis following deep anterior lamellar keratoplasty. Indian J Ophthalmol 2016;64:597-600.
7. Wilhelmus KR, Hassan SS. The prognostic role of donor corneoscleral rim cultures in corneal transplantation. Ophthalmology 2007;114:440-5.
8. Jain R, Murthy SI, Motukupally SR. Clinical outcomes of corneal graft infections caused by multi-drug resistant *Pseudomonas aeruginosa*. Cornea 2014;33:22-6.

Case Report

"Ocular Surface Squamous Neoplasia Mimicking as Vascularised Corneal Opacity" – An Unusual Case

ABSTRACT

To discuss the management of a rare case of ocular surface squamous neoplasia (OSSN) mimicking a vascularized corneal opacity. A 71-year-old patient presented with a gradually progressive painless white lesion in the right eye for 1 year and was diagnosed as vascularized corneal opacity elsewhere and referred to our clinic for corneal transplantation. On careful examination, the lesion was elevated, gelatinous, purely corneal, originating from the inferior limbus and had feeder vessels. Clinical suspicion of OSSN prompted rapid evaluation with anterior segment optical coherence tomography (AS-OCT) and impression cytology, thus confirming the diagnosis. He was treated with 4 cycles of topical Mitomycin C (MMC) 0.02% which resulted in complete resolution and restoration of normal visual acuity. No recurrence and MMC toxicity were noted at 1-year follow-up. OSSN is a challenging diagnosis requiring high degrees of clinical suspicion by the general ophthalmologist. Even though the common site of lesion is limbus or conjunctiva, it may rarely present as a purely corneal lesion too, as seen in our case. Careful clinical examination, AS-OCT and impression cytology are rapid and noninvasive methods of diagnosis in such cases. And timely instillation of topical chemotherapy helps in salvaging useful vision with maximum efficacy, debarring the surgical complications.

Keywords: Anterior segment optical coherence tomography, corneal mass, impression cytology, ocular malignancy, ocular surface squamous neoplasia

INTRODUCTION

Ocular surface squamous neoplasia (OSSN) represents a spectrum of dysplastic and neoplastic lesions of the conjunctival and corneal epithelium, ranging from mild dysplasia to invasive squamous cell carcinoma.[1-7] It is the most common non-pigmented malignancy of the ocular surface and typically arises from the limbal region. Risk factors include ultraviolet radiation exposure, advanced age, immunosuppression, and human papillomavirus infection. Clinically, OSSN may present with a variety of appearances such as leukoplakic, papilliform, gelatinous, or nodular lesions, often associated with feeder vessels. However, atypical presentations may mimic benign ocular surface conditions such as pterygium, pinguecula, or vascularized corneal opacity, leading to diagnostic challenges. Early and accurate diagnosis is essential because delayed recognition may result in local invasion and visual morbidity. This report highlights an unusual case of OSSN presenting as a vascularized corneal opacity and emphasizes the role of careful clinical examination and non-invasive diagnostic modalities in establishing the diagnosis.[1-7]

CASE REPORT

A 71-year-old farmer presented with a gradually progressive painless whitish lesion over the right eye for 1 year. There

Hitisha Mittal, Gaurav Gupta[1]

Department of Ophthalmology, VMMC and Safdarjung Hospital, New Delhi, India, [1]Department of Ophthalmology, Eye Sure Super Speciality Eye Hospital, Bathinda, Punjab, India

Address for correspondence: Dr. Gaurav Gupta,
Eye Sure Super Speciality Eye Hospital, Bathinda - 151 001, Punjab, India.
E-mail: gauravucms08@gmail.com

Submitted: 29-01-2026 **Revised:** 26-02-2026
Accepted: 28-02-2026 **Published:** ***

Access this article online

Website: https://journals.lww.com/saao

DOI: 10.4103/SAOJ.SAOJ_23_26

Quick Response Code

How to cite this article: Mittal H, Gupta G. "Ocular surface squamous neoplasia mimicking as vascularised corneal opacity" – An unusual case. South Asian Acad Ophthalmol J 2026;XX:XX-XX.

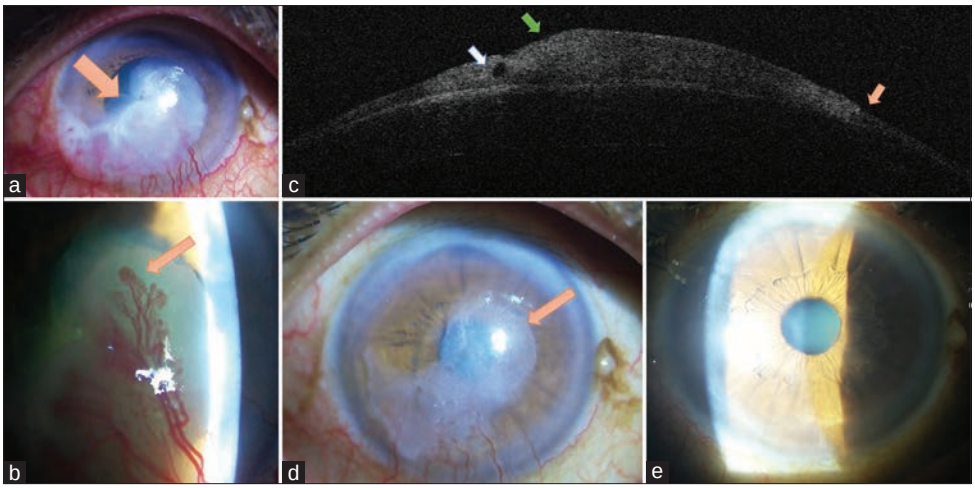

Figure 1: (a) Slit lamp photograph of the right eye showing an elevated gelatinous vascular mass (marked by arrow) extending from inferior limbus and encroaching nearly two-thirds of cornea. (b) Magnified view of feeder vessels showing hairpin configuration (marked by arrow) and arborizing pattern over the lesion. (c) anterior segment optical coherence tomography scan through lesion showing thickened hyper-reflective corneal epithelium (marked by green arrow), abrupt transition from healthy to abnormal cornea (marked by orange arrow), and dilated feeder vessel (marked by white arrow). (d) Dramatic reduction in lesion size and vascularity after the first cycle of topical Mitomycin C (MMC). (e) Complete resolution of lesion after completion of 3 cycles of topical MMC

was no history of preceding ocular trauma or surgery. He was diagnosed as vascularized corneal opacity elsewhere and referred to our clinic for corneal transplantation.

At presentation, his best corrected visual acuity (BCVA) was finger counting close to the face and 20/20 in the right and left eye, respectively. Slit lamp examination of the right eye revealed a whitish, vascularized lesion over the cornea. On careful examination, we noted that the lesion was originating from the inferior limbus, was elevated, gelatinous lesion with pseudopodia configuration, and encroached up to two-thirds of the cornea [Figure 1a]. There were multiple dilated vessels with hair pin configuration and an arborizing pattern suggestive of feeder vessels [Figure 1b]. The left eye was normal. There were no palpable cervical lymph nodes.

Clinical findings raised suspicion of ocular surface squamous neoplasia (OSSN). An anterior segment optical coherence tomography (AS-OCT) scan through the lesion revealed thickened hyperreflective corneal epithelium and an abrupt transition from healthy to abnormal cornea, and the presence of a vessel in the mass [Figure 1c]. Diagnosis of OSSN was confirmed with impression cytology, which revealed atypical squamous cells. Patient tested negative for Human Immunodeficiency Virus.

The patient was started on topical Mitomycin C (MMC) 0.02% four times a day for 1 week, followed by a drug holiday for 1 week. There was a significant reduction in size and vascularity after the first MMC cycle [Figure 1d]. Topical MMC was continued for 3 more cycles, which resulted in complete resolution of the lesion [Figure 1e] and BCVA of 20/25. The patient was followed up closely and did not show any recurrence at 1 year. The patient is currently under follow-up every 3 months and did not show any signs of MMC toxicity at 1-year follow-up.

DISCUSSION

OSSN is a broad term encompassing corneal and conjunctival squamous epithelial malignancies, namely corneal epithelial dysplasia, conjunctival intra-epithelial neoplasia, squamous cell carcinoma and mucoepidermoid carcinoma.[1]

OSSN lesion is usually a limbal location but can rarely present as a purely corneal lesion too. A rapidly growing gelatinous mass arising from the limbus and encroaching over the surface of the cornea; feeder vessels with hairpin configuration and arborizing pattern; and keratinization over the surface should raise suspicion of malignancy. Early OSSN lesions with conjunctival involvement should be differentiated from the common conjunctival degenerative conditions like pterygium and pinguecula by a thorough history and examination, as untreated OSSN can rapidly progress to invade the eye and orbit. Similarly, OSSN lesions with pure corneal involvement should be carefully differentiated from a vascularized corneal opacity (as in our case). A general ophthalmologist should carefully examine such patients to arrive at the diagnosis. While corneal OSSN lesions present as an elevated, gelatinous, rapidly growing mass with corneal thickening, a corneal opacity is associated with corneal thinning and a preceding history of either ocular surgery, trauma, inflammation or infection. An accurate diagnosis in such cases is pertinent to avoid performing keratoplasty (as

noted in our case) which can prove fatal due to seeding and metastasis of malignant cells during surgery.[2]

Careful clinical examination is of paramount importance and helps in making a clinical diagnosis in most of the cases. Non-invasive, rapid and advanced modalities such as high-resolution AS-OCT and impression cytology aid in OSSN diagnosis. Incision biopsy is not preferred due to the risk of local spread.[3,4]

Treatment options include medical therapy (topical chemotherapy and immunotherapy) and surgery. While surgical excision is the gold standard, there are several morbid challenges associated with this approach, including extensive scarring, symblepharon formation, limbal stem cell deficiency (LSCD), cosmetic disfigurement, and recurrence due to residual tumor. Also, in our case, isolated large corneal OSSN lesions cannot be surgically excised due to the risk of perforation, postoperative corneal scarring, and loss of vision.[5]

To combat these surgical challenges, medical therapy with MMC was preferred in our patient. It was instilled in a cyclical manner (1 week on and 1 week off) to maximise efficacy and minimize complications such as conjunctival congestion, punctal stenosis, and epithelial toxicity. MMC was compounded for each cycle under sterile conditions in the clinic and dispensed to the patient for easy use at home. It was refrigerated at 2°C–6°C for 7 days (I cycle) and discarded at the end of each cycle. Even though the lesion completely resolved after 3 cycles, MMC was completed for 4 cycles, and the patient was followed up every 2 weeks for 3 months, every 4 weeks for the next 6 months, and every 3 months thereafter.

Studies have reported LSCD secondary to topical MMC therapy due to the inhibition of cell division of malignant and limbal stem cells. There is no common consensus on the frequency and duration of follow-up in such patients. However, the treating ophthalmologists often monitor these patients closely for recurrent or persistent epithelial defects, corneal vascularization, and whorl-like epitheliopathy, as these signs can develop months to years after cessation of MMC.[6,7]

To summarise, OSSN may mimic a vascularized corneal opacity. Careful clinical examination, high-resolution AS-OCT, and impression cytology help in rapid diagnosis and timely institution of topical chemotherapy, which aids in complete resolution, as seen in our patient.

Declaration of patient consent

The authors certify that they have obtained all appropriate patient consent forms. In the form, the patient has given his consent for his images and other clinical information to be reported in the journal. The patient understands that name and initials will not be published and due efforts will be made to conceal identity, but anonymity cannot be guaranteed.

Financial support and sponsorship

Nil.

Conflicts of interest

There are no conflicts of interest.

REFERENCES

1. Alvarez OP, Zein M, Galor A, Karp CL. Management of ocular surface squamous neoplasia: Bowman club lecture 2021. BMJ Open Ophthalmol 2021;6:e000842.
2. Gurnani B, Kaur K. Current concepts and recent updates in the treatment of ocular surface squamous neoplasia. Expert Rev Ophthalmol 2023;18:281-7.
3. Singh S, Mittal R, Ghosh A, Tripathy D, Rath S. High-resolution anterior segment optical coherence tomography in intraepithelial versus invasive ocular surface squamous neoplasia. Cornea 2018;37:1292-8.
4. Singh R, Joseph A, Umapathy T, Tint NL, Dua HS. Impression cytology of the ocular surface. Br J Ophthalmol 2005;89:1655-9.
5. Nanji AA, Moon CS, Galor A, Sein J, Oellers P, Karp CL. Surgical versus medical treatment of ocular surface squamous neoplasia: A comparison of recurrences and complications. Ophthalmology 2014;121:994-1000.
6. Cicinelli MV, Marchese A, Bandello F, Modorati G. Clinical management of ocular surface squamous neoplasia: A review of the current evidence. Ophthalmol Ther 2018;7:247-62.
7. Lichtinger A, Pe'er J, Frucht-Pery J, Solomon A. Limbal stem cell deficiency after topical mitomycin C therapy for primary acquired melanosis with atypia. Ophthalmology 2010;117:431-7.

Case Report

Donor Rim Culture Guided Management of Postpenetrating Keratoplasty *Enterococcus faecalis* Endophthalmitis

ABSTRACT

We report the case of a 27-year-old male who developed early-onset endophthalmitis following penetrating keratoplasty which was done for pseudophakic bullous keratopathy due to a malplaced intraocular lens, implanted during cataract surgery done previously following trauma. Despite a nil visual prognosis, the patient opted for keratoplasty primarily for cosmetic rehabilitation. On postoperative day 1, the graft was clear with a healthy graft-host junction. On the second postoperative day, he developed severe anterior segment inflammation and hypopyon. Ultrasonography revealed dense vitreous echoes suggestive of endophthalmitis. Crucially, routine microbiological evaluation of the donor corneoscleral rim and Cornisol medium (Aurolab, Madurai, India) – mandated by our institutional protocol – grew *Enterococcus faecalis*, and the antibiotic sensitivity report enabled prompt, targeted antimicrobial therapy. Intravitreal piperacillin–tazobactam with dexamethasone, supplemented with topical antimicrobial treatment, led to the resolution of infection. This case highlights the potential utility of donor rim culture at the time of transplantation, a practice that enables early detection and targeted management of donor-transmitted infections.

Keywords: Donor rim culture, endophthalmitis, *Enterococcus faecalis*, intravitreal piperacillin–tazobactam, penetrating keratoplasty

INTRODUCTION

Donor-to-host infection remains one of the most feared complications of corneal transplantation, occurring in up to 2% of grafts and often leading to graft failure or globe loss. A large meta-analysis of 17,614 keratoplasties demonstrated that positive donor rim cultures conferred a 12-fold higher risk of postoperative endophthalmitis, underscoring the strong predictive value of rim microbiology – even before clinical signs emerge.[1] Although fungal contaminants have frequently been implicated, Gram-positive bacteria such as *Enterococcus faecalis* – a nosocomial pathogen with intrinsic multidrug resistance – are increasingly recognized as causes of fulminant postkeratoplasty infections.[2] Economic evaluations further support routine rim culturing in high-volume or resource-limited settings, where early organism-specific therapy markedly improves outcomes.[1,2] In this report, we describe a case of early-onset *E. faecalis* endophthalmitis following penetrating keratoplasty (PK) and highlight how our institution's practice of routine donor rim culture enabled prompt, targeted management that preserved both graft clarity and globe integrity.

Access this article online	
Website: https://journals.lww.com/saao	Quick Response Code
DOI: 10.4103/SAOJ.SAOJ_44_26	

Neha Pathak, Gagan Deep Kaur, Pratima Mishra[1], Amit Mishra, Virendra Agrawal, Vishal Agrawal[2]

Dr Virendra Laser Phaco Surgery Centre, Jaipur, Rajasthan, India, [1]Advanced Eye Care and Retina Centre, Jaipur, Rajasthan, India, [2]Department of Ophthalmology, Agrawal Hospital, Jaipur, Rajasthan, India

Address for correspondence: Dr. Neha Pathak, E-251, Udai Path, Shyam Nagar, Sodala, Ajmer Road, Jaipur - 302 019, Rajasthan, India.
E-mail: pthknh@gmail.com

Submitted: 02-02-2026 **Revised:** 23-02-2026
Accepted: 25-02-2026 **Published:** ***

How to cite this article: Pathak N, Kaur GD, Mishra P, Mishra A, Agrawal V, Agrawal V. Donor rim culture guided management of postpenetrating keratoplasty *Enterococcus faecalis* endophthalmitis. South Asian Acad Ophthalmol J 2026;XX:XX-XX.

CASE REPORT

A 27-year-old male presented with a history of whitening of the cornea in the right eye from past 1½ years. He reported trauma to the right eye in childhood, for which he had undergone cataract surgery with intraocular lens (IOL) implantation. At presentation, his best-corrected visual acuity in the right eye was perception of light present with inaccurate projection of rays in the nasal and superior quadrants. The fellow eye was unremarkable with a normal disc and macula.

Slit-lamp biomicroscopy of the right eye revealed diffuse stromal thickening and opacification. Notably, a three-piece IOL was observed to be stuck over the iris tissue with superior haptic touching the corneal endothelium. The pupillary opening was barely visible. Indirect pupillary reaction in the left eye was sluggish and ill sustained. The posterior segment of the right eye could not be visualized. B-scan ultrasonography of the right eye revealed an acoustically clear vitreous cavity without retinal/choroidal detachment or globe distortion, ruling out phthisis bulbi. Visual evoked potential showed no waveform in the right eye, indicating profound visual dysfunction.

The patient was extensively counselled regarding the poor-nil visual prognosis. However, given the cosmetic disfigurement, he opted for surgical correction. The option of anterior stromal puncture and corneal tattooing using a tattoo gun was also considered, but the patient did not opt for it, citing that the outcome might be cosmetically very different from the "natural eye." Moreover, tattooing without removing the anterior chamber intraocular lens will not stop ongoing mechanical irritation of the endothelium, causing possible recurrence of bullae and epithelial breakdown because the causative haptic contact remains. Hence, PK with IOL explantation was planned and performed uneventfully under local anesthesia.

The donor graft was prepared postcorneal marking and partial trephination of the host cornea in the operating room, after being maintained at room temperature for 30 min before transplantation. It was harvested from a 27-year-old phakic male donor from a hospital-based source. The endothelial cell density was 2667 cells/mm^2. The death-to-preservation interval was 10 h, and the tissue was stored in Cornisol medium (containing gentamicin) for 72 h prior to use. Slit-lamp and specular microscope examinations of the graft, performed at the eye bank, revealed mild to moderate stromal edema with several mild to moderate Descemet's folds.

On postoperative day 1, the corneal graft was optically clear with a healthy graft-host junction and sutures and an anterior chamber reaction of grade 0.5+ cells (according to Standardization of Uveitis Nomenclature Working Group)[3] with no flare. However, by day 2, 4+ anterior chamber cells and dense fibrinous reaction with 1 mm hypopyon and relatively clear graft were noted. Repeat B-scan revealed newly developed hyperechoic foci in the vitreous cavity, suggestive of early endophthalmitis [Figure 1a and b]. Concurrently, the donor corneoscleral rim along with Cornisol medium solution which was sent for microbiological examination at the time of transplantation, grew *E. faecalis* on aerobic pyogenic culture after 24 h of incubation.

Antibiotic sensitivity testing done by Kirby–Bauer Disc Diffusion Method demonstrated the isolated organism to be multidrug resistant.[4] and showed maximum zones of inhibition to Beta-lactam/Beta Lactamase Inhibitor combination group and Linezolid [Figure 2].

Based on the recommendation by our Retina Surgeon due to their previous good experience with the drug, we decided to promptly treat the eye with intravitreal piperacillin–tazobactam (IVPT) injection (225 µg/0.1 mL) combined with dexamethasone (400 µg/0.1 ml) on postoperative day 2. The vitreous tap sample also grew *E. faecalis* on culture. He began showing clinical improvement by postoperative day 4–2 days after the initial injection – and subsequently received further intravitreal injections on days 4 and 6. The rapid, favorable response to IVPT was evident on the slit lamp [Figures 3-5]. The patient was also started simultaneously on topical fortified piperacillin–tazobactam (PT) (hourly), linezolid 0.2% (every 2 h), prednisolone acetate 1% (QID), and atropine 1% (TID). The anterior segment exudates and fibrinoid reaction started retracting, and follow-up ultrasonography showed a marked reduction in vitreous opacities. Although visual acuity remained limited due to pre-existing optic nerve damage, anatomical integrity of the eye was preserved, and graft clarity was maintained.

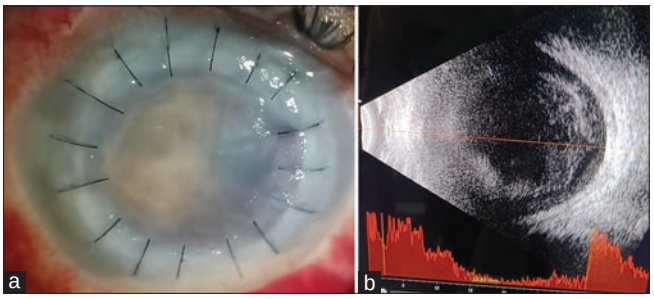

Figure 1: (a) Dense fibrinous reaction and 1mm hypopyon in anterior chamber with relatively clear graft seen on postoperative day 5 (after 1st intravitreal piperacillin–tazobactam injection). (b) B-scan revealing hyper-echoic foci in vitreous cavity on postoperative day 3

Organism Grown : **Enterococcus faecalis**

Antibiotic Sensitivity :

Antibiotics	Zone diameter in mm.				
	Resistant	Intermediate	Sensitive	Result	Interpretation
PENICILLINS					
AMPICILLIN	16		17	20	Sensitive
PENICILLIN -G	14		15	20	Sensitive
CEPHALOSPORINS					
CEFEPIME	14	15-17	18	6	Resistant
CEFOTAXIME	14	15-22	23	6	Resistant
CEFPODOXIME	17	18-20	21	6	Resistant
CEFTRIAXONE	13	14-20	21	6	Resistant
CEFUROXIME	14	15-17	18	6	Resistant
B -LACTAMS/B L I COMBINATIONS					
AMOXYCILLIN/CLAVULANIC ACID	19		20	22	Sensitive
AMPICILLIN/ SULBACTAM	11	12-14	15	23	Sensitive
PIPERACILLIN / TAZOBACTAM	17		18	22	Sensitive
CARBAPENEMS					
ERTAPENEM	13	14-15	16	17	Sensitive
IMIPENEM	13	14-15	16	18	Sensitive
MEROPENEM	13	14-15	16	18	Sensitive
AMINOGLYCOSIDES					
AMIKACIN	14	15-16	17	6	Resistant
GENTAMICIN	12	13-14	15	6	Resistant
NETILMICIN	12	13-14	15	6	Resistant
TOBRAMYCIN	12	13-14	15	6	Resistant
FLUOROQUINOLONES					
CIPROFLOXACIN	15	16-20	21	6	Resistant
LEVOFLOXACIN	15	16-18	19	6	Resistant
MOXIFLOXACIN	20	21-23	24	6	Resistant
OFLOXACIN	14	15-17	18	6	Resistant
MACROLIDES					

Figure 2: Antibiotic sensitivity report showing maximum sensitivity of isolated organism to BetaLactam/BetaLactamase Inhibitor combination group and Linezolid

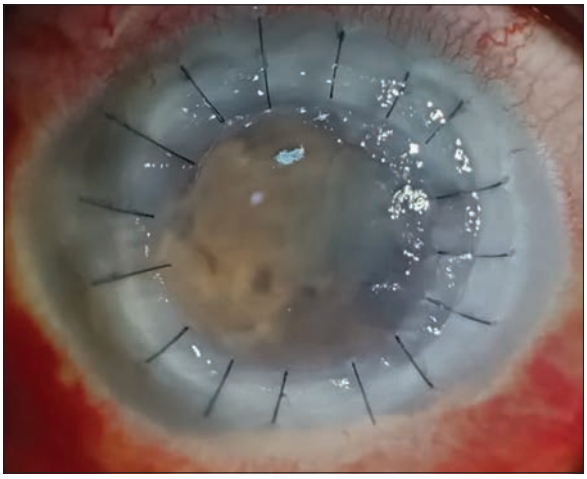

Figure 3: Retracting anterior chamber exudates and receding hypo-yon on postoperative day 5 (after 2nd Intravitreal piperacillin–tazobactam injection)

DISCUSSION

Donor-transmitted infections are among the most feared complications of corneal transplantation, and although relatively rare, they can have devastating consequences. *E. faecalis*, a facultative anaerobic Gram-positive coccus, has emerged as a significant nosocomial pathogen in corneal transplantation, particularly in tissue retrieved from hospital or mortuary settings.[5] While often commensal in the gastrointestinal tract, *E. faecalis* can induce fulminant ocular infections due to its ability to develop intrinsic and acquired antibiotic resistance.[6]

Routine microbiological assessment of donor corneoscleral rims remains a debated practice. There is no published national survey giving a single percentage for how often Indian surgeons send donor corneoscleral rims for microbiological work-up. Proponents argue that positive culture results can facilitate early organism-specific therapy, particularly in cases where clinical signs emerge before culture results of the infected host tissue are available. Critics, however, cite concerns regarding false positives and cost-effectiveness, especially since not all positive rim cultures result in clinical infection.[7]

In our case, the early availability of culture results from the donor rim allowed for swift initiation of targeted intravitreal antibiotic therapy, effectively halting the progression of a potentially devastating infection. Ozkiriş *et al*. studied the safety of IVPT in rabbits using electroretinographic, histopathologic, and morphometric analysis and concluded that 250 microg/0.1 mL PT is the highest nontoxic dose to the normal retinas of adult albino rabbits as intravitreal injection and that PT may be a new,

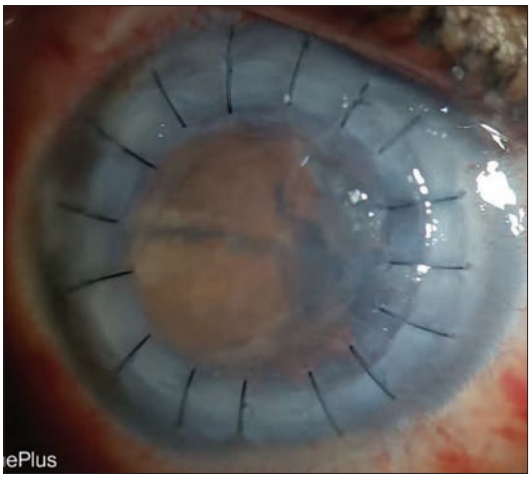

Figure 4: Almost resolved anterior chamber exudates and hypopyon on postoperative day 7 (after 3rd intravitreal piperacillin–tazobactam injection)

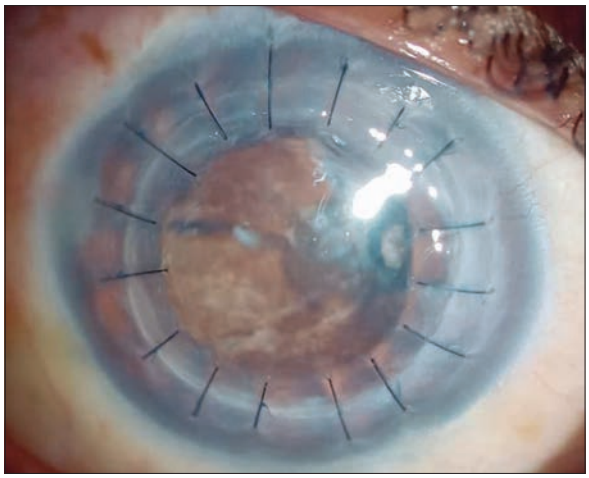

Figure 5: One month postsurgery, the graft was absolutely clear with nil anterior chamber reaction

potentially important drug in the treatment of endophthalmitis as it has a broad antimicrobial spectrum.[8]

Ozkiriş *et al*. also compared the efficacy of intravitreal PT with ceftazidime[9] and vancomycin[10] in experimental *Pseudomonas aeruginosa* and *Staphylococcus epidermidis* endophthalmitis, respectively and concluded that all these drugs were equally effective in treating the respective conditions and therefore, IVPT may be an alternative therapeutic option in the treatment of *P. aeruginosa* and *S. epidermidis* endophthalmitis.

After thorough literature search, eight case reports were found documenting the use of IVPT in endophthalmitis of varying etiologies.[11-18] To the best of our knowledge, ours is the first case of multidrug-resistant *E. faecalis* endophthalmitis after PKP with IOL explantation, treated successfully with IVPT.

Thus, our case underscores the clinical utility of rim cultures, especially in high-volume centers or regions where tissue retrieval occurs in resource-constrained environments prone to nosocomial contamination. Moreover, the case contributes to the growing body of evidence advocating for defined protocols that include routine donor rim cultures as part of the standard transplant workflow.

Declaration of patient consent

The authors certify that they have obtained all appropriate patient consent forms. In the form, the patient(s) has/have given his/her/their consent for his/her/their images and other clinical information to be reported in the journal. The patients understand that their names and initials will not be published and due efforts will be made to conceal their identity, but anonymity cannot be guaranteed.

Financial support and sponsorship

Nil.

Conflicts of interest

There are no conflicts of interest.

REFERENCES

1. Wilhelmus KR, Hassan SS. The prognostic role of donor corneoscleral rim cultures in corneal transplantation. Ophthalmology 2007;114:440-5.
2. Vislisel JM, Goins KM, Wagoner MD, Schmidt GA, Aldrich BT, Skeie JM, *et al.* Incidence and outcomes of positive donor corneoscleral rim fungal cultures after keratoplasty. Ophthalmology 2017;124:36-42.
3. Jabs DA, Nussenblatt RB, Rosenbaum JT, Standardization of Uveitis Nomenclature (SUN) Working Group. Standardization of uveitis nomenclature for reporting clinical data. Results of the first international workshop. Am J Ophthalmol 2005;140:509-16.
4. Basak S, Singh P, Rajurkar M. Multidrug resistant and extensively drug resistant bacteria: A study. J Pathog 2016;2016:4065603.
5. Sudana P, Chaurasia S, Joseph J, Mishra DK. Delayed postoperative interface keratitis due to *Enterococcus faecalis* after descemet membrane endothelial keratoplasty. BMJ Case Rep 2021;14:e238389.
6. D'Oria F, Galeone A, Pastore V, Cardascia N, Alessio G. Multi-drug resistant *Enterococcus faecium* in late-onset keratitis after deep anterior lamellar keratoplasty: A case report and review of the literature. Medicine (Baltimore) 2019;98:e17140.
7. Kiatos E, Armstrong JJ, Hutnik CM, Tsioros SM, Malvankar-Mehta MS, Hodge WG. The value of corneoscleral rim cultures in keratoplasty: A systematic review and cost-effectiveness analysis. Clinicoecon Outcomes Res 2017;9:459-74.
8. Ozkiriş A, Evereklioglu C, Kontaş O, Oner AO, Erkiliç K. Determination of nontoxic concentrations of piperacillin/tazobactam for intravitreal application. An electroretinographic, histopathologic and morphometric analysis. Ophthalmic Res 2004;36:139-44.
9. Ozkiriş A, Evereklioglu C, Akgün H, Eşel D, Caner F, Erkiliç K. A comparison of intravitreal piperacillin/tazobactam with ceftazidime in experimental *Pseudomonas aeruginosa* endophthalmitis. Exp Eye Res 2005;80:361-7.
10. Ozkiriş A, Evereklioglu C, Eşel D, Akgün H, Erkiliç K. The efficacy of intravitreal piperacillin/tazobactam in rabbits with experimental *Staphylococcus epidermidis* endophthalmitis: A comparison with

vancomycin. Ophthalmic Res 2005;37:168-74.
11. Suganeswari G, Shah D, Anand AR. Intravitreal piperacillin-tazobactam in endophthalmitis caused by *Mycobacterium abscessus in silico* ne-filled eye: A case report. Indian J Ophthalmol 2020;68:1471-3.
12. Pathengay A, Mathai A, Shah GY, Ambatipudi S. Intravitreal piperacillin/tazobactam in the management of multidrug-resistant *Pseudomonas aeruginosa* endophthalmitis. J Cataract Refract Surg 2010;36:2210-1.
13. Singh TH, Pathengay A, Das T, Sharma S. Enterobacter endophthalmitis: Treatment with intravitreal tazobactam – Piperacillin. Indian J Ophthalmol 2007;55:482-3.
14. Goel N, Bhambhwani V, Ghosh B. Multidrug-resistant *Pseudomonas aeruginosa* endophthalmitis in a silicone oil-filled eye treated with piperacillin/tazobactam: Report of a case and review of literature. Int Ophthalmol 2015;35:599-602.
15. Uy HS, Leuenberger EU, de Guzman BB, Natividad FF. Chronic, postoperative *Pseudomonas luteola* endophthalmitis. Ocul Immunol Inflamm 2007;15:359-61.
16. Relhan N, Albini T, Pathengay A, Flynn HW Jr. Bilateral endogenous endophthalmitis caused by vancomycin-resistant *Staphylococcus epidermidis* in a neonate. J Ophthalmic Inflamm Infect 2015;5:11.
17. Bhavsar MM, Devarajan TV, Nembi PS, Ramakrishnan N, Mani AK. Metastatic endogenous endophthalmitis: A rare presentation with methicillin-resistant *Staphylococcus aureus* prostatic abscess. Indian J Crit Care Med 2017;21:172-5.
18. Kaur M, Titiyal JS, Sharma N, Chawla R. Successful re-implantation of implantable collamer lens after management of post-ICL methicillin-resistant *Staphylococcus epidermidis* endophthalmitis. BMJ Case Rep 2015;2015:bcr2015212708.

Case Report

Choroidal Neovascularization: A Consequence of Central Serous Chorioretinopathy

ABSTRACT

Central serous chorioretinopathy (CSR) is usually a self-limiting retinal disease associated with serous detachment of the neurosensory retina and alterations of the retinal pigment epithelium, complicated by persistent subretinal fluid accumulation or multiple recurrences. Case description: A 75 years female with best corrected visual acuity of 6/24 was diagnosed with right eye CSR as evidenced by clinical examination of fundus revealing elevation of the retina. Optical Coherence Tomography (OCT) of macula showed presence of subretinal fluid and pigment epithelial detachment in the same eye. Patient was treated with topical NSAIDs. During her three months follow up, her condition did not improve and fundus examination showed presence of subretinal hemorrhage and exudates in the same eye. FFA done showed areas of leakage thus confirming the development of choroidal neovascular membrane (CNVM). She was then treated with anti-VEGF intravitreal injections with her vision improving to 6/9. Conclusion: CSR is a common disease and CNVM seems to be a natural complication of the prolonged disease course. Chronic cases of CSR that persist over an extended period may lead to the development of CNVM.

Keywords: Central serous chorioretinopathy, choroidal neovascularization, pigment epithelial detachment, subretinal fluid

INTRODUCTION

Central serous chorioretinopathy (CSR) is usually a self-limiting retinal disease associated with serous detachment of the neurosensory retina and alterations of the retinal pigment epithelium. Most of the cases resolve spontaneously within several months with good visual recovery, but some may be complicated by persistent subretinal fluid accumulation or multiple recurrences. In such cases, there may be a risk of development of Choroidal neovascular membrane (CNVM).

CASE REPORT

A 75-year-old female presented with gradual painless diminution of vision in the right eye for six months. Her best-corrected distance visual acuity at the time of presentation was 6/24. Posterior segment examination revealed elevation of the retina in the right eye in the foveal region. Macular optical coherence tomography (OCT) of the same eye showed typical feature of CSR [Figure 1], showing subretinal fluid and pigment epithelial detachment (PED). She was given topical nonsteroidal anti-inflammatory drugs and was suggested for lifestyle modification.

On three months of follow-up, her symptoms did not improve. Spectral-domain OCT and fundus fluorescein angiography (FA) were done. FA revelaed leakage at different points in the late phase [Figure 2]. The patient was diagnosed with choroidal neovascularization membranes (CNVM) secondary to chronic CSR [Figure 3]. The patient was treated with two intravitreal injections of bevacizumab (0.5 ml/1.25 mg). After two

Rachni Gurung, Meenali Karna, Eli Pradhan
Department of Medical Retina, Tilganga Institute of Ophthalmology, Kathmandu, Nepal

Address for correspondence: Dr. Rachni Gurung, Tilganga Institute of Ophthalmology, Kathmandu, Nepal.
E-mail: grgrachni@gmail.com

Submitted: 07-06-2025
Accepted: 27-01-2026 **Published:** ***

Access this article online	
Website: https://journals.lww.com/saao	Quick Response Code
DOI: 10.4103/SAOJ.SAOJ_3_26	

How to cite this article: Gurung R, Karna M, Pradhan E. Choroidal neovascularization: A consequence of central serous chorioretinopathy. South Asian Acad Ophthalmol J 2026;XX:XX-XX.

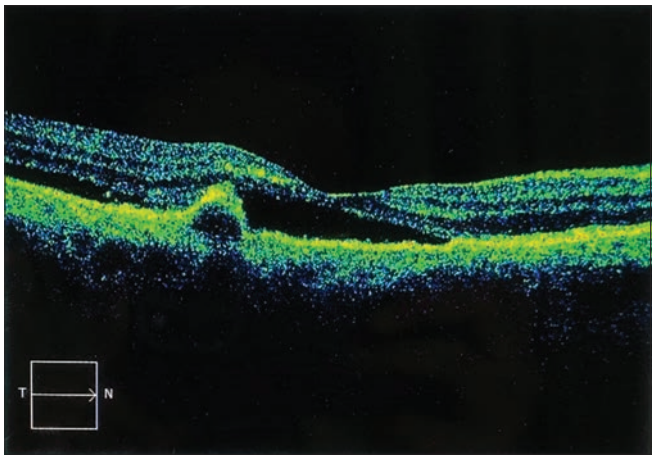

Figure 1: RE optical coherence tomography shows hyperreflective material with subretinal fluid and pigment epithelial detachment

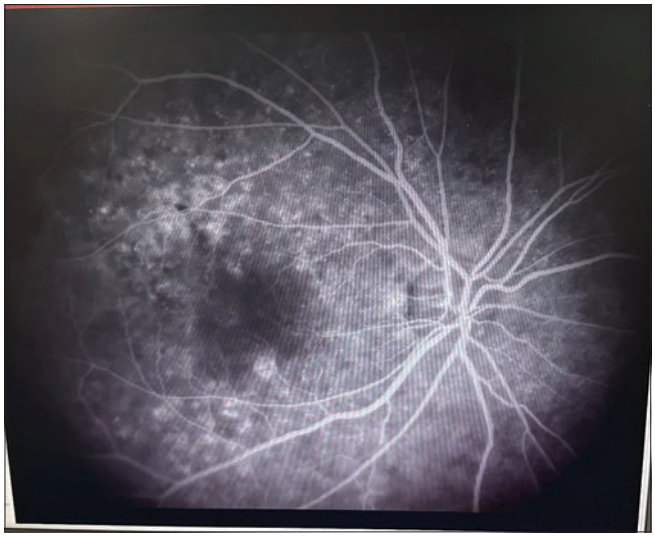

Figure 2: Late phase fundus fluorescein angiography shows increase in intensity of hyperfluorescence areas with leakage at 3 different points

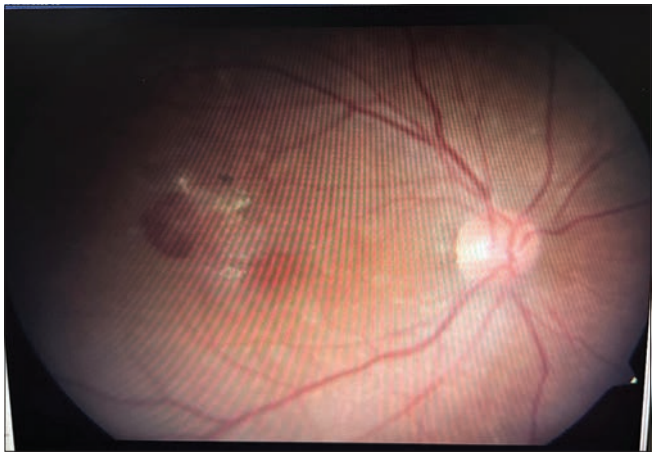

Figure 3: Color fundus photography shows subretinal exudates and subretinal hemorrhage in the macular area in the right eye

intravitreal injections of bevacizumab, her vision improved to 6/9. There was no recurrence of symptoms till date.

DISCUSSION

CNVM in chronic CSR is included in the group of pachychoroid neovasculopathy, which is defined as type 1 neovascularization associated with choroidal thickening in the absence of characteristic age-related macular degeneration or degenerative changes.[1] CSR is a common disease, and choroidal neovascularization (CNV) seems to be a natural complication of the prolonged disease course.[2] It is difficult in detecting a CNV component as the clinical features can be seen in chronic CSR both with and without CNV. Chronic CSR with CNVM may have features such as retinal PED, Subretinal fluid (SRF), intraretinal fluid, cystoid macular degeneration, retinal atrophy, and diffuse irregular hyperfluorescence on FA.[3]

Early CNV detection, with prompt and adequate treatment, is crucial for a good visual outcome. CNVM may be more prevalent in patients over 50 years of age with chronic CSR.[4] Recent studies have shown that anti-vascular endothelial growth factor (VEGF) intravitreal injections have shown effectiveness in treating CNVMs secondary to CSR.[5]

CONCLUSION

Chronic cases of central serous retinopathy (CSR) that persist over an extended period may lead to the development of choroidal neovascular membrane (CNVM). Administering anti-VEGF intravitreal injections in these instances may prove advantageous for enhancing visual outcomes.

Declaration of patient consent

The authors certify that they have obtained all appropriate patient consent forms. In the form, the patient(s) has/have given his/her/their consent for his/her/their images and other clinical information to be reported in the journal. The patients understand that their names and initials will not be published and due efforts will be made to conceal their identity, but anonymity cannot be guaranteed.

Financial support and sponsorship

Nil.

Conflicts of interest

There are no conflicts of interest.

REFERENCES

1. Pang CE, Freund KB. Pachychoroid neovasculopathy. Retina 2015;35:1-9.
2. Spaide RF, Campeas L, Haas A, Yannuzzi LA, Fisher YL, Guyer DR, *et al*. Central serous chorioretinopathy in younger and older adults. Ophthalmology 1996;103:2070-9.
3. Sulzbacher F, Schütze C, Burgmüller M, Vécsei-Marlovits PV, Weingessel B. Clinical evaluation of neovascular and non-neovascular chronic central serous chorioretinopathy (CSC) diagnosed by swept source optical coherence tomography angiography (SS OCTA). Graefes Arch Clin Exp Ophthalmol 2019;257:1581-90.
4. Shiragami C, Takasago Y, Osaka R, Kobayashi M, Ono A, Yamashita A, *et al.* Clinical features of central serous chorioretinopathy with type 1 choroidal neovascularization. Am J Ophthalmol 2018;193:80-6.
5. Cozzupoli GM, Sacconi R, Tombolini B, Fantaguzzi F, Servillo A, Menean M, *et al*. Long-term predictors of anti-VEGF treatment response in patients with neovascularization secondary to CSCR: A longitudinal study. Graefes Arch Clin Exp Ophthalmol 2024;262:73-80.

Case Report

Demystifying Pseudo Papilledema: A Case of Optic Disc Drusen

ABSTRACT

Pseudopapilledema due to optic disc drusen (ODD) can closely mimic true papilledema, creating a diagnostic challenge in patients presenting with chronic headaches. We report a 26-year-old male referred for evaluation of suspected papilledema. Visual acuity, color vision, and pupillary reactions were normal. Fundus examination revealed bilaterally elevated optic discs with ill-defined margins, irregular "lumpy-bumpy" contours, and absent physiologic cups without hyperemia or vessel obscuration. B-scan ultrasonography demonstrated a highly reflective elevated optic nerve head with persistent reflectivity on reduced gain, confirming ODD. Multimodal imaging assists in differentiating pseudopapilledema from true optic disc edema. Early recognition of ODD prevents unnecessary neuroimaging and invasive investigations in patients with headache.

Keywords: Optic Disc Drusen, papilledema, pseudo papilledema

Pseudopapilledema, often masquerading as true papilledema, poses a diagnostic conundrum in patients with chronic headaches, potentially leading to unnecessary neuroimaging or invasive procedures. Optic disc drusen (ODD), calcified axonal deposits within the optic nerve head, represent the most common etiology, affecting up to 2% of the population and mimicking raised intracranial pressure (ICP) in 75% of bilateral cases. Distinguishing these benign anomalies from life-threatening papilledema is paramount to avert misdiagnosis.

A 26-year-old male with complaints of chronic headache was referred from the neuromedicine department to rule out any features of papilledema.

On examination, his UCVA was 20/20 OU, color vision normal, and pupils were bilaterally brisk.

On dilated fundus examination, we were surprised to see that the disc margins in both eyes were ill-defined, irregular, with a "lumpy-bumpy" appearance and absent cup, without hyperemia or vessel obscuration. The clinical diagnosis of ODD OU was made [Figure 1].

Access this article online	
Website: https://journals.lww.com/saao	Quick Response Code
DOI: 10.4103/SAOJ.SAOJ_2_26	

B-scan also revealed that optic nerve head was elevated and highly reflective OU which maintained the high signal density even on decreasing the gain settings [Figures 2 and 3].

The diagnosis of pseudo papilledema due to ODD OU was made in this patient who was referred to rule out papilledema!!!

This case exemplifies ODD's propensity for pseudopapilledema, particularly in young adults, where buried drusen evade superficial detection until adolescence.[1] Multimodal imaging – fundus autofluorescence for hyperautofluorescence, ultrasonography for acoustic shadowing, and optical

J. Nimmy

Department of Ophthalmology, Government Medical College, Thrissur, Kerala, India

Address for correspondence: Dr. J. Nimmy, Department of Ophthalmology, Government Medical College, Thrissur - 680 596, Kerala, India.
E-mail: nimmyj90@gmail.com

Submitted: 25-01-2026
Accepted: 27-01-2026 **Published:** ***

How to cite this article: Nimmy J. Papilloedema or pseudopapilloedema?? South Asian Acad Ophthalmol J 2026;XX:XX-XX.

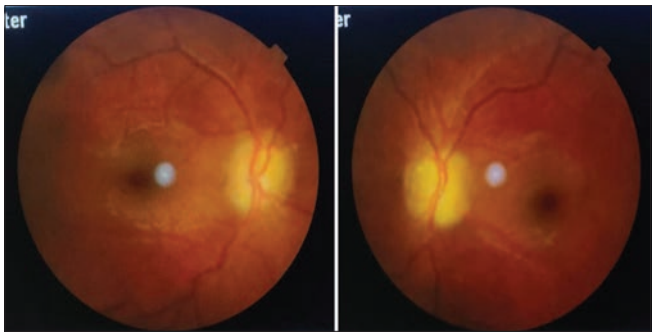

Figure 1: Fundus photo OD and OS

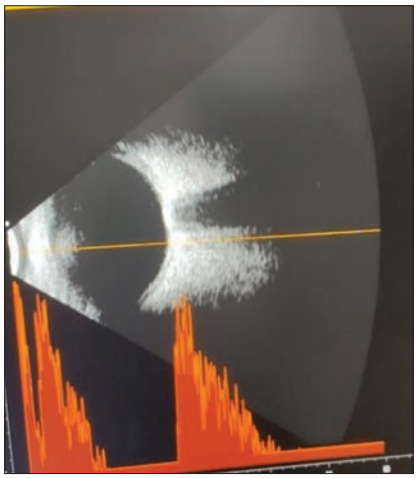

Figure 2: B scan OD

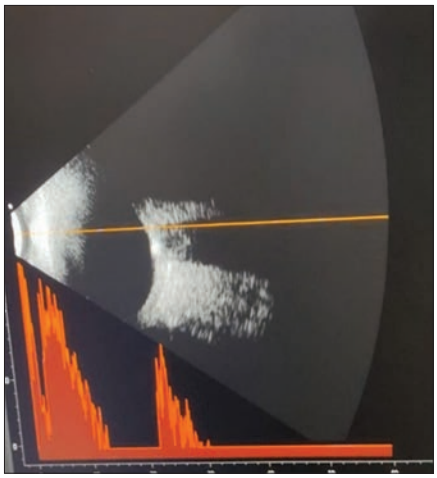

Figure 3: B SCAN OS

coherence tomography (OCT) for peripapillary nerve fiber layer defects – helps differentiation from true edema.[2] Complications such as anterior ischemic optic neuropathy (AION) or field loss occur in 75% but rarely impair acuity.[3] Associations with retinitis pigmentosa or angioid streaks warrant systemic evaluation.[4]

This vignette encapsulates ODD's chameleonic guise, where buried drusen forge pseudopapilledema, confounding headache workups.[5] Fundus hallmarks – lumpy elevation, vascular tortuosity, and cup absence – herald suspicion, yet superficial obscurity in youth delays detection until teens, when extrusion unveils pearl-like nodules.[6] Our patient's adult presentation aligns with gradual unmasking, evading birth absence but courting misattribution to migraine or tension cephalalgia.

The pathogenesis implicates axonal debris calcification amid dysplastic vasculature and compressive ischemia.[2] Bilateral predilection (75%) and sporadic dominance underscore genetic mosaicism, although associations with retinitis pigmentosa (via MFRP mutations), angioid streaks (25% co-occurrence), or Alagille syndrome (90%) mandate syndromic scrutiny.[7] The complications, although infrequent include AION in younger people with prior visual obscurations, field defects (arcuate or blind spot) in 75%, and rare neovascular sequelae.[8]

B-scan detects calcification through persistent reflectivity and shadowing.[3] FAF elicits autofluorescence from mitochondrial-rich drusen, while OCT quantifies peripapillary thinning or peripapillary hyperreflective ovoid mass-like structures, distinguishing edema's fluid halo.[9] In pseudotumor cerebri overlaps, ODD prevalence surges, confounding ICP metrics and advocating OCT volumetry.

This report reinforces algorithmic triage: Suspect pseudopapilledema in atypical discs, deploy ultrasonography foremost, and reserve lumbar puncture for validated edema.[5]

CONCLUSION

Vigilant ophthalmoscopy and targeted B-Scan ultrasonography demystify pseudopapilledema, safeguarding patients from iatrogenic harm. This report advocates routine ODD screening in headache referrals, underscoring imaging's role in precision diagnostics.

Declaration of patient consent

The authors certify that they have obtained all appropriate patient consent forms. In the form, the patient has given his consent for his images and other clinical information to be reported in the journal. The patient understands that name and initials will not be published and due efforts will be made to conceal identity, but anonymity cannot be guaranteed.

Financial support and sponsorship

Guidance and support from the faculty at Government Medical College, Thrissur.

Conflicts of interest

There are no conflicts of interest.

REFERENCES

1. Hoover DL, Robb RM, Petersen RA. Optic disc drusen in children. J Pediatr Ophthalmol Strabismus 1988;25:191-5.
2. Sibony PA, Kupersmith MJ, Kardon RH. Optical coherence tomography neuro-toolbox for the diagnosis and management of papilledema, optic disc edema, and pseudopapilledema. J Neuroophthalmol 2021;41:77-92.
3. Genizi J, Meiselles D, Arnowitz E, Segal I, Cohen R, Goldenberg-Cohen N. Optic nerve drusen is highly prevalent among children with pseudotumor cerebri syndrome. Front Neurol 2021;12:789673.
4. El-Gendy RS, El-Hamid AS, Galhom AE, Hassan NA, Ghoneim EM. Diagnostic dilemma of papilledema and pseudopapilledema. Int Ophthalmol 2024;44:272.
5. Carter JE, Merren MD, Byrne BM. Pseudodrusen of the optic disc. Papilledema simulating buried drusen of the optic nerve head. J Clin Neuroophthalmol 1989;9:273-6.
6. Lam BL, Morais CG Jr., Pasol J. Drusen of the optic disc. Curr Neurol Neurosci Rep 2008;8:404-8.
7. Gutteridge IF. Optic nerve drusen and pseudopapilledema. Am J Optom Physiol Opt 1981;58:671-6.
8. Asensio-Sánchez VM, Trujillo-Guzmán L. SD-OCT to distinguish papilledema from pseudopapilledema. Arch Soc Esp Oftalmol 2015;90:481-3.
9. Vienne-Jumeau A, Lebranchu P, Akhenak I, Bremond-Gignac D, Robert MP. Peripapillary hyperreflective ovoid mass-like structure (PHOMS) and optic disc drusen in pediatric pseudo-papilledema. Graefes Arch Clin Exp Ophthalmol 2025;263:1725-32.

The Ocular Eclipse

Congenital hypertrophy of the retinal pigment epithelium (CHRPE) is a benign, flat, pigmented retinal lesion that is frequently encountered in routine fundus examinations. Despite its characteristic appearance, CHRPE is not uncommonly misdiagnosed as a choroidal nevus or melanoma, leading to unnecessary patient anxiety and referrals to ocular oncology services.[1]

We present a wide-field color fundus photograph and corresponding fundus autofluorescence image of an asymptomatic patient referred with a presumptive diagnosis of "suspicious choroidal melanoma [Figure 1]."

The color fundus image demonstrates a solitary, well-circumscribed, flat, jet-black lesion located in the superotemporal peripheral retina. The lesion has smooth margins, uniform pigmentation, and absence of surrounding subretinal fluid, orange pigment, or hemorrhage. There is no distortion of adjacent retinal vasculature or elevation suggestive of a choroidal mass.

Fundus autofluorescence imaging reveals a sharply demarcated area of dense hypoautofluorescence corresponding to the lesion, consistent with marked melanin content and absence of lipofuscin. This autofluorescence pattern is pathognomonic for CHRPE and helps reliably differentiate it from choroidal nevus or melanoma, which typically demonstrate variable autofluorescence due to lipofuscin accumulation.[2]

Based on clinical examination and multimodal imaging, a definitive diagnosis of solitary CHRPE was made. The patient was reassured regarding the benign nature of the lesion, and no treatment or oncologic surveillance was advised.

This case highlights the importance of careful clinical evaluation and multimodal imaging in avoiding overdiagnosis of ocular malignancy. Recognition of CHRPE is essential for retina specialists, comprehensive ophthalmologists, and ocular oncologists alike to prevent unnecessary referrals, investigations, and patient distress.[3]

Written informed consent was obtained from the patient.

Financial support and sponsorship

Nil.

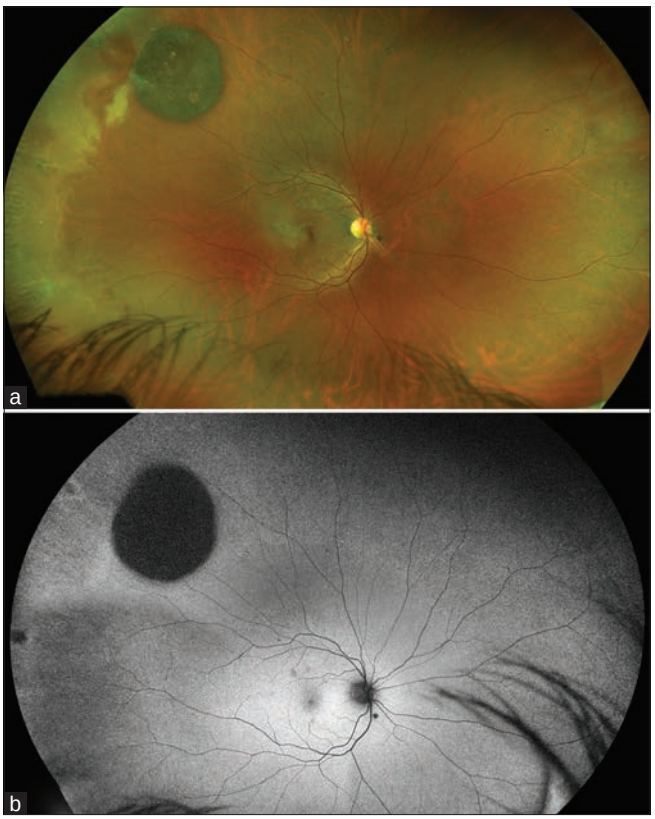

Figure 1: (a) Ultra-widefield color fundus photograph showing a flat, well-defined, uniformly pigmented lesion in the superotemporal peripheral retina consistent with congenital hypertrophy of the retinal pigment epithelium, (b) Fundus autofluorescence image demonstrating dense hypoautofluorescence corresponding to the lesion, confirming the diagnosis of congenital hypertrophy of the retinal pigment epithelium

Conflicts of interest

There are no conflicts of interest.

Dhaivat Shah, Nicey Roy Thomas, Kubra Banu, Aathira Surendranathan

Department of Ophthalmology, Ahalia Eye Care, Abu Dhabi, UAE

Address for correspondence: Dr. Dhaivat Shah, Ahalia Eye Care, Abu Dhabi, UAE.
E-mail: dhaivatkshah@gmail.com

Submitted: 26-01-2026
Accepted: 27-01-2026 **Published:** ***

REFERENCES

1. Shields CL, Mashayekhi A, Ho T, Cater J, Shields JA. Solitary congenital hypertrophy of the retinal pigment epithelium: Clinical features and frequency of enlargement in 330 patients. Ophthalmology 2003;110:1968-76.

2. Shields JA, Shields CL. Pigmented lesions of the retina and choroid. Ophthalmol Clin North Am 2005;18:85-102.
3. Kanski JJ, Bowling B. Clinical Ophthalmology: A Systematic Approach. 8th ed. Abu Dhabi, UAE; Elsevier; 2016. p. 543-5.

Access this article online

Website: https://journals.lww.com/saao

DOI: 10.4103/SAOJ.SAOJ_5_26

Quick Response Code

How to cite this article: Shah D, Thomas NR, Banu K, Surendranathan A. The ocular eclipse. South Asian Acad Ophthalmol J 2026;XX:XX-XX.

Photo Essay

Caviar Fish Eggs Mirage: Intraocular Lens Adorned by Emulsified Silicone Oil

Silicone oil has become a mainstay as an internal tamponade following pars plana vitrectomy, particularly in complex cases of retinal detachment and proliferative vitreoretinopathy. We present a 67-year-old male who underwent vitrectomy for retinal detachment in his right eye a decade ago and now presents for a routine ophthalmic evaluation with nystagmus, a best-corrected visual acuity of 0.167 (LogMAR), and normal intraocular pressure. On slit-lamp examination, emulsified silicone oil droplets delicately adhered to the anterior surface of the intraocular lens, resembling caviar fish eggs in their clustered, pearlescent appearance [Figure 1]. The persistent nystagmus likely generated repetitive shear forces at the silicone–aqueous interface, accelerating emulsification.[1] This case strikingly illustrates how refractile emulsified oil droplets can cling to the lens surface – transforming a postoperative complication into an image of ethereal beauty.

Declaration of patient consent

The authors certify that they have obtained all appropriate patient consent forms. In the form, the patient has given his consent for his images and other clinical information to be reported in the journal. The patient understands that his name and initials will not be published and due efforts will be made to conceal his identity, but anonymity cannot be guaranteed.

Financial support and sponsorship

Nil.

Conflicts of interest

There are no conflicts of interest.

C. Supriya, Sumitha Calaivanane[1], S. Sivaranjani[2]

Cornea Services, Aravind Eye Hospital, Puducherry, India, [1]Glaucoma Services, Aravind Eye Hospital, Puducherry, India, [2]Vitreo Retina Services, Aravind Eye Hospital, Puducherry, India

Address for correspondence: Dr. S. Sivaranjani, 41, Library Street, Ganapathy Nagar, Murungapakkam, Puducherry - 605 004, India.
E-mail: drsivaranjani.s@gmail.com

Submitted: 27-01-2026 **Accepted:** 12-02-2026 **Published:** ***

REFERENCE

1. Yilmaz T, Güler M. The role of nystagmus in silicone oil emulsification after pars plana vitrectomy and silicone oil injection for complex retinal detachment. Eur J Ophthalmol 2008;18:150-4.

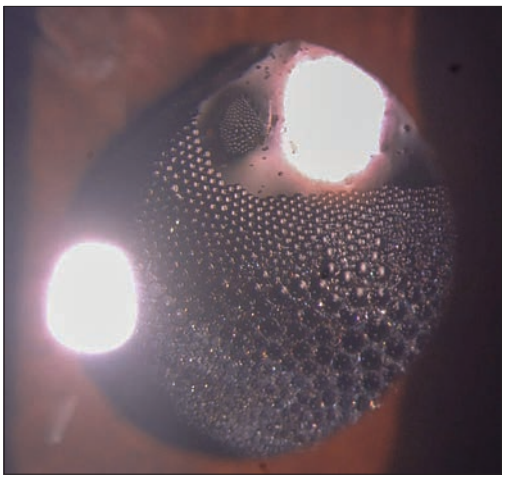

Figure 1: Emulsified silicone oil droplets delicately adhered to the anterior surface of the intraocular lens, resembling caviar fish eggs in their clustered, pearlescent appearance

Access this article online	
Website: https://journals.lww.com/saao	Quick Response Code
DOI: 10.4103/SAOJ.SAOJ_13_26	

How to cite this article: Supriya C, Calaivanane S, Sivaranjani S. Caviar fish eggs mirage: Intraocular lens adorned by emulsified silicone oil. South Asian Acad Ophthalmol J 2026;XX:XX-XX.

Photo Essay

Posterior Embryotoxon

INTRODUCTION

Posterior embryotoxon is a congenital anomaly characterized by prominence of the Schwalbe's ring Figure 1.[1] Axenfield described posterior embryotoxon and iris strands adherent to the anterior displaced Schwalbe's line.[2]

Axenfield syndrome, an autosomal dominant disorder associated with ocular and systemic developmental abnormalities secondary to genetic defects resulting from developmental arrest of the neural crest cells with their retention in the anterior chamber angle during gestation, results in incomplete development of the trabecular meshwork or Schlemm's canal.[2]

Glaucoma is seen in almost 50% of the cases. Although glaucoma may result in early infancy, it is mostly seen during adolescence or early adulthood.

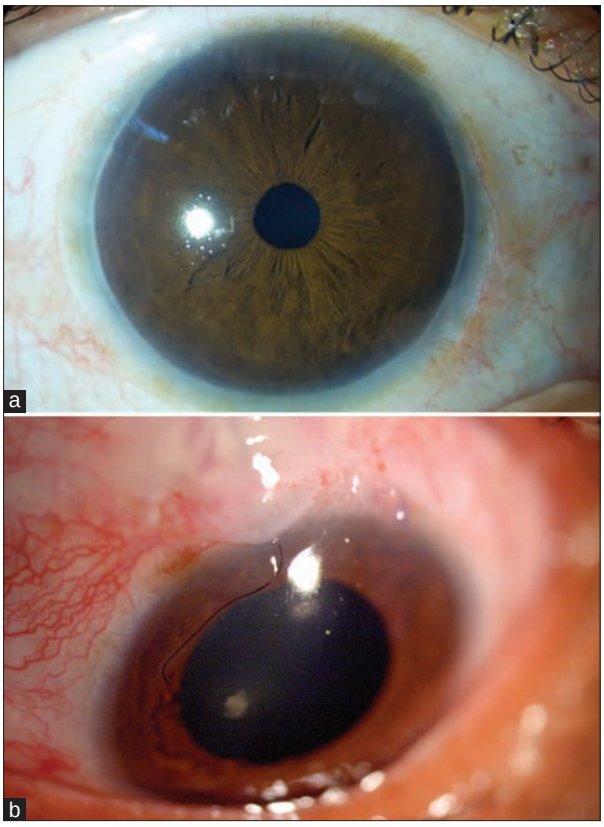

Figure 1: (a) Prominence of the anterior border ring of Schwalbe's line with iris stromal atrophy and (b) Postop showing well-functioning bleb with releasable suture intact

Differential

Axenfeld–Rieger syndrome, primary congenital glaucoma, iris hypoplasia, Peters anomaly.

Acknowledgments

We would like to sincerely acknowledge the team of optometrists at our institute for assisting us in taking photographs of the patient.

Financial support and sponsorship

Nil.

Conflicts of interest

There are no conflicts of interest.

Amit C. Porwal, Amitesh Satsangi[1]

Department of Glaucoma, Choithram Netralaya, Indore, Madhya Pradesh, India, [1]Department of Ophthalmology, CARE CHL Hospitals, Indore, Madhya Pradesh, India

Address for correspondence: Dr. Amit C. Porwal, Department of Glaucoma, Choithram Netralaya, Shriram Talawali, Dhar Road, Indore - 453 001, Madhya Pradesh, India.
E-mail: amitcporwal@yahoo.com

Submitted: 27-01-2026 **Revised:** 02-02-2026
Accepted: 13-02-2026 **Published:** ***

REFERENCES

1. Malik S, Singh G, Gupta AK. Posterior embryotoxon. Indian J Ophthalmol 1969;17:115-6.
2. Axenfeld TH. Embryotoxon cornea posterius. Klin Monatsbl Augenheilkd 1920;65:381-2.

Access this article online	
Website: https://journals.lww.com/saao	Quick Response Code
DOI: 10.4103/SAOJ.SAOJ_12_26	

How to cite this article: Porwal AC, Satsangi A. Posterior embryotoxon. South Asian Acad Ophthalmol J 2026;XX:XX-XX.

A Case of Traumatic Phacocele Causing Meridional Visual Impairment

Traumatic phacocele has not been associated with a meridional visual impairment earlier. A 55-year-old female had a sudden diminution of vision and distorted image perception in the left eye (LE) following blunt trauma. The LE had a best-corrected visual acuity (BCVA) of LogMAR +1.5. The slit examination showed a well-delineated subconjunctival mass in the superonasal quadrant, appearing to be a dislocated lens [Figure 1a]. The anterior segment optical coherence tomography showed an anterior chamber angle of 42.9° and a 3.59-mm thick mass in the superonasal quadrant. The LE had keratometry readings of 52.12 diopters at 36° and 36.90 diopters at 126°, depicting corneal flattening at the axis tangential to the displaced lens [Figure 1b]. Three months following lens extraction, LE had BCVA of LogMAR +0.5, and keratometry readings of 49.57 diopters at 38° and 37.93 diopters at 128°, depicting persistent corneal flattening at the same axis [Figure 1c and d]. Besides aphakia, corneal distortion with a profoundly altered keratometry caused visual impairment in phacocele.[1-4]

Declaration of patient consent

The authors certify that they have obtained all appropriate patient consent forms. In the form, the patient has given her consent for her images and other clinical information to be reported in the journal. The patient understands that her name and initials will not be published and due efforts will be made to conceal her identity, but anonymity cannot be guaranteed.

Financial support and sponsorship

Nil.

Conflicts of interest

There are no conflicts of interest.

Punita Kumari Sodhi, Avilasha Mohapatra, Aastha Singh

Department of Ophthalmology, Guru Nanak Eye Centre Affiliated with Maulana Azad Medical College, New Delhi, India

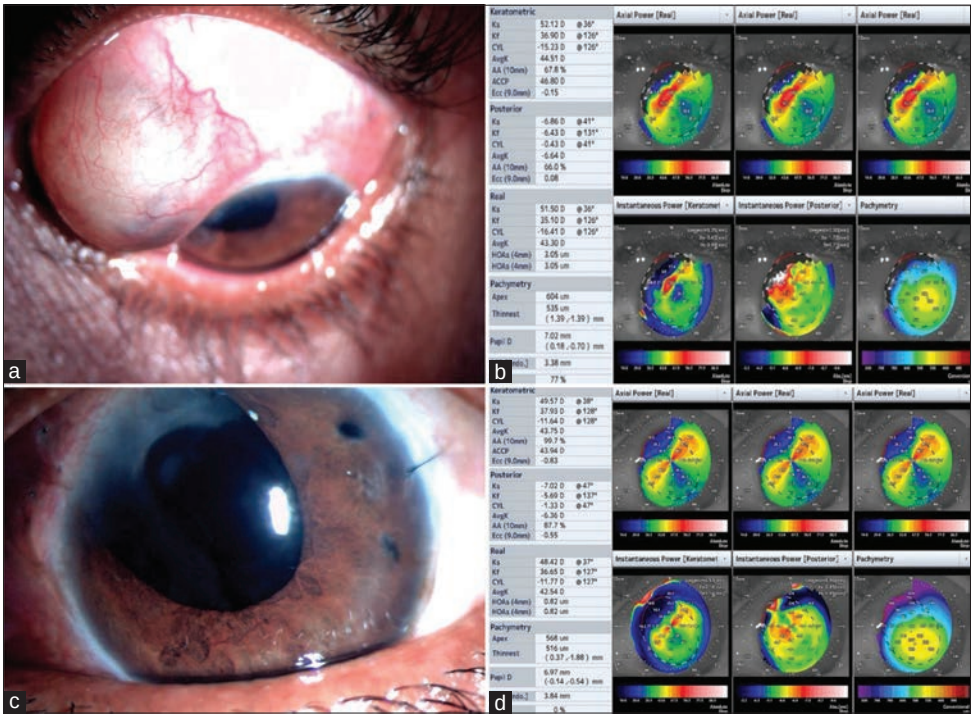

Figure 1: (a) Colour photo of the left eye showing superonasal dislocation of lens, (b) Corneal topography showing flattening of cornea at the axis tangential to the displaced lens, (c) Colour photo of the left eye following lens extraction showing aphakia with superonasal iris defect, (d) Corneal topography after lens extraction showing persistent flattening of cornea at the same axis

Address for correspondence: Prof. Punita Kumari Sodhi, Department of Ophthalmology, Guru Nanak Eye Centre Affiliated with Maulana Azad Medical College, New Delhi, India.
E-mail: punitasodhi222@gmail.com

Submitted: 01-02-2026 **Revised:** 03-02-2026
Accepted: 16-02-2026 **Published:** ***

REFERENCES

1. Bhattacharjee K, Bhattacharjee H, Deka A, Bhattacharyya P. Traumatic phacocele: Review of eight cases. Indian J Ophthalmol 2007;55:466-8.
2. Sharma R, Yadav V, Maurya G, Singh SK. Traumatic subconjunctival phacocele –Rare and sui generis. Indian J Ophthalmol Case Rep 2024;4:733-5.
3. Neupane S, Das D, Korgaonkar S. Migrated subconjunctival cystalline lens: A traumatic phacocele. BMJ Case Rep 2020;13:e237014.
4. Chaniyara MH, Rathi A, Pujari A, Urkude JS. Traumatic phacocele: A rare but unique scenario. BMJ Case Rep 2017;2017:bcr2017220755.

Access this article online

Website: https://journals.lww.com/saao

Quick Response Code

DOI: 10.4103/SAOJ.SAOJ_38_26

How to cite this article: Sodhi PK, Mohapatra A, Singh A. A case of traumatic phacocele causing meridional visual impairment. South Asian Acad Ophthalmol J 2026;XX:XX-XX.